DEVELOPMENT OF PLANT-PRODUCED SUBUNIT VACCINES TO ELICIT THE

IMMUNOGENICITY AGAINST SARS-CoV-2 VARIANT VIRUSES

Mr. Narach Khorattanakulchai

จุฬาลงกรณ์มหาวิทยาลัย

CHULALONGKORN UNIVERSITY

A Dissertation Submitted in Partial Fulfillment of the Requirements

for the Degree of Doctor of Philosophy in Pharmaceutical Sciences and Technology

FACULTY OF PHARMACEUTICAL SCIENCES

Chulalongkorn University

Academic Year 2022

Copyright of Chulalongkorn University

การพัฒนาวัคซีนหน่วยย่อยที่ผลิตจากพืชเพื่อกระตุ้นภูมิคุ้มกันต่อไวรัส ซาร์ส-โควี-2 กลายพันธุ์

นายนรัช คอรัตนกุลชัย

Thesis Title   DEVELOPMENT OF PLANT-PRODUCED SUBUNIT
                      VACCINES TO ELICIT THE IMMUNOGENICITY AGAINST
                      SARS-CoV-2 VARIANT VIRUSES
By   Mr. Narach Khorattanakulchai
Field of Study   Pharmaceutical Sciences and Technology
Thesis Advisor   Associate Professor WARANYOO PHOOLCHAROEN, Ph.D.

Accepted by the FACULTY OF PHARMACEUTICAL SCIENCES, Chulalongkorn University in Partial Fulfillment of the Requirement for the Doctor of Philosophy

.... Dean of the FACULTY OF
PHARMACEUTICAL SCIENCES
(Professor PORNANONG ARAMWIT, Ph.D.)

DISSERTATION COMMITTEE
.... Chairman
(Associate Professor Anchanee Kubera, Ph.D.)
.... Thesis Advisor
(Associate Professor WARANYOO PHOOLCHAROEN, Ph.D.)
.... Examiner
(Assistant Professor NATAPOL PORNPUTTAPONG, Ph.D.)
.... Examiner
(Associate Professor JITTIMA LUCKANAGUL, Ph.D.)
.... Examiner
(Associate Professor CHATCHAI CHAOTHAM, Ph.D.)

นรัช คอรัตนกุลชัย : การพัฒนาวัคซีนหน่วยย่อยที่ผลิตจากพืชเพื่อกระตุ้นภูมิคุ้มกันต่อไวรัส ซาร์ส-โควี-2 กลายพันธุ์. (DEVELOPMENT OF PLANT-PRODUCED SUBUNIT VACCINES TO ELICIT THE IMMUNOGENICITY AGAINST SARS-CoV-2 VARIANT VIRUSES) อ.ที่ปรึกษาหลัก : รศ. ดร.วรัญญู พูล เจริญ

ตั้งแต่มีการระบาดของโรคระบาดใหญ่ไวรัสโคโรนาในปี ค.ศ. 2019 (โควิด-19) ทำให้การพัฒนาวัคซีนที่มีประสิทธิภาพเพื่อต่อสู้กับการติดเชื้อเพิ่มขึ้นทั่วโลก ขณะที่ ไวรัสโคโรนาก่อโรคหายใจรุนแรงเฉียบพลัน-2 (ซาร์ส-โควี-2) ที่กลายพันธุ์ในส่วนบริเวณจับตัวรับ (Receptor-binding domain, RBD) ที่เกี่ยวกับการเพิ่มความสามารถในการแพร่กระจาย การเพิ่มความสามารถในการติดเชื้อ และการหลบหลีกภูมิคุ้มกันจากการฉีดวัคซีน ที่เป็นการระบาดหลักในขณะนี้ วัคซีนที่มีประสิทธิภาพต่อสายพันธุ์ที่น่ากังวล (VOC) และกลยุทธ์ในการฉีดเข็มกระตุ้นอย่างเหมาะสมเป็นสิ่งที่จำเป็นอย่างมาก ในที่นี้ ยีนที่ถอดรหัสเป็น RBD 7 สายพันธุ์ที่แตกต่างกัน (สายพันธุ์บรรพบุรุษ (อู่ฮั่น) แอลฟา บีตา แกมมา แคปปา เดลตา และเอปไซลอน) เชื่อมด้วยส่วนที่ตกผลึกได้ (Fragment crystallizable region, Fc) ของ IgG1 มนุษย์ (RBD-Fc) ถูกสร้างและโคลนเข้าสู่เวกเตอร์การแสดงออกในพืช และผลิตใน *Nicotiana benthamiana* โดยการแสดงออกแบบชั่วคราว นอกจากนี้ การกระตุ้นภูมิคุ้มกันของวัคซีนหน่วยย่อยของ RBD-Fc ที่กลายพันธุ์ ที่ผลิตจากพืชถูกทดสอบในลิงแสม ในขั้นแรก ลิงถูกฉีดกระตุ้นภูมิเข้ากล้ามเนื้อแบบเข็มหลัก-กระตุ้น และ เข็มกระตุ้นหลังจากนั้น 4 เดือน ด้วยวัคซีน RBD-Fc อู่ฮั่น ใบยาซาร์สโควีทูแวกซ์ 1 (Baiya SARS-CoV-2 Vax 1) ในวันที่ 0 21 และ 133 ในขั้นที่สอง ลิงแต่ละกลุ่มลิงถูกฉีดกระตุ้นภูมิเข้ากล้ามเนื้อ 3 ครั้ง ด้วยวัคซีน RBD-Fc กลายพันธุ์ ในวันที่ 0 21 และ 42 ต่อมาตัวอย่างเลือดถูกเก็บเพื่อประเมินแอนติบอดีที่จำเพาะต่อแอนเจนและนิวทรัลไลซ์ ซาร์ส-โควี-2 กลายพันธุ์ ลิงที่ได้รับ ใบยาซาร์สโควีทูแวกซ์ 1 กระตุ้นระดับของแอนติบอดี anti-RBD สูงอย่างมีนัยสำคัญ น่าสนใจที่ ซีรั่มที่เก็บจากลิงได้รับเข็มกระตุ้นที่ 4 เดือน แสดงการตอบสนองของแอนติบอดีนิวทรัลไลซ์แบบข้ามต่อ ซาร์ส-โควี-2 กลายพันธุ์ แอลฟา บีตา แกมมา เดลตา และ โอไมครอน การให้วัคซีนสามครั้งของวัคซีน RBD-Fc กลายพันธุ์ กระตุ้นระดับของแอนติบอดีที่จำเพาะต่อแอนติเจนและนิวทรัลไลซ์สูงขึ้น โดยเฉพาะในกลุ่มของวัคซีน เดลตา และ เอปไซลอน อย่างไรก็ตาม ความสามารถในการนิวทรัลไลซ์ที่สูงขึ้นจากการกระตุ้นภูมิด้วยวัคซีนกลายพันธุ์ แสดงให้เห็นอย่างเจาะจงว่ามีผลต่อสายพันธุ์กลายพันธุ์ที่คล้ายคลึงกัน การค้นพบครั้งนี้แนะนำว่า การฉีดกระตุ้นในระยะยาวอาจมีประโยชน์สำหรับการป้องกันต่อ ซาร์ส-โควี-2 กลายพันธุ์ในข้างหน้า และวัคซีนที่จำเพาะต่อการกลายพันธุ์อาจถูกประยุกต์เป็นวัคซีนเข็มกระตุ้นหรือค็อกเทล เพื่อกระตุ้นแอนติบอดีนิวทรัลไลซ์อย่างกว้างขวาง ผลนี้เผยศักยภาพสำหรับการใช้วัคซีนหน่วยย่อยที่ผลิตจากพืชในการต่อสู้กับ ซาร์ส-โควี-2

สาขาวิชา	เภสัชศาสตร์และเทคโนโลยี	ลายมือชื่อนิสิต ....
ปีการศึกษา	2565	ลายมือชื่อ อ.ที่ปรึกษาหลัก ....

6271012833 : MAJOR PHARMACEUTICAL SCIENCES AND TECHNOLOGY

Narach Khorattanakulchai : DEVELOPMENT OF PLANT-PRODUCED SUBUNIT VACCINES TO ELICIT THE IMMUNOGENICITY AGAINST SARS-CoV-2 VARIANT VIRUSES. Advisor: Assoc. Prof. WARANYOO PHOOLCHAROEN, Ph.D.

Since the emergence of the coronavirus pandemic in 2019 (COVID-19), the development of effective vaccines to combat the infection has accelerated worldwide. While the severe acute respiratory syndrome-coronavirus 2 (SARS-CoV-2) with mutations in the receptor-binding domain (RBD) with high transmissibility, enhanced infectivity, and immune escape from vaccination is also predominantly emerging. Effective vaccines against variant of concern (VOC) and optimized booster vaccination strategies are thus highly required. Here, the gene encoding seven different RBD (ancestral (Wuhan), Alpha, Beta, Gamma, Kappa, Delta, and Epsilon variants) fused with the fragment crystallizable region (Fc) of human IgG1 (RBD-Fc) was constructed and cloned into the plant expression vector and produced in *Nicotiana benthamiana* by transient expression. Further, the immunogenicity of plant-produced variant RBD-Fc subunit vaccines was tested in cynomolgus monkeys. First, monkeys were intramuscularly immunized with prime-booster and 4-month booster dose with the Wuhan RBD-Fc vaccine (Baiya SARS-CoV-2 Vax 1) on day 0, 21, and 133. Second, each group of monkeys were intramuscularly injected thrice with different variant RBD-Fc vaccines on day 0, 21, and 42. Then, the blood samples were collected for evaluating the antigen-specific and neutralizing antibodies against SARS-CoV-2 variants. Baiya SARS-CoV-2 Vax 1 immunized monkeys elicited significantly high levels of anti-RBD antibodies. Interestingly, the sera collected from 4-month booster dose monkeys showed cross-neutralizing antibody response against the SARS-CoV-2 variants; Alpha, Beta, Gamma, Delta, and Omicron. The three doses of variant RBD-Fc vaccines also elicited high levels of antigen-specific and neutralizing antibodies, especially in Delta and Epsilon vaccine groups. However, the high neutralizing activity of immunized variant vaccine sera was demonstrated specifically against the homologous variants. These findings suggested that the long-term booster dose might be helpful for protecting against further SARS-CoV-2 variants and the variant-specific vaccine might be applied as a booster or cocktail vaccine to induce broadly neutralizing antibodies. These results revealed the potential for using the plant-produced protein subunit vaccines in the fight against SARS-CoV-2.

Field of Study:	Pharmaceutical Sciences and Technology	Student's Signature ....
Academic Year:	2022	Advisor's Signature ....

ACKNOWLEDGEMENTS

TABLE OF CONTENTS

LIST OF TABLES

LIST OF FIGURES

CHAPTER I INTRODUCTION

1 Coronavirus disease 2019 (COVID-19)

Infectious disease control relies on the understanding of pathogen structure, disease pathology and its mode of transmission which helps to develop suitable vaccines or therapeutic interventions against that particular infection. The ongoing pandemic coronavirus disease 2019 (COVID-19) is caused by severe acute respiratory syndrome coronavirus 2 (SARS-CoV-2). The pandemic causes devastating impact on human lives and economy. The virus structure, infection, past outbreaks, and adaptation of virus was briefly explained in this section.

1.1 Coronavirus

Coronaviruses (CoVs) are enveloped RNA viruses and classified in the *Nidovirales* order, *Coronaviridae* family, which are classified into 4 genera: *Alphacoronavirus* (α-coronavirus), *Betacoronavirus* (β-coronavirus), *Gammacoronavirus* (γ-coronavirus), and *Deltacoronavirus* (δ-coronavirus) (1). The genome of CoVs is positive-sense single-stranded RNA (+ssRNA), measuring approximately 30 kb by 5'-cap and 3'-poly-A tail. The genomic RNA acts as a template for the synthesis of both non-structural proteins (nsps) and structural proteins with various open reading frames (ORFs) (Figure 1A).

The nsps genes, polyprotein 1a/1ab (pp1a/pp1ab), located in ORF1a/b and encoded 16 nsps (nsp1-16), except γ-coronavirus (nsp2-16). Between the ORF1a and ORF1b has -1 frameshift to translate two polypeptides, pp1a and pp1ab. After that, viral proteases, one or two papain-like protease and chymotrypsin-like protease (3CL^{pro}) or main protease (M^{pro}), cleave pp1a and pp1ab into 15 or 16 nsps (2, 3). In double-membrane vesicles (DMVs), nsps form the replication-transcription complex (RTC). Accordingly, RTC synthesizes a set of subgenomic RNAs (sgRNAs), which are 5'-3' messenger RNAs (mRNAs), to terminate transcription (4, 5). Then, a leader RNA appears at transcription regulatory sequences that are located between open reading frames (ORFs) and the minus-strand sgRNAs become the templates for the production of subgenomic mRNAs (6, 7).

The 3' terminus of the genome contains ORFs that are translated to structural proteins and accessory proteins. The four major structural proteins consist of spike or surface (S), membrane (M), envelope (E), and nucleocapsid (N) proteins (Figure 1B). S protein is a transmembrane protein located on the outer viral surface, which form homotrimer as a crown-like structure. S protein is cleaved by host furin-like protease into 2 subunits, S1 and S2. The S1 unit contains a receptor-binding domain (RBD) that interacts with the host cell receptor while S2 is involved in fusion and transmission to enter into the host cell (8-10). M protein plays a major role in the structure and shape of the virus. This protein can attach to all structural proteins, especially N protein to stabilize the nucleocapsid (11, 12). Next, E protein participates in viral production, assembly, maturation, and pathogenesis (13-15). N protein is bound to the viral genome that plays a key role in the processes of the viral genome, viral replication, and infection (9, 16, 17).
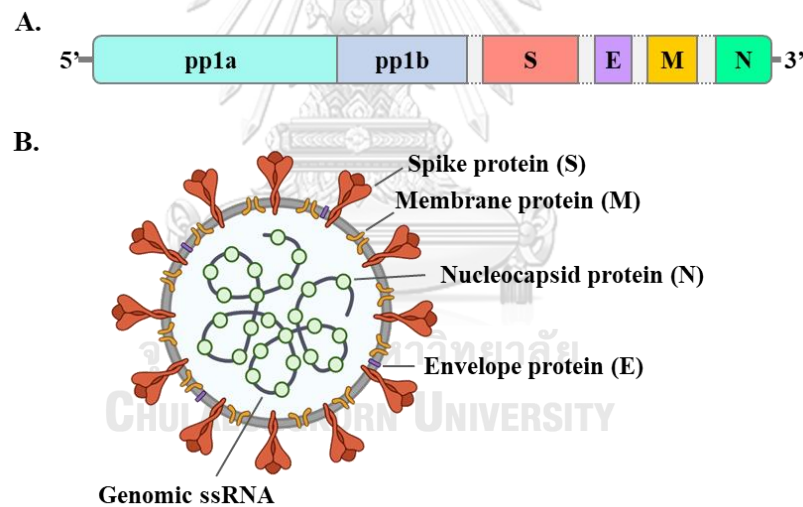
Figure 1 Genomic structure (A) and virion of CoV (B).

ssRNA: single-stranded RNA, pp1a/b: nsp polyprotein 1a/1b, S: spike protein, M: membrane protein, N: nucleocapsid protein, E: envelope protein, dashed line: accessory protein. Modified from (1, 18).

1.2 Outbreaks caused by CoVs

In the past, humans dealt with two epidemic respiratory syndromes namely severe acute respiratory syndrome (SARS) and Middle East respiratory syndrome

(MERS). Both diseases were caused by β-coronaviruses such as SARS-CoV and MERS-CoV, respectively.

In 2002, the first confirmed case of SARS in humans was reported in the Guangdong province, China (19). After that, the 26 countries were affected by SARS, more than 8,000 cases and 700 deaths were reported in 2003. The transmission of this disease might be caused by zoonotic transfer of virus from civet cats to humans and then human-to-human transmission occur, *via*., respiratory secretions or body fluids. The symptoms including high fever, cough, breath shorten, and diarrhea were reported which rapidly progressed to severe respiratory distress in severe cases (20, 21).

MERS, the second epidemic, occurred in several countries in the Middle East, South Asia, and Africa in 2012 (22). The initial human case was confirmed in Saudi Arabia in 2012. Since 2012, the MERS spread to 27 countries, with 2562 cases, and 881 deaths were reported with the mortality rate of 34% (22). Still the origin of MERS-CoV is unclear and suggested to be transmitted by animals to humans (23). The bats might be the origin of this virus and transfer to dromedary camels, a reservoir, and then transmitted to humans (22, 24). However, human-to-human transmission needs close contact with patients, families, or health care workers, without appropriate protection. The symptoms of MERS are similar to SARS, in addition MERS virus can develop into renal disease in weakened patients (25).

1.3 SARS-CoV-2 Pandemic

Since December 2019, the world has been faced with the new pandemic novel coronavirus disease (2019-nCoV or COVID-19) which is caused by SARS-CoV-2 (26). The first case was confirmed in Wuhan, Hubei Province, China. The beginning of the disease was suggested that it connected to wild animal trading at the Wuhan fish market (27). However, no evidence can confirm the source of the disease (28). The hosts are believed to be bats and pangolin, which showed 96% and 99% genetic similarity, respectively, to SARS-CoV-2 found in humans (29, 30). COVID-19 spread around the world with a high transmission rate and over 641 million cases, and 6.6 million deaths were reported (data on 30th November 22) (31, 32). The patients mostly show

symptoms of fever, dry cough, and tiredness (33). In severe cases, the patients are faced with lung injury by cytokine storm and immunosuppression (34, 35). COVID-19 spreads through infected saliva or droplets even during the incubation period (36). Moreover, the dramatical infection rate of COVID-19 was suggested that it might be an airborne transmission, small droplet (aerosol) spread in the air (37, 38). On the other hand, most patients are asymptomatic-infected, those can spread the virus without any symptoms (39), which makes the diagnosis and prevention of COVID-19 difficult (40). Moreover, the incubation time of SARS-CoV-2 was estimated to be ranged from 2 - 11 days (mean = 5 days) (41, 42), and could be up to 24 days (43). When compared with the previous CoVs, SARS and MERS showed the same as COVID-19 with a range of 2 - 10 days (mean = 5 days) and 2 - 14 days (mean = 5-7 days), respectively (44, 45).

Earlier reports suggested that SARS-CoV-2, similar to SARS-CoV (46), binds to human angiotensin-converting enzyme 2 (hACE2) receptor *via.,* spike or surface (S) glycoprotein for infection (47-49). S protein plays an important role in host cell attachment, cleaved into S1 and S2 subunits by the host proteases during the infection process. In particular, the receptor-binding domain (RBD), located in the S1 subunit of SARS-CoV-2, recognizes hACE2 in the host cell and plays a crucial role in host cell entry. Therefore, the S, S1 or RBD proteins are the primary targets for neutralizing antibodies and therapeutic vaccine development (50-53).

1.4 SARS-CoV-2 variants

The viral genome normally has the adaptive mutation to modify their ability to survive against the immune response and obscure vaccine development from any single amino acid change (54). In SARS-CoV-2, the mutations occurred over time and created many variants that are different from the ancestral strain. The mutation in early pandemic of SARS-CoV-2 was minimal with the appearance of main variant called D614G, which was related with increase transmissibility without any effect in disease severity (55). After that, the new variants of SARS-CoV-2 have been predominately emerging worldwide (56, 57), which were classified for tracking SARS-CoV-2 genetic lineages and named by WHO using letters of the Greek Alphabet (58). The emerging

variants were grouped into variant of concerns (VOCs) and variant of interest (VOIs). VOCs exhibit high virulence, fast transmission, and reduced susceptibility to neutralizing antibodies. Data as of 29th June, 2022, Omicron variant (B.1.1.529) was mentioned as currently circulating VOCs. In addition, Alpha (B.1.1.7), Beta (B.1.351), Gamma (P.1), and Delta (B.1.617.2) variants were former VOCs.

In December 2020, the new VOC was reported from SARS-CoV-2 positive patients in UK, described as B.1.1.7 lineage, GRY, or Alpha (59, 60). Alpha genome consists of 8 mutations, Δ69-70, Δ144, N501Y, A570D, P681H, T716I, S982A, D1118H, which are located in S protein (61). N501Y was reported as enhance transmission and attachment to host cell by increasing binding affinity to human ACE2 (62). This variant was reported as predominate strain in UK with 43% - 82% increase transmissibility (63). Moreover, the mortality rate (~1.6 time) of Alpha virus infected patients was higher than ancestral strain infected (64, 65)

Another new SARS-CoV-2 variant was reported in South Africa in October 2020, namely, GH501Y.V2, lineage B.1.351, or Beta (66). Beta variant also has multiple mutation sites at S protein (L18F, D80A, D215G, R246I, K417N, E484K, N501Y, D614G, and A701V) (61). In addition, K417N, E484K, and N501Y sites are located in RBD, which are related to increase the ACE2 binding affinity and evade host immune system (67, 68). Moreover, Beta strain was reported as high transmission rate and decrease neutralizing activities from monoclonal antibody, convalescent sera, and vaccine immunized sera (69-71).

In Brazil, the third VOC was reported in December 2020, known as P.1 lineage, GR/501Y.V3, or Gamma (72). Gamma variant includes many mutation sites at S protein (L18F, T20N, P26S, D138Y, R190S, K417T, E484K, N501Y, D614G, H655Y, T1027I, V1176F) (61). Gamma variant also shares the mutation sites (L18F, E484K, N501Y) that are located in RBD like Beta variant and has an effect on antibody neutralizations (70).

The fourth strain was first identified in India, known as lineage B.1.617.2, G/478K.V1 or Delta in December 2020 (73). Delta strain contains ten mutations in S protein (T19R, G142D, E156G, ΔF157, ΔR158, L452R, T478K, D614G, P681R, D950N) (61). RBD mutation sites (L452R, T478K), L452R was also reported in Epsilon strain (B.1.429 lineage) as involved in increase in both transmissibility and viral replication (74, 75). For

T478K site, it is suggested that associates with the infection and immune evasion, like E484K mutation (76). In the past, Delta and its sub lineages used to dominantly infect India and all other the world (77, 78)

Omicron variant (B.1.1.529 lineage or GR/484A) is the fifth VOC that was reported in South Africa in November 2021 (79). With multiple mutations, more than 30 sites including insertion and deletion (A67V, Δ69-70, T95I, Δ142-144, Y145D, Δ211, L212I, ins214EPE, G339D, S371L, S373P, S375F, K417N, N440K, G446S, S477N, T478K, E484A, Q493R, G496S, Q498R, N501Y, Y505H, T547K, D614G, H655Y, N679K, P681H, N764K, D796Y, N856K, Q954H, N969K, L981F) in S protein (80). Omicron was reported with higher transmissible than the Delta strain and affects even the vaccinated people (81). Moreover, Omicron illustrated more evasive immunity ability than Beta in *in vitro* study (82). However, no uncommon symptom was recognized in the Omicron patients and some are asymptomatic (83). Many researchers suggested that Omicron strain could increase transmissibility, decrease efficiency of vaccine, and enhance risk of reinfection (84, 85).

VOIs are described as the variant that contain specific mutation markers involved in increased transmissibility or virulence, decreased neutralizing activity of antibodies from natural infection or vaccination, evasion ability of detection, or reduced the effective of therapeutics or vaccination. WHO has informed eight VOIs that has previously circulated, Epsilon (B.1.427 and B.1.429), Zeta (P.2), Eta (B.1.525), Theta (P.3), Iota (B.1.526), Kappa(B.1.617.1), Lambda (C.37) and Mu (B.1.621) (58).

2 Candidate for COVID-19 vaccines

Vaccines and vaccination protect us from infectious diseases and prevent the spread of the pathogen. Several vaccines were developed against SARS-CoV-2. This section explains the types, function, and efficacy of vaccines that were developed to prevent COVID-19 infection.

2.1 Type of vaccines

From the WHO report (86), abouts candidate COVID-19 vaccines in clinical trials, shows many types of vaccine (inactivated, non-replicating and replicating viral vectors, DNA, RNA, protein subunits, and VLPs).

The inactivated virus vaccine is the most common vaccine which widely used in many viral diseases (87). Virus inactivation methods employ chemical reagents, detergents or heat are used to inactive the virus (88, 89). Previously, the inactivated SARS vaccines were reported which showed antibody-dependent enhancement (ADE) in SARS-CoV infection (90, 91). Recently, the inactivated vaccines against COVID-19 were developed and approved (92, 93) such as CoronaVac (Sinovac, China), Covilo (Sinopharm/BBIBP, China), and Covaxin (Bharat Biotech, India). The inactivated virus vaccine recipients were not affected by changing percentage of lymphocytes or a cytokine storm that can potentially cause of death in SARS-CoV-2 patients (92).

The viral vector vaccine generates a high-level protein expression and long-term stability, and can induce robust the immunity (94, 95) which can be either non-replicating or replicating vector. For non-replicating vector vaccine, host cells were infected and virus antigens are produced. In contrast, replicating vector can generate new virus to infect new host cell to increase antigen production (96). Both types of viral vectors were employed for COVID-19 vaccine development and showed to be promising in preventing the infection (97-99). In this platform, adenovirus type-5 (Ad5), Ad26, and vesicular stomatitis virus (VSV) viral vectors are generally used. AZD1222 or ChAdOx1 nCoV-19 (Vaxzevria or Covishield, Oxford/ AstraZeneca), JNJ-78436735 (Ad26.COV2.S, Janssen (Johnson & Johnson)), and Ad5-nCoV (Convidecia, CanSino Biologics) have been listed as non-replicating viral vector COVID-19 EUL vaccines from WHO. In T-cell response, the releasing of IFN-γ, TNF, and IL-2 were detected from $CD4^+$ and $CD8^+$ T cells (100). However, induced antibodies and T-cell responses were moderately reduced in the recipients that used to get immunity against adenovirus (100).

The virus genomic sequence could also be used for establishing vaccines in both DNA and RNA form which offer great flexible antigen manipulation and high-speed development (94). Firstly, DNA vaccine is based on the plasmid that encodes S protein

and induces immunity. Moreover, this kind of vaccine is high scalable, stable, and cold-chain free (101). In the past, both SARS (102, 103) and MERS (104, 105) DNA vaccines were developed which led the promising to develop SARS-CoV-2 DNA vaccine. Recently, the COVID-19 DNA vaccines were developed (50, 106). Next, the RNA vaccine is based on the messenger RNA (mRNA), encoding virus antigen protein, especially S protein or RBD, to induce innate immune response both SARS and SARS-CoV-2 (107, 108). The RNA vaccine is mostly formulated in lipid nanoparticles for enhance transportation into host cells after intramuscular injection (IM) (109). In principle, when the mRNA vaccine is delivered into the cells and it will be translated into the protein antigen in the cytoplasm (110). Then, the released antigen is processed and presented by antigen-presenting cells (APCs) *via* major histocompatibility complex I (MHC I) to activate CD8^{+} T-cells following MHC II to activate CD4^{+} T cells and B-cells by mounting of an antibody response. These processes stimulate both humoral and cell-mediated antigen-specific responses (110-112). In addition, secreted antigens were absorbed by macrophages, then, pro-inflammatory cytokines and chemokines were released for activating the innate immune response. In addition, IFN-γ, IL-2, and IL-12p70 were detected in mRNA vaccine recipients, indicating the T helper type 1 (Th1) bias, but not the Th2 response (113). BNT162b2 (Comirnaty, Pfizer/ BioNTech) and mRNA-1273 (Spikevax, Moderna) were demonstrated the promising efficacy both in pre-clinical and clinical studies, then, are approved by WHO EUL COVID-19 vaccines (114, 115).

The protein subunit vaccines are alternative way to be candidate vaccine developed by using virus protein structure or subunits. The S protein is the major candidate for COVID-19 subunit vaccine (116), especially RBD (117), Which is the main domain that interacts with host cell receptor. However, full-length of S protein vaccines may induce unwanted antibodies from non-neutralizing epitopes. In SARS-CoV challenge in animal, the inflammatory and liver damage or enhancing infection were observed after infection that related in antibody-mediated disease enhancement (ADE) (118-120). In contrast, the fragment of S protein or RBD of SARS-CoV vaccines showed highly neutralizing antibodies response without any adverse effects in SARS-CoV challenged mice (121, 122). Moreover, the immunoinformatic approach might be the alternative way to create the candidate multi-epitope peptide vaccines from MHC

epitopes of B-cells (123). Protein subunit vaccines mainly elicit antibody-mediated immune responses *via* Th2 with a low level of T-cell induction. Adjuvants are required to boost the immune response and enhance vaccine efficacy of protein subunit vaccines (124). NVX-CoV2373 (Nuvaxovid, Novavax) was recently approved in WHO EUL COVID-19 vaccine with promising safety and efficacy in phase 3 clinical trial (125). With the Matrix-M adjuvanted NVX-CoV2373, Th1 cytokines, IFN-γ, TNF-α, and IL-2, in CD4$^+$ and CD8$^+$ T cells were detected in higher level than IL-4 and IL-5 (Th2 cytokines) secretion from CD4$^+$ T cells (126, 127).

The virus-like particles (VLPs), the co-expressed recombinant virus structural proteins that mimics the virus virion without virus genome were developed for COVID-19 vaccine to induce immunity (128, 129). The proteins on the VLP surface are presented as antigens or epitopes for enhanced activation of B-cells and antibody responses (130). Recently, plant-derived COVID-19 VLP vaccine (CoVLP or Covifenz), developed by Medicago Inc., Canada, was approved for human use in Canada (131).

Recently, WHO has approved some SARS-CoV-2 candidate vaccines under emergency use listing (EUL) as shown in Table 1 (132).

Table 1 WHO EUL COVID-19 vaccines.

Name of vaccine	Developed by	Type of Vaccine
Comirnaty (BNT162b2)	Pfizer/BioNTech, USA	mRNA
Spikevax (mRNA-1273)	Moderna, USA	mRNA
Vaxzevria or Covishield (AZD1222 or ChAdOx1 nCoV-19)	Oxford/AstraZeneca, UK	Viral vector (non-replicating)
Ad26.COV2.S (JNJ-78436735)	Janssen (Johnson & Johnson), USA	Viral vector (non-replicating)
Convidecia (Ad5-nCoV)	CanSino Biologics, China	Viral vector (non-replicating)
CoronaVac	Sinovac, China	Inactivated
Covilo (BBIBP-CorV)	Sinopharm/BBIBP, China	Inactivated

Name of vaccine	Developed by	Type of Vaccine
Covaxin (BBV152)	Bharat Biotech, India	Inactivated
Nuvaxovid or COVOVAX (NVX-CoV2373)	Novavax, USA	Protein subunit

2.2 Efficacy of approved vaccines against SARS-CoV-2 VOCs

SARS-CoV-2 VOCs have multiple mutations, especially in the RBD or S protein, that relate to increase in transmission and evade the immune response. Some of the crucial mutations are remarked to decrease the efficacy of approved vaccines (133). BNT162b2 (Pfizer/BioNTech) induced neutralizing antibodies against the Alpha and Beta variants as 2.6-fold and 8.8-fold reduction, respectively, compared to the Wuhan (134). However, neutralizing titers against the Delta and the Beta variants were reduced as 3-fold and 16-fold decrease when compared to the Alpha variant, respectively (135). NVX-CoV2373 (Novavax) showed efficacy against non-B.1.17 strain (96.4%) higher than B.1.17 (86.3%) in the clinical trial phase 3 (125). Furthermore, efficacy against the Beta variant (60%) of NVX-CoV2373 was lower than the Alpha and D614G stains (136). Additional, neutralizing titers of ChAdOx1_nCoV-19 vaccine (Oxford/AstraZeneca) against the Delta and the Beta strains were decreased as 5-fold and 9-fold compared to the Alpha strain (135). The neutralizing responses of both BNT162b2 and ChAdOx1_nCoV-19 vaccines were detected against the Delta variant only after the second dose (135). In BNT162b2 vaccinated sera showed 40-fold reduction in neutralizing response against Omicron compared to the Wuhan. Moreover, neutralizing response against Omicron in the CoronaVac (Sinovac) recipients' sera was not detected (137).

Hence urgent research is required to fulfill the knowledge of effective vaccine and treatment on SARS-CoV-2 and its variants in order to combat its infection and further variant outbreak.

3. Plant-produced vaccines

The cost-effective recombinant vaccine production platform might reduce the vaccine cost, reduce the financial burden, and improve vaccine accessibility, especially in developing countries. Recently, the plant expression system is considered as an alternative to conventional platforms to produce recombinant proteins, such as enzymes, antigens, antimicrobial peptides, diagnostic reagents, and antibodies, especially during emergency situations (138-141). In this section, plant-based expression system, their types, and plant-produced vaccines were reviewed.

3.1 Plant-based recombinant protein production systems

During the pandemic or epidemic outbreaks, many therapeutic agents, vaccines and diagnostic reagents are required to prevent or control the outbreak. The demand for vaccination during COVID-19 pandemic has increased in all the countries. The rapid production and effective material are involved in the major concern of the vaccine industry. In developing countries, the cost-effective investment is also related.

On a commercial scale, recombinant therapeutic proteins are mostly produced in bacterial expression systems for simple proteins without a post-translational process. However, mammalian cell expression systems are famously used for producing complex structural or functional proteins with required post-translational modification (142-144). However, the mammalian cell system requires a high investment and handling costs (145). At present, plants are alternative recombinant protein expression systems with low cost, scalability, and providing post-translation modifications (146, 147). Moreover, the plant-produced process is more safety without contamination by any mammalian or human pathogens (148). From above, the plant-produced recombinant protein system is cost-effective, which can be used especially in developing countries (149). Anyway, the downstream process for biopharmaceutical production is similar to the mammalian system, which requires high purity and sterility. The summary of comparison advantages and disadvantages of each recombinant protein expression system was shown in Table 2 (Modified from (18)).

Table 2 Comparison of recombinant protein production systems efficiency.

Organism	Yield	Scalability	Cost	Glycosylation	Safety	Timescale
Bacteria	Moderate	High	Low	None	Low	Weeks
Yeast	High	Low	Moderate	High mannose	Unknown	Weeks
Insect	Moderate to High	Low	Moderate to High	Mannose terminal	Moderate	Weeks to months
Mammalian cell	Moderate to High	Low	High	Correct	Moderate	Months
Plant						
Cell suspension	Moderate	Moderate	Moderate		High	Weeks to months
Transient	High	High	Low	Plant specific	High	Days to weeks
Transgenic	Moderate	Moderate	Low		High	Months to years

There are several methods to produce recombinant proteins in plant systems, stable transformation, transient expression, and cell suspension cultures (150). In the past, the stable expression system was mostly used for producing proteins in plants by transformed the foreign gene into the host genome. While transient expression method was done by modified viral-derived vectors and agroinfiltration. Moreover, transgenic plant cell suspension system was alternatively used for producing protein by culturing the plant cells in bioreactors, like bacterial and mammalian cells (151). The brief process of recombinant protein production in plants is shown in Figure 2 (18).
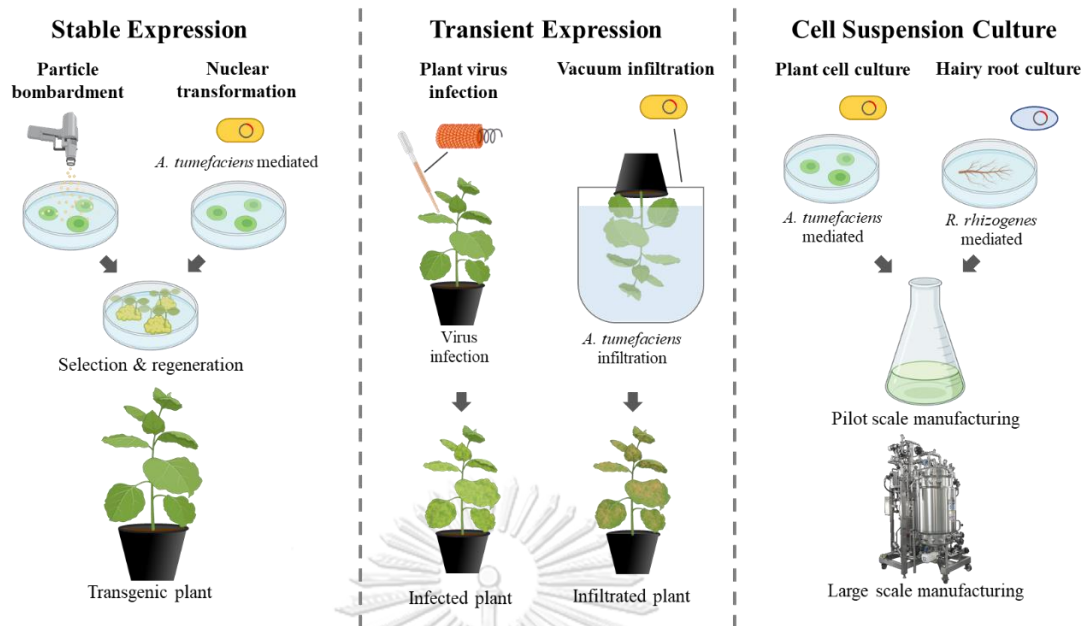
Figure 2 Schematic representation of different expression methods available for the production of the recombinant proteins in plants.

Tobacco (*Nicotiana tabacum* and *Nicotiana benthamiana*) is a well-known plant to use for expressing recombinant proteins, including recombinant therapeutic proteins. Moreover, tobacco is not food-crop or animal feed plant which will be saved for contaminating genetically modified (GM) (142, 152). Previously, tobacco was used mainly to develop transgenic plants (stable transformation). However, the long duration for developing and producing proteins in transgenic plant makes it not suitable to use during disease outbreaks (153, 154).

Transient transformation, which can rapidly scale up the recombinant, has become famous method at present (155). The transient expression is mediated by *Agrobacterium tumefaciens via*., nonvirulent tumor inducing plasmid (Ti-plasmid) by releasing transfer-DNA (T-DNA) to plant cells. *N. benthamiana* is commonly used as transient expression host (152). *N. benthamiana*-based rapid antibody manufacturing platform (RAMP) was established to fight against EBOV outbreak by using magICON, tobacco mosaic virus (TMV) vector expression system (156). The geminiviral vector is the next generation of transient expression, using bean yellow dwarf virus (BeYDV)

derived vector (157) to produce high copy recombinant DNA which refers to high level of transcription of gene of interest (GOI).

The pBeYDV (pBY) expression vector series were reconstructed from Ti-plasmid that contains modified T-DNA from BeYDV DNA e.g., pBYR2eK2Md (pBYR2eK) (Figure 3), which mimics the virus replicon without viral structure proteins. These vectors use cauliflower mosaic virus (CaMV) 35S promoter for strong expression. The mechanism of this expression system starts after T-DNA from *Agrobacterium* was transfer to the genome of infected plant cells, called rolling circle replication mechanism. Firstly, the replication initiator protein (Rep) is translated from C1/C2 by host replication elements, then, nicks the template at long intergenic region (LIR). After that, template is replicated again at nicked LIR and stop at short intergenic region (SIR), which contains poly A tail signal. Then, Rep performs as terminase to release from template and suddenly ligates the copied DNA to form circular DNA. Finally, many circular DNA insides host nucleus will be transcription and translation to produce GOI that is inserted in T-DNA. Which results high yield recombinant proteins (157). To prevent the silencing from host RNA interference (RNAi), p19 suppressor protein of tomato bushy stunt virus (TBSV) was added to T-DNA cassette.
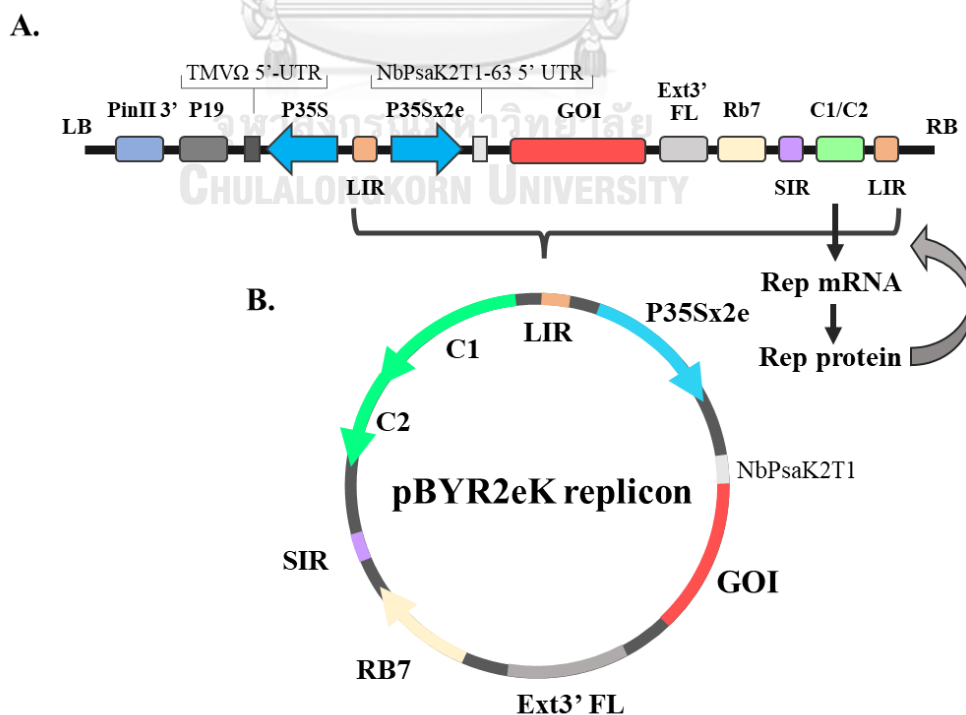
Figure 3 Structure of T-DNA from pBYR2eK2Md (pBYR2eK) (A) and its replicon (B).

LB (left border), PinII 3′ (potato proteinase inhibitor II gene terminator), P19 (tomato bushy stunt virus (TBSV) P19 gene), TMVΩ 5′-UTR (tobacco mosaic virus Ω 5′ untranslated region), P35S (cauliflower mosaic virus (CaMV) 35S promoter), LIR (bean yellow dwarf virus (BeYDV) long intergenic region), NbPsaK2T 5′UTR (5′ untranslated region), GOI (gene of interest), Ext3′FL (3′ full length of the tobacco (N. tabacum) extension gene), RB7 (tobacco RB7 promoter), SIR (BeYDV short intergenic region of), C2/C1 (BeYDV open reading frames C1 and C2 encoding for replication initiation protein (Rep) and RepA), RB (right border). GOI Gene of Interest Modified from (157, 158)

3.2 Plant-produced recombinant vaccines

Since the advancements of plant genetic engineering in the 1980s, plants have been used for the production of economically valuable, biologically active non-native proteins or biopharmaceuticals, the concept termed as plant molecular farming (PMF) (159). The first plant-produced vaccine against Newcastle disease virus to prevent poultry infection, has been approved by the US Department of Agriculture (160). Moreover, several plant-based candidate vaccines have been investigated to induce immunogenicity and demonstrated safety in both preclinical and clinical studies (Table 3, Modified from (18)).

In COVID-19 candidate vaccines, plant platform showed the potential to develop effective vaccine. Virus-like particle (CoVLP, Medicago Inc., Canada) and protein subunit (KBP-201, Kentucky BioProcessing, Inc., USA; Baiya SARS-CoV-2 Vax 1 and Baiya SARS-CoV-2 Vax 2, Baiya Phytopharm Co., Ltd., Thailand) vaccines are on-going in clinical trials. CoVLP or Covifenz, *N. benthamiana*-produced virus-like particle vaccine adjuvanted with AS03, is recently approved for human used, age 18 – 64 years old, in Canada (131). Moreover, CoVLP was cross-effective against SARS-CoV-2 variants with transient adverse effects without any concerns in the clinical trial phase 3 (161). KBP-201, RBD-based vaccine produced from *N. benthamiana* with CpG adjuvant, is under the clinical trial phase 1/2 (86). Baiya SARS-CoV-2 Vax 1, RBD fused with fragment crystallizable (Fc) vaccine from *N. benthamiana* adjuvanted with alum, is the first

generation COVID-19 vaccine of BaiyaPharming™ platform starting phase 1 of the clinical trial and performs effective immunogenicity and safety in pre-clinical studies (162-164). Baiya SARS-CoV-2 Vax 2 is the second generation vaccine under the clinical trial phase 1 (165).

These successes could increase the reliability of plant-produced biopharmaceutical proteins on human treatment. In addition, the plant-based vaccines can be given an opportunity for development and commercialization in further.

Table 3 List of plant-produced candidate vaccines against viral diseases that are in clinical studies.

Disease	Developer	Plant Species	Type	Clinical Trial	Reference
Influenza	Medicago Inc.		Quadrivalent Virus-like particle	Phase 3 (NCT03321968, NCT03301051, NCT03739112)	(166)
	Kentucky BioProcessing Inc.		Protein Subunit	Phase 1 (NCT04439695)	(167)
H5N1 influenza	Medicago Inc.		Virus-like particle	Phase 2 (NCT01991561, NCT01244867)	(168)
	Fraunhofer, CMB	*N. benthamiana*	Protein Subunit	Phase 1 (NCT01250795)	(169)
H1N1 influenza	Fraunhofer, CMB		Protein Subunit	Phase 1 (NCT01177202)	(169)
	Medicago Inc.		Virus-like particle	Phase 1 (NCT01302990)	(170)
H7N9 influenza	Medicago Inc.		Virus-like particle	Phase 1 (NCT02022163)	(171)
	Kentucky BioProcessing, Inc.		Protein Subunit	Phase 1/2 (NCT04473690)	(86)
COVID-19	Medicago Inc.		Virus-like particle	Phase 3 (NCT05040789)	(161)
	Baiya Phytopharm Co., Ltd.		Protein Subunit	Phase 1 (NCT04953078)	(86)
				Phase 1 (NCT05197712)	(165)
Anthrax	Fraunhofer, CMB		Protein Subunit	Phase 1 (NCT02239172)	(169)
Malaria			Virus-like particle	Phase 1 (NCT02013687)	(169)
Follicular Lymphoma	Icon Genetics GmbH		Full-idiotypic immunoglobulin	Phase 1 (NCT01022255)	(172)
Rabies	Thomas Jefferson University	Spinach	Glycoprotein and nucleoprotein fusion	Phase 1	(173)

3.3 Alum adjuvant

Due to the poor immunogenic response of some recombinant antigens, the adjuvant formulation is required to boost the immune response of the vaccines (174) Adjuvants are classified into three groups. First, immunomodulatory molecules are innate receptor ligands, such as toll-like receptors (TLRs), NOD-like receptors (NLRs), C-type lectins, and RIG-I–like receptors. Second, the delivery systems that promotes more effective delivery of vaccine antigens (lipid vesicle-based or liposome). Third, the combined actions of the above systems such as squalene-based emulsion (MF59), aluminum salts, and adjuvants combination (Figure 4) (175).
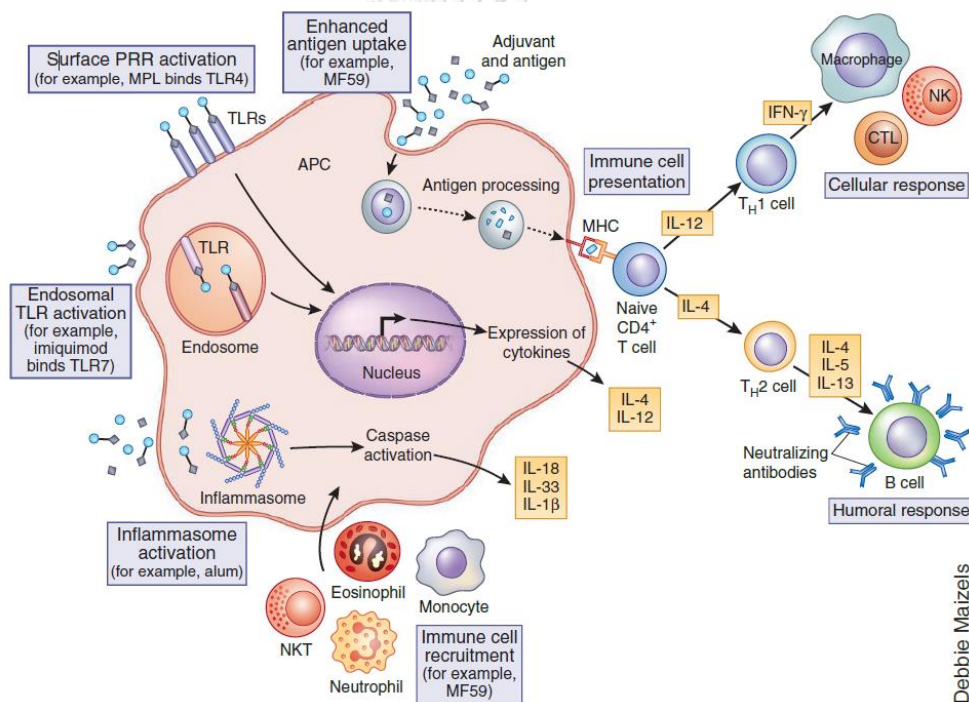
Figure 4 Proposed mechanisms of action of adjuvants.

Many mechanisms have been proposed through which adjuvants mediate their activity in the immune response. Some adjuvants can activate innate immunity by acting as ligands for pattern recognition receptors (PRRs). Then, transcription factors can be activated by receptor signaling. After that, cytokines and chemokines production have been induced that help through especially immune response, such as a Th1 or Th2 response, as well as impact the immune cells that are recruited to the site of injection. Some adjuvants have also been reported as associated activation of the inflammasome that leads to the production of proinflammatory cytokines.

Moreover, some adjuvants also influence antigen presentation by MHC. Many adjuvants can perform through multiple mechanisms (175).

Alum, aluminum salt-based, is well known as a generally used adjuvant in vaccines and has been used for many decades (176-178). Alum adjuvants are referred to as non-crystalline gels mostly based on hydroxide gel (aluminum oxy-hydroxide) or phosphate gel (aluminum hydroxyphosphate) (179). Aluminum in vaccine adjuvant plays an important role in absorbing negative net charge antigen with positive net charge aluminum particles. The action mechanism of alum adjuvant is proposed in 3 major ways, functioning by increasing the antigen recognition and uptake of antigen, recruits various types of immune cells, and promotes proinflammatory cytokines through cell signaling (175). Alum formulation vaccines show strongly stimulate Th2, which produce IL-4, IL-5, and IL-10, and induce adaptive immunity by Th2 cells helping follicular B cells (180, 181). Moreover, alum adjuvant also activates innate immunity through pattern recognition receptors (PRR) (182). The benefits of alum in vaccine adjuvants are included antibody responses induction, antigen stabilization, and safety profile (179).

4. Objectives of the Study

This study aimed to expand our horizon of the previous knowledge on plant-produced SARS-CoV-2 RBD-Fc vaccines, by investigating the immune response of low dose of our vaccines with three-dose regimen in cynomolgus monkeys. Further the ability of antibodies elicited by RBD-Fc vaccines to neutralize SARS-CoV-2 variants were also elucidated. In this study, plant-produced SARS-CoV-2 ancestral (Wuhan) RBD and SARS-CoV-2 variant RBD proteins, Alpha (N501Y, A570D, D614G), Beta (K417N, E484K, N501Y, D614G), Gamma (K417T, E484K, N501Y, D614G), Kappa (L452R, E484Q, D614G), Delta (L452R, T478K, D614G), and Epsilon (L452R, D614G), were fused with Fc region for subunit vaccine development. The *in vivo* immunogenicity of the low dose (10 µg) of plant-produced RBD-Fc, Baiya SARS-CoV-2 Vax 1, and variant vaccines were tested in cynomolgus macaques. Further, the ability of neutralizing against original SARS-CoV-2 (Wuhan) and its variants was also evaluated in these plant-produced vaccines.

CHAPTER II EXPERIMENTAL

1. Research framework

pBYR2eK-SARS-CoV-2 RBD-Fc

pBYR2eK-SARS-CoV-2 Alpha Beta RBD-Fc

A. tumefaciens GV3101 transformation

Gene construction (Gamma, Kappa, Delta, Epsilon RBD-Fc)
by site-directed mutation PCR

Transient expression in *N. benthamiana*
via Agrobacterium-infiltration

Ligation pBY2eK-SARS-CoV-2 Gamma, Kappa, Delta, Epsilon RBD-Fc

Protein purification
by protein A affinity chromatography

A. tumefaciens **GV3101 transformation**

Protein characterization
by SDS-PAGE, western blot, ELISA

Transient expression in *N. benthamiana*
via Agrobacterium-infiltration

Immunogenicity in monkeys
Including 2 groups (n=5)
G.1: 10 µg RBD-Fc + excipients + alum
G.2: excipients + alum (control)

Protein purification
by protein A affinity chromatography

RBD-specific total IgG titer by ELISA

Protein characterization
by SDS-PAGE, western blot, ELISA

Microneutralization assay using live virus *in vitro*

Immunogenicity in monkeys
Including 7 groups (n=5)
G.1: 10 µg Alpha RBD-Fc + excipients + alum
G.2: 10 µg Beta RBD-Fc + excipients + alum
G.3: 10 µg Gamma RBD-Fc + excipients + alum
G.4: 10 µg Kappa RBD-Fc + excipients + alum
G.5: 10 µg Delta RBD-Fc + excipients + alum
G.6: 10 µg Epsilon RBD-Fc + excipients + alum
G.7: excipients + alum (control, n=3)

Neutralization assay using pseudovirus *in vitro*

RBD-specific total IgG titer by ELISA

Microneutralization assay using live virus *in vitro*

Neutralization assay using pseudovirus *in vitro*

2. Equipment and chemicals

2.1 Equipment and machines

- 0.45 µm S-Pak membrane filters (Merck, USA)

- 0.22 µm polyethersulfone (PES) syringe filter (Merck, USA)

- Amicon® ultracentrifugal filter 50K (Merck, USA)

- High binding 96-well plate (Greiner Bio-one, Austria)

- 0.45 µm nitrocellulose membrane (Bio-rad, USA)

- T100™ Thermal Cycle (Bio-Rad, USA)

- Mini-PROTEAN® Tetra system (Bio-rad, USA)

- MicroPulser (Bio-Rad, USA)

- 1.5mL Graduated Microcentrifuge tube (Molecular BioProducts, USA)

- 1mL Pipet tips, blue (Molecular BioProducts, USA)

- 1-200 µl Pipet tips, yellow (Molecular BioProducts, USA)

- 0.1-20 µl Pipet tips (Molecular BioProducts, USA)

- Microplate incubator (Hercuvan Lab systems, Malaysia)

- Spectramax M5 microplate reader (Molecular Devices, USA)

2.2 Chemical reagents

Agarose (Vivantis, Malaysia), Ampicillin (ITW Reagents, Germany), Kanamycin (Bio Basic, Canada), Rifampicin (Thermo Fischer Scientific, USA), Gentamicin (ITW Reagents, Germany), 2-N-morpholino-ethanesulfonic acid (MES) (ITW Reagents, Germany), Magnesium Sulphate ($MgSO_4$) (Merck, USA), Tris (Vivantis, Malaysia), Glycine (Vivantis, Malaysia), Sucrose (Merck, USA), Enhanced Chemiluminescence (ECL) plus detection reagent (Abcam, UK), color reagent A (stabilized peroxide solution) and color reagent B (stabilized chromogen solution) (R&D Systems, USA), InstantBlue® coomassie protein stain (Abcam, UK), rProtein A Sepharose Fast Flow antibody purification resin (Cytiva, USA), Medical X-ray Green/MXG Flim (Carestream, China), β-mercaptoethanol (Merck, USA), Skim milk (BD Difco, USA), TMB stabilized substrate (Promega, USA), Sulfuric acid (H_2SO_4) (Merck,

USA), Alhydrogel® adjuvant 2% (Aluminium hydroxide gel) (Invivogen, USA), 1X Phosphate buffered saline (PBS) (Hyclone, USA)

2.3 Gene synthesized

- SARS-CoV-2 RBD gene (Accession No: YP_009724390.1, F318-C617) (GeneWiz, China)

- SARS-CoV-2 Alpha RBD gene (Accession No: QQX0 1934.1, F318-C617) (GeneWiz, China)

- SARS-CoV-2 Beta RBD gene (Accession No: QSH75306.1, F318-C617) (GeneWiz, China)

2.4 Enzymes

- *Bam*HI (New England Biolabs, USA).

- *Xba*I (New England Biolabs, USA)

- *Sac*I (New England Biolabs, USA).

- T4 DNA ligase (New England Biolabs, USA).

- Taq DNA polymerase (Vivantis, Malaysia)

- Q5 DNA polymerase (New England Biolabs, USA)

2.5 Cloning and Expression vector

- pGEMT-Easy Vector (Promega, USA) (Appendix A)

- pBYR2eK2Md Vector (Appendix B)

2.6 Molecular Biology kits

- AccuPrep Nano-Plus Plasmid Mini Extraction kit protocol (Bioneer, Korea)

- AccuPrep Gel Purification Kit (Bioneer, Korea)

2.7 Bacteria

- *Escherichia coli* strain DH10B

- *Agrobacterium tumefaciens* strain GV3101

2.8 Antibodies and recombinant protein

- Goat anti-human IgG-HRP (Southern Biotech, USA)

- Anti-SARS-CoV-2 RBD conjugated HRP (Sino Biological, China)

- Goat anti-monkey IgG HRP conjugated (Abcam, UK)

- SARS-CoV-2 Spike protein (RBD, His Tag) (GenScript, USA)

2.9 Buffer

2.9.1 Buffer for variant RBD-Fc purification

Extraction buffer & Washing buffer

137 mM Sodium chloride (NaCl), 2.7 mM Potassium Chloride (KCl), 8.1 mM Sodium hydrogen phosphate (Na2HPO4), 1.5 mM Potassium dihydrogen phosphate (KH2PO4) pH 7.4

Eluting buffer

0.1 M Glycine, pH 2.0-3.0

2.9.2 DNA loading 6x dye

38% (w/v) Glycerol, 0.08% (w/v) Bromophenol blue, 0.08% (w/v) Xylencyanol

2.9.3 Z-buffer non-reducing dye

125 mM Tris HCl, 12% Sodium Dodecyl Sulphate, 10% Glycerol, 0.001% Bromophenol blue pH 6.8

2.9.4 Z-buffer reducing dye

125 mM Tris HCl, 12% Sodium Dodecyl Sulphate, 10% Glycerol, 0.001% Bromophenol blue, 22% β-mercaptoethanol pH 6.8

2.9.5 1X Phosphate-buffered saline (PBS)

137 mM NaCl, 2.7 mM Potassium Chloride (KCl), 8.1 mM Sodium hydrogen phosphate (Na_2HPO_4), 1.5 mM Potassium dihydrogen phosphate (KH2PO4) pH 7.4

2.9.6 Phosphate-buffered saline-Tween (PBST)

1X PBS, 0.05% Tween 20

2.9.7 1X Running buffer (SDS-PAGE)

25 mM Tris, 192 mM Glycine, 1% SDS

2.9.8 1X Transfer buffer (Western blot)

25 mM Tris, 192 mM Glycine, 15% Methanol

2.9.9 1X Infiltration buffer

10 mM MES, 10mM MgSO4 pH 5.5

2.10 Media

2.10.1 Luria Bertani (LB) Broth

1% NaCl, 0.5% Yeast, 1% Peptone

2.10.1 Luria Bertani (LB) Agar

1% NaCl, 0.5% Yeast, 1% Peptone, 1.5% Agar

3. Methods

3.1 Construction of recombinant expression vector

For the construction of receptor-binding domain (RBD) genes, the SARS-CoV-2 Wuhan RBD sequence (Accession: YP_009724390.1, F318-C617) with 1XGGGGS linker containing *Xba*I and *Bam*HI restriction enzyme sites at 5' and 3', respectively, was codon-optimized and synthesized by Genewiz (China) as previously described (163). For SARS-CoV-2 variant RBD genes, the Wuhan RBD gene was used as a template to generate a series of RBD point mutations with the same amino acid sequence length. The construct of Alpha (N501Y, A570D, D614G) and Beta (K417N, E484K, N501Y, D614G) RBD genes with 1XGGGGS linker containing *Xba*I and *Bam*HI sites at 5' and 3', respectively, were codon-optimized and synthesized by Genewiz (China) as previously described (183). Then, the RBD-Fc genes were created by ligation at the 5' *Bam*HI site of the Fc region of human IgG1 (Accession: 4CDH_A, P35-K255) containing 2XGGGGS linker and 3' *Sac*I site by T4 DNA ligase (New England Biolabs, USA). After that, the RBD-Fc gene was ligated with *Xba*I and *Sac*I overhang of the recombinant bean yellow dwarf geminiviral plasmid pBYR2eK2Md (pBYR2eK) (157) by T4 DNA ligase. The ligation mixture was transformed into *Escherichia coli* strain DH10B competent cells by heat shock method. The cells were spread on selective Luria-Bertani (LB) agar plate containing 50 µg/mL kanamycin (ITW Reagents, Germany) and incubated at 37°C overnight. The selected colonies were picked from the plate for colony polymerase chain reaction (PCR) using *Xba*I-SP-F/Fc-KDEL-*Sac*I-R primers (Table 4). The confirmed colonies were inoculated into 50 µg/mL kanamycin in LB broth and incubated at 37°C overnight in a shaking incubator. The recombinant plasmids were extracted from

bacteria by following the protocol from DNA-spin™ Plasmid DNA Purification Kit (iNtRON Biotechnology, Korea) and stored at -20 °C.

For the other variant RBD genes, Gamma (K417T, E484K, N501Y, D614G), Kappa (L452R, E484Q, D614G), Delta (L452R, T478K, D614G), and Epsilon (L452R, D614G) RBD genes was constructed by site-directed mutation primers (Table 4) with PCR. Briefly, the Gamma RBD was constructed with K417T replacement by using *Xba*I-SP-F/K417T-R and K417T-F/D614G-R primers, and the Beta RBD-Fc gene as a template. The Epsilon RBD was generated L452R and D614G mutations by using SP-F/L452R-R and L452R-F/D614G-R primers, and the Wuhan RBD-Fc as a template. Epsilon RBD was used as the template for generating the Kappa RBD (E484Q) with SP-F/E484Q-R and E484Q-F/D614G-R primers, and the Delta RBD (T478K) with SP-F/T478K-R and T478K-F/D614G-R primers. Then, all new variant RBD genes was ligated with Fc region and pBYR2eK plasmid and then the recombinant plasmids were screened as above described. All recombinant pBYR2eK plasmids with variant RBD-Fc are shown in Figure 4. List of primers used in the study for the generation of variant RBD-Fc constructs are provided in Table 4.

Table 4 List of primers used in the study for the generation of variant RBD-Fc constructs. The underlined sequence showed the mutated region/sites.

Primer Name	Sequence (5'→3')
*Xba*I -SP-F	CCTCTAGAACAATGGGCTGG
*BamH*I-2XGGGGS-F	GGATCCGGAGGTGGAGGTTCTGGAGGTGGAGGTTCACCACCATGTCCAGCTCCAG
FC-KDEL- *Sac*I-R	GAGCTCTTAAAGCTCATCCTTCTCAGACTTGCCAGGGGACAAAGAAAGG
D614G-R	GGATCCACCACCACCAGAGATATCGCAGTTCAC<u>ACC</u>CTGGTAAAGAACTGCCACC
K417T-F	CCTGGTCAGACCGGA<u>ACC</u>ATCGCTGACTACAAC
K417T-R	GTTGTAGTCAGCGAT<u>GGT</u>TCCGGTCTGACCAGG
L452R-F	GCAATTACAACTAC<u>CGC</u>TACCGGCTGTTCCGGAAG
L452R-R	CTTCCGGAACAGCCGGTA<u>GCG</u>GTAGTTGTAATTGC
T478K-F	CTATCAGGCTGGTTCT<u>AAG</u>CCTTGCAACGGTGTT
T478K-R	AACACCGTTGCAAGG<u>CTT</u>AGAACCAGCCTGATAG
E484Q-F	CCCCTTGCAACGGTGTT<u>CAG</u>GGTTTCAACTGCTAC
E484Q-R	GTAGCAGTTGAAACC<u>CTG</u>AACACCGTTGCAAGGGG
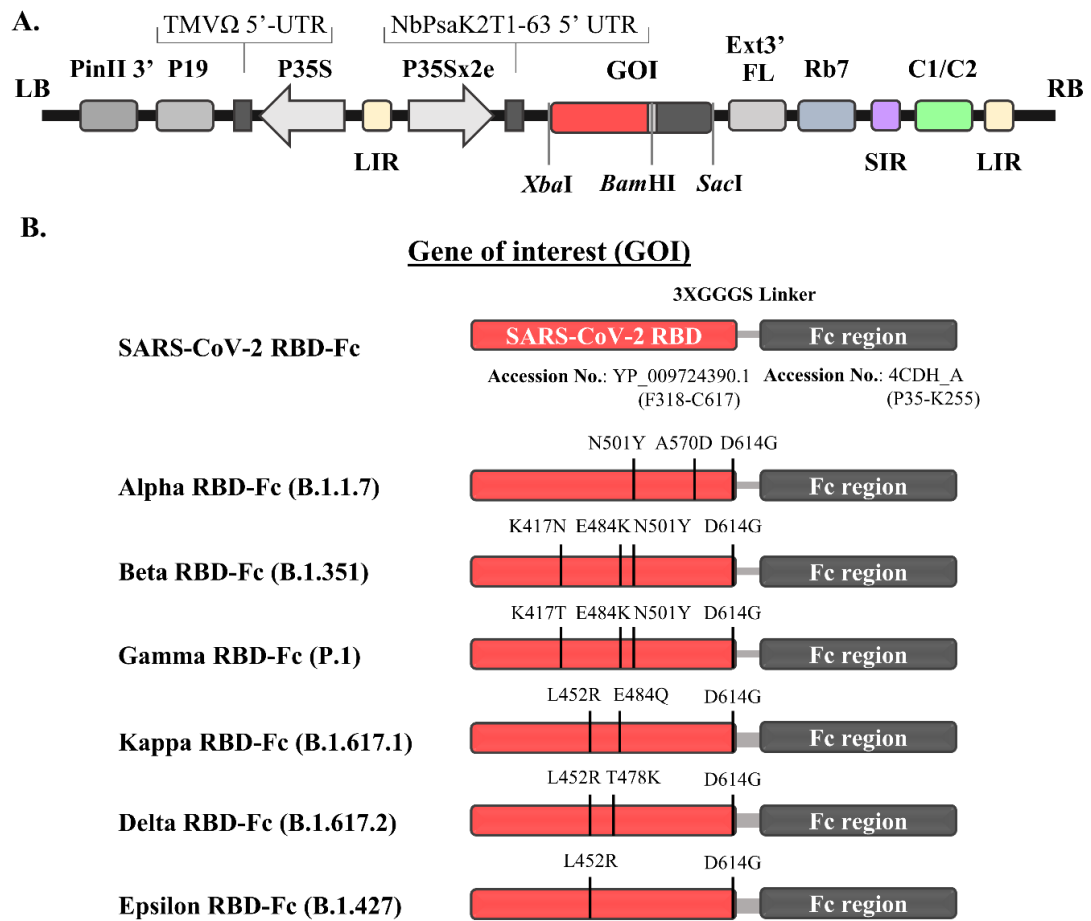
Figure 5 Schematic representation of geminiviral vector (pBYR2eK) T-DNA region of SARS-CoV-2 RBD-Fc and variant RBD-Fc fusion protein.

This vector was used for expression in N. benthamiana with gene of interest (GOI) (A). Illustration image of the SARS-CoV-2 RBD-Fc and variant RBD-Fc fusion proteins with the predicted mutation sites compared to the RBD of original strain (Wuhan) was indicated (B).

3.2 Genetic transformation into *Agrobacterium tumefaciens*

The recombinant SARS-CoV-2 RBD-Fc and variant RBD-Fc plasmids were transformed into *A. tumefaciens* GV3101 competent cells by electroporation by MicroPulser (Bio-Rad, USA). The transformed *A. tumefaciens* cells were spread on an LB RGK agar plate, containing 50 µg/mL kanamycin, 50 µg/mL rifampicin (Thermo Fischer Scientific, USA), and 50 µg/mL gentamicin (ITW Reagents, Germany), and

incubated at 28 °C for 24-48 h. The colonies on the plates were selected and verified by colony PCR for confirming the successful gene insertion. After that, the confirmed colonies were cultured at 28 °C for overnight in 5 mL LB RGK broth on the shaker at 250 rpm. Then, the bacteria were inoculated into 1:100 fresh LB RGK medium and propagated at 28 °C for overnight on the shaker at 250 rpm for plant infiltration.

3.3 Transient expression of recombinant proteins in *Nicotiana benthamiana*

Wild-type *N. benthamiana* plants were grown from seeds in the plant room with 28 °C and 16:8 light cycle for 4-5 weeks old. The healthy plants were used for *Agrobacterium* infiltration.

The cultured *Agrobacteria* was collected by centrifugation at 4,000 xg for 15 minutes at 4 °C. The cells were resuspended and diluted in the infiltration buffer, (10 mM 2-(N-morpholino)ethanesulfonic acid (MES) and 10 mM $MgSO_4$, pH 5.5, at the optimal density at 600 nm (OD_{600}) of 0.2 - 0.4 for infiltration. In the preliminary expression, the leaves were equally separated and infiltrated with *Agrobacteria* solution *via.,* syringe without a needle. For large-scale expression, the plants were infiltrated under vacuum condition by dipping the plant leaves in the *Agrobacteria* solution. Infiltrated leaves were harvested 2-6 days post infiltration (dpi) depending on the signal. After the infiltrated leaves have a signal, the leaves were harvested for the extraction or stored at -80°C for the long term.

3.4 Purification of recombinant proteins

The infiltrated leaves were minced in extraction buffer 1XPBS (phosphate-buffered saline; 137 mM NaCl, 2.68 mM KCl, 10.1 mM Na_2HPO_4, 1.76 mM KH_2PO_4, pH 7.4) using blender. After that, the minced solution was centrifuged at 12,000 xg at 4 °C for 1 hour. The supernatant was filtered using 0.45 μm membrane filters (Merck, Ireland) before purifying by protein A affinity chromatography (GE Healthcare, USA) as previously described (183). Briefly, the filtered solution was loaded into the gravity flow column containing protein A beads. Then, the beads were washed with 10 column

volume of 1XPBS pH 7.4. After that, the recombinant protein was eluted by 0.1 M glycine buffer pH 2 – 3 and immediately neutralized by 1.5 M Tris- HCl pH 8.8. The eluted protein was concentrated and buffer exchanged with 1XPBS by Amicon® ultracentrifugal filter (Merck, USA). The purified RBD-Fc protein was filtered by 0.22 µm polyethersulfone (PES) syringe filter (Merck, USA) and stored at -80 °C for further studies.

3.5 Protein characterization

The purified SARS-CoV-2 RBD-Fc and variant RBD-Fc proteins were analyzed both in reducing and non-reducing conditions by sodium dodecyl sulfate-polyacrylamide gel electrophoresis (SDS-PAGE) and confirmed by western blotting with goat anti-human IgG-HRP (Southern Biotech, USA), and anti-SARS-CoV-2 RBD conjugated HRP (Sino Biological, China). Briefly, the purified RBD-Fc was loaded into gradient 5-12 % SDS-polyacrylamide gel by using Mini-PROTEAN® Tetra system (Bio-rad, USA). The gel was stained by InstantBlue® coomassie protein stain (Abcam, UK). For western blotting, the gel was transferred to nitrocellulose membrane (Bio-rad, USA). Then, the transferred membrane was blocked with 5% w/v skim milk (BD Difco, USA) in 1XPBS. The membrane was probed with 1:10,000 of anti-human IgG-HRP or 1:4,000 of anti-SARS-CoV-2 RBD conjugated HRP diluted in 3% w/v skim milk in 1XPBS. The membrane was washed by 1XPBST (1XPBS plus 0.05% Tween-20) three times between each step. After that, the membrane was developed by enhanced chemiluminescent (ECL) (Promega, USA) following manufacturer's instruction.

The concentration of each recombinant RBD-Fc was determined by direct ELISA with anti-human IgG-HRP detection and human IgG (Abcam, UK) as standard as previously described (163). Briefly, high binding 96-well plate (Greiner Bio-one, Austria) was coated with two-fold serial dilution of human IgG standard from 1000 ng/mL to 31.25 ng/mL or RBD-Fc with estimate dilutions and incubated at 4 °C for overnight. Then, plate was blocked with 5% w/v in 1XPBS and incubated at 37 °C for 3 hours. After that, 1:2,000 of anti-human IgG-HRP in 1XPBS was added and incubated at 37 °C for 1 hour. The plate was washed by 1XPBST three times between each step. Then,

TMB solution (Promega, US) was added as substrate of colorimetric reaction. Finally, 1M H_2SO_4 was added to stop the reaction. The absorbance at 450 nm (A_{450}) was measured using SpectraMax® M3 Microplate Reader (Molecular Devices, USA) and calculated the concentration of recombinant RBD-Fc with human IgG standard curve.

3.6 Vaccine formulation

The dose of 10 µg purified plant-produced SARS-CoV-2 RBD-Fc and variant RBD-Fc formulated with 0.5 mg/dose of aluminum (Al) content of Alhydrogel® adjuvant 2% (InvivoGen, France), aluminum hydroxide (alum), containing 5% w/v sucrose (Merck, Germany) and 3% w/v glycine (Vivantis technologies, Malaysia) as excipients in 1XPBS pH 7.0-7.2 (HyClone™, USA). The alum containing excipients in 1XPBS without plant-produced RBD-Fc was used as control. A total volume of 0.5 ml was injected intramuscularly in the quadricep femoris muscle of monkeys.

3.7 Monkey immunization

The monkey immunization studies were performed in the National Primate Research Center of Thailand-Chulalongkorn University (NPRCT-CU; AAALAC International Accredited facility). The cynomolgus monkeys (*Macaca fascicularis*) originated from Thailand was supplied by the NPRCT-CU breeding facility. The specific pathogen free (SPF) animals free from tuberculosis, B virus, SRV, SIV, STLV and SARS-CoV-2 was used. The anesthesia was used during vaccine administration and blood collection. The animal use and the experimental procedures have been approved by the NPRCT-CU Animal Care and Use Committee (Protocol review no. 2075015, 2175005, and 2175007).

In plant-produced SARS-CoV-2 RBD-Fc vaccine, ten female monkeys were randomly divided into two groups (*n*=5). The 10-µg dose of plant-produced RBD-Fc vaccine and control groups were intramuscularly injected with 0.5 mL dose of either vaccine or adjuvant alone on days 0, 21 and 133 for investigating the 2nd-booster dose efficacy (Figure 5A). The blood samples were collected on day 0 (before the first

injection) and day 133 (before the third injection), and day 14, 35, and 147 (14 days after each immunization).

In plant-produced variant (Alpha, Beta, Gamma, Kappa, Delta, and Epsilon) RBD-Fc vaccines, thirty-three male and female monkeys were randomly divided into seven groups. The 10-μg dose of plant-produced variant RBD-Fc vaccines (*n*=5) and control groups (*n*=3) were intramuscularly injected with 0.5 mL dose of vaccines or adjuvant alone on days 0, 21 and 42 for investigating the efficacy of variant vaccines (Figure 5B). The blood samples were collected on day 0 (before the first injection), and day 14, 35, and 56 (14 days after each immunization).

The immunized monkey sera were used to assess the RBD-specific antibody titer, live virus neutralizing antibody, and for pseudovirus neutralization antibody titers.
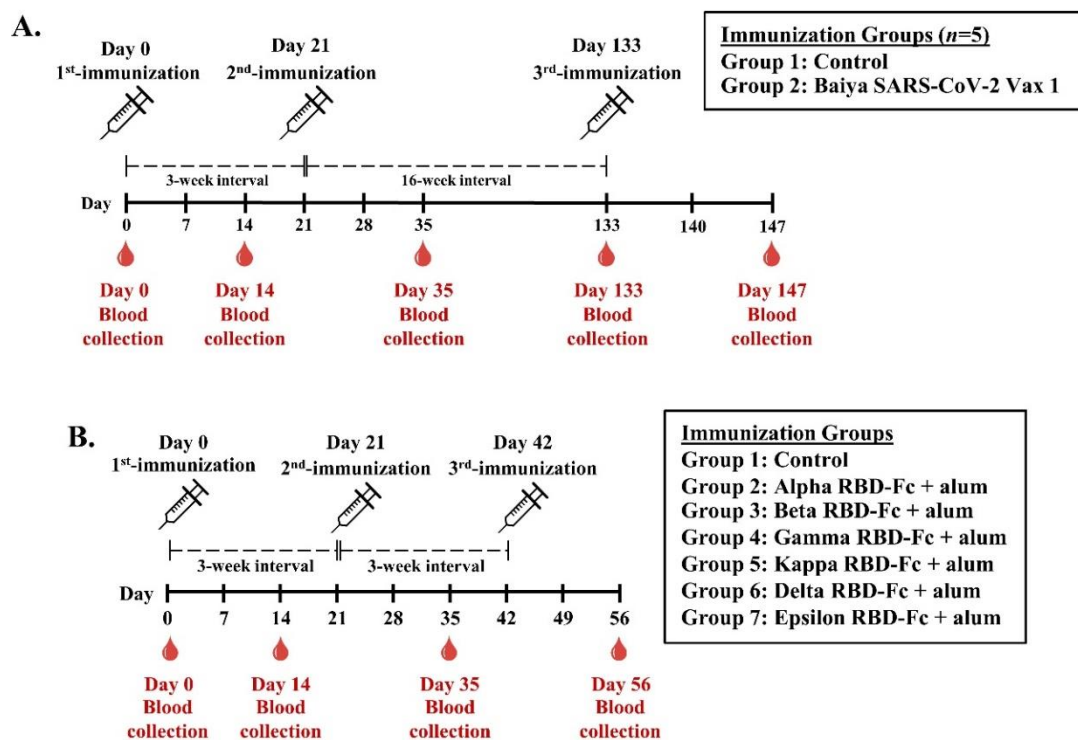
Figure 6 The immunization and blood collection schedules of plant-produced variant RBD-Fc vaccines in monkeys.

The 10 monkeys were separated into Baiya SARS-CoV-2 Vax 1 and control, n=5, and immunized on day 0, 21, and 133 (A). The 33 monkeys were separated into 7 groups, variant RBD-Fc vaccines, n=5, and control, n=3, and immunized on day 0, 21, and 35 (B). Blood was collected on day 0 and every 14 days after immunization.

3.8 RBD-specific total IgG titer by ELISA

SARS-CoV-2 spike RBD-His protein (Cat. No. Z03479; GenScript, USA) at 2 µg/mL 50 µL/well (100 ng/well) was coated on high binding 96-well plate (Greiner Bio-One, Austria) and incubated for overnight at 4°C. Subsequently, the wells were blocked with 200 µL 5% w/v skim milk in 1XPBS pH 7.4 for 2 hours at 37°C. Then, the monkey sera were prediluted by starting at 1:100 with 2-fold serial dilutions in 1XPBS. The diluted sera were loaded in each well as duplicates and incubated for 2 hours at 37°C. After that, 1:2,000 of goat anti-monkey IgG HRP conjugated (Abcam, UK) in 1XPBS was added and incubated for 2 hours at 37°C. TMB was added as a substrate for detection to the plates, and then 1M H_2SO_4 was added to stop the reactions. The absorbance at 450 nm (A_{450}) was measured by microplate reader. The plates were washed three times by 1XPBST between each step. The endpoint titers were determined as the highest dilution of immunized sera, which has A_{450} more than the cut-off value calculated from A_{450} of pre-immunized sera (Day 0) at 1:100 dilution as previous described (184). The data were plotted as a geometric mean titer (GMT) with ± 95% confidence interval (CI) by GraphPad Prism software version 9.0 (GraphPad Software, USA). Statistical significance was calculated by two-way analysis of variance (ANOVA). The *p*-value < 0.05 considered statistically significant.

3.9 Live-virus microneutralization

Microneutralization assay was performed in 96-well microplates containing confluent Vero E6 cell line and live SARS-CoV-2 viruses isolated from a COVID-19 patient as shown in Table 5. The experiment was conducted in a certified biosafety level (BSL) 3 facility of Microbiology Department, Faculty of Science, Mahidol University, Thailand, as previously described (163, 185).

Table 5 List of strain and isolate of live SARS-CoV-2 viruses used in the

microneutralization assay.

Strain name	Isolate name	Provided from
Wuhan	SARS-CoV-2/human/ THA/LJ07_P3/2020	Bamrasnaradura Infectious Diseases Institute, Nonthaburi, Thailand.
Alpha (B.1.1.7)	SARS-CoV-2/human/ THA/NH657_P3/2021	Ramathibodi Chakri Naruebodindra Hospital, (Chakri Naruebodindra Medical Institute), Samut Prakan, Thailand
Beta (B.1.351)	SARS-CoV-2/human/ THA/NH088_P3/2021	Division of Genomic Medicine and Innovation Support, Department of Medical Sciences, Ministry of Public Health, Nonthaburi, Thailand
Delta (B.1.617.2)	SARS-CoV2/human/ THA/OTV007_P3/2021	Ramathibodi Chakri Naruebodindra Hospital, (Chakri Naruebodindra Medical Institute), Samut Prakan, Thailand

Briefly, immunized monkey sera and the convalescent serum from COVID-19 patients (positive control) was heat-inactivated at 56°C for 30 minutes. Two-fold serial dilution of sera was mixed with 100 of 50% tissue culture infective dose ($TCID_{50}$) of SARS-CoV-2 variant in Dulbecco's Modified Eagle Medium (DMEM) at 37°C for 1 hour. Each sample was prepared in duplicates. The control virus and cell wells were included in each plate. Next, Vero cell monolayer wells were added by the mixture and incubated at 37°C for 2 days. Then, the cells were washed with 1XPBS, fixed, and permeabilized with cold fixative solution (1:1 methanol/acetone) at 4°C for 20 minutes. The plates were washed three times with 1XPBST and blocked with 2% BSA at room temperature (RT) for 1 hour. The 1:5,000 of anti-SARS-CoV/SARS-CoV-2 nucleocapsid (N) monoclonal antibody (Sino Biological, China) in 1XPBS was added as a primary antibody for detecting viral infection and incubated at 37°C for 1 hour. Then, 1:2,000 of goat anti-rabbit polyclonal antibodies conjugated HRP (Dako, Denmark) in 1XPBS was added as a secondary antibody and incubated at 37°C for 1 hour. The TMB substrate (KPL Sureblue™ TMB, SeraCare, USA) was added followed by 1N HCl was added to stop the reaction. The A_{450} was measured using a Sunrise™ microplate reader (Tecan, Männedorf, Switzerland). The ΔA_{450} of samples was equated to the 50% of the

cut point value, which was calculated as previously mentioned (186). The data was presented as GMT ± 95% CI by GraphPad Prism software version 9.0. Statistical significance was calculated by two-way analysis of variance (ANOVA). The *p*-value < 0.05 considered statistically significant.

3.10 Psudovirus neutralization

Pseudovirus neutralization will be performed at Virology and Cell Technology Laboratory, National Center for Genetic Engineering and Biotechnology (BIOTEC), Thailand.

Lentiviral pseudoviruses presenting CoV spike was constructed as previously mentioned (187) with some changes. Briefly, the mixture of plasmids including pCSFLW (provided by Dr. Nigel Temperton); the lentivirus backbone expressing a firefly luciferase reporter gene, pCMVΔR8.91; the expression plasmid expressing HIV-1 structural/regulatory proteins, and pCAGGS; the expression plasmid expressing the codon-optimized spike genes (Wuhan, Alpha, Beta, Gamma, and Delta variants) will be used to produce pseudoviruses. Then, HEK293T/17 producer cells were seeded in 6-well plates at 7.5×10^5/well for 24 hours After that, the cells were transfected with the 600 ng pCMVΔR8.91, 600 ng pCSFLW, and 500 ng of pCAGGS-Spike, in OptiMEM (Gibco, USA) containing 10 µL of polyethyleneimine (PEI). The transfected cells were incubated at 37 °C, 5% CO_2 for 12 hours. Next, the cells were washed and cultured in DMEM containing 10% fetal bovine serum (FBS) (DMEM-10%). After 72 hours of transfection, the supernatants of pooled harvests containing pseudoviruses were collected by centrifuged at 1,500 × g for 10 minutes at 4°C to eliminate the cellular debris, and stored at -80 °C.

For pseudovirus titrations, HEK 293T/17-ACE2 cells were transfected with the expression plasmid encoding for human TMPRSS2 using Fugene HD (Promega, USA). After 24 hours of transfection, the supernatants were changed by DMEM-10%. Then, the transfected cells were used as pseudovirus infection targets. The mixtures containing pseudoviruses were serially two-fold diluted in a DMEM and loaded into 96-well plate. Next, HEK 293T/17-ACE2 expressing TMPRSS2 cells were added to each well

at 1×10^4 cells/well and incubated for 72 hours. Subsequently, the luminescence of cell cultures was evaluated in Relative Luminescence Units (RLUs) by Synergy Plate Reader luminometry (Agilent, USA) using the Bright-Glo™ Luciferase Assay System (Promega, Italy). will be evaluated

In the neutralizing activity measurement, the sample sera were heat-inactivated and prepared serially 2-fold dilution in high glucose DMEM. The sera were preincubated with pseudoviruses presenting spike variant of interest (1×10^5 RLU/well) in a 1:1 v/v ratio in a 96-well plate and incubated for 1 hour at 37 °C. Then, HEK293T-ACE-2 expressing human TMPRSS2 (2×10^4 cell/mL) cell suspensions were combined with the pre-inucubated serum-pseudovirus. After that, the mixture will be added into each well of CulturPlate™ Microplates (PerkinElmer, USA) and incubated at 37 °C for 48 hours. The neutralizing antibodies were evaluated by luciferase activity as previously described (188). The data was presented as GMT ± 95% CI by GraphPad Prism software version 9.0. Statistical significance was calculated by two-way analysis of variance (ANOVA). The p-value < 0.05 was considered statistically significant.

CHAPTER IV RESULTS

1. Construction of recombinant variant RBD-Fc gene construct

Previously, recombinant pBYR2eK vectors containing Wuhan RBD-Fc, Alpha RBD-Fc, and Beta RBD-Fc were cloned as previously described (163, 183). These recombinant vectors were confirmed by cleaved at *Xba*I and *Sac*I sites (Figure 6) before being used as templates for generation of other variant RBD genes.
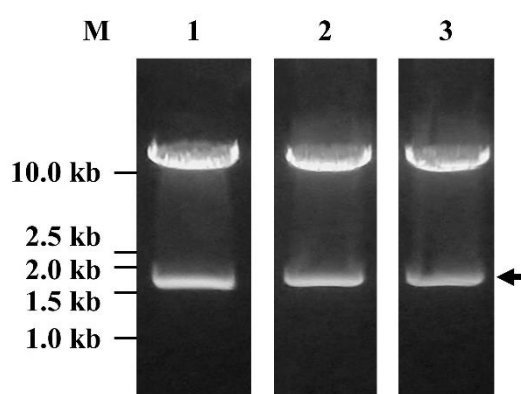
Figure 7 The confirmation of restriction enzyme cleavage of pBYR2eK Wuhan RBD-Fc, Alpha RBD-Fc, and Beta RBD-Fc constructs.

The recombinant pBYR2eK vectors were cleaved by XbaI and SacI enzymes. Lane M: VC 1kb DNA Ladder; Lane 1: Wuhan-RBD-Fc; Lane 2: Alpha-RBD-Fc; Lane 3: Beta-RBD-Fc. Arrow mark indicated the expected band.

Then, the variant RBD genes were constructed by PCR site-directed mutagenesis. In the first step (Figure 7A), pBYR2eK Beta RBD-Fc was used as the template with K417T replacement by using *Xba*I-SP-F/K417T-R primers to generate left-handed (400 bp) and K417T-F/D614G-R primers to generate right-handed (682 bp) Gamma RBD gene. Next, pBYR2eK Wuhan RBD-Fc was used as the template with L452R and D614G replacements by using SP-F/L452R-R to generate left-handed (508 bp) and L452R-F/D614G-R primers to generate right-handed the Epsilon RBD (536 bp). After that, the Epsilon RBD gene was used as the template with E484Q replacement with SP-F/E484Q-R to generate left-handed (601 bp) and E484Q-F/D614G-R primers to generate right-handed Kappa RBD (443 bp), and with T478K replacement with SP-F/T478K-R to generate left-handed (583 bp) and T478K-F/D614G-R primers to generate right-handed

Delta RBD (460 bp). Subsequently, each left-handed and right-handed fragments of each variant RBD were annealed by PCR and the expected products were observed at 1,010 bp (Figure 7B).
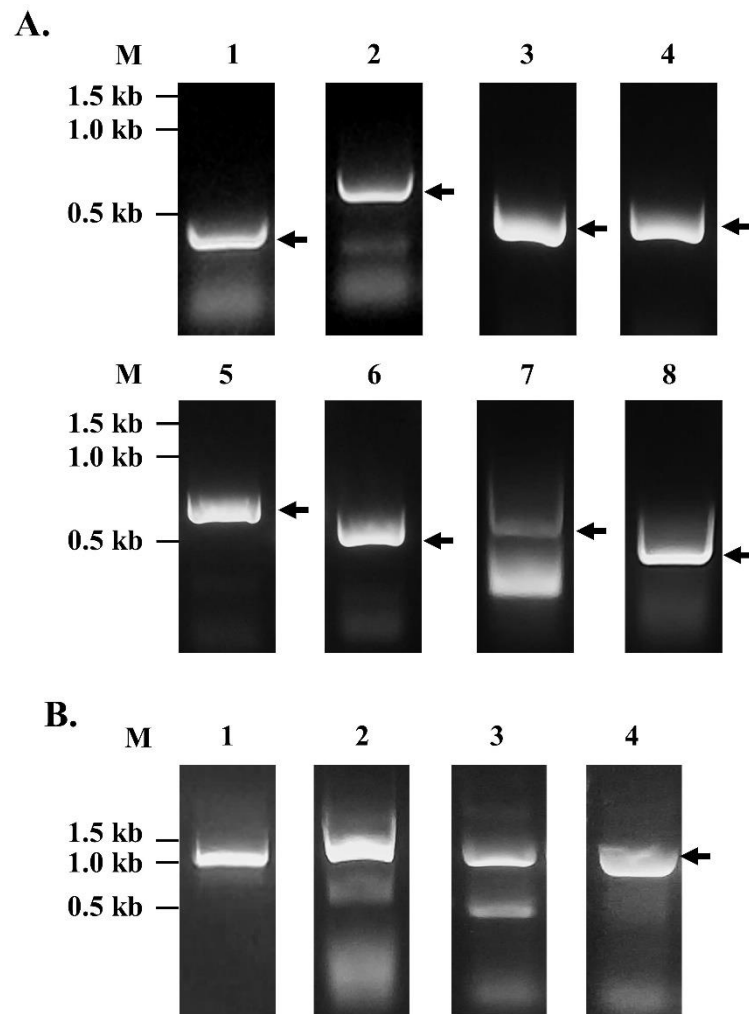
Figure 8 Site-directed mutagenesis of Gamma RBD, Epsilon RBD, Kappa RBD, and Delta RBD constructs by PCR.

Mutagenesis step of RBD genes were amplified by specific primer pairs (A). Lane M: VC 1kb DNA Ladder; Lane 1: Left-handed Gamma RBD; Lane 2: Right-handed Gamma RBD; Lane 3: Left-handed Epsilon RBD Lane 4: Right-handed Epsilon RBD; Lane 5: Left-handed Kappa RBD Lane 6: Right-handed Kappa RBD; Lane 7: Left-handed Delta RBD Lane 8: Right-handed Delta RBD. The annealing step of RBD genes were annealed and amplified by XbaI-SP-F/D614G-R primers (B). Lane M: VC 1kb DNA Ladder; Lane 1:

Gamma RBD; Lane 2: Epsilon RBD; Lane 3: Kappa RBD; Lane 4: Delta RBD. Arrow mark indicated the expected band.

Then, variant RBD genes were purified from agarose gel and ligated into pGem®-T Easy vector (Promega, USA). After that, *E. coli* strain DH10B competent cell was transformed with each ligation mixture of variant RBD gene by heat-shock and was screened by blue-white colony screening technique. The white colonies were amplified by PCR with *Xba*I-SP-F/D614G-R primers and the expected products were observed at around 1,010 bp (Figure 8).
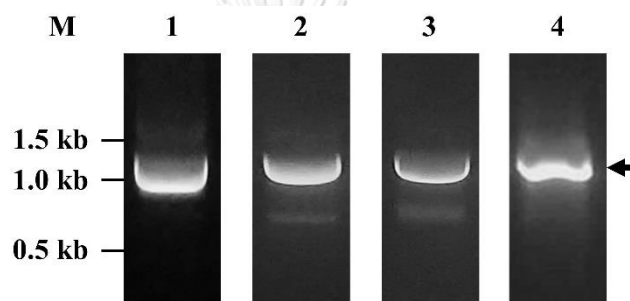
Figure 9 Screening of E. coli transformed recombinant pGEM®-T Easy Gamma RBD, Epsilon RBD, Kappa RBD, and Delta RBD constructs by PCR.

The transformed E. coli DH10B were amplified by XbaI-SP-F/D614G-R primers. Lane M: VC 1kb DNA Ladder; Lane 1: Gamma RBD; Lane 2: Epsilon RBD; Lane 3: Kappa RBD; Lane 4: Delta RBD. Arrow indicated the expected band.

The selected *E. coli* colonies containing the variant RBD gene were cultured and the plasmids were isolated. Then, the recombinant pGEM®-T Easy variant RBD genes, 2XGGGGS-Fc, and pBYR2eK vector were cleaved at *Xba*I-*Bam*HI, *Bam*HI-*Sac*I, and *Xba*I-*Sac*I sites, respectively (Figure 9). The expected bands were eluted from the gel and purified.
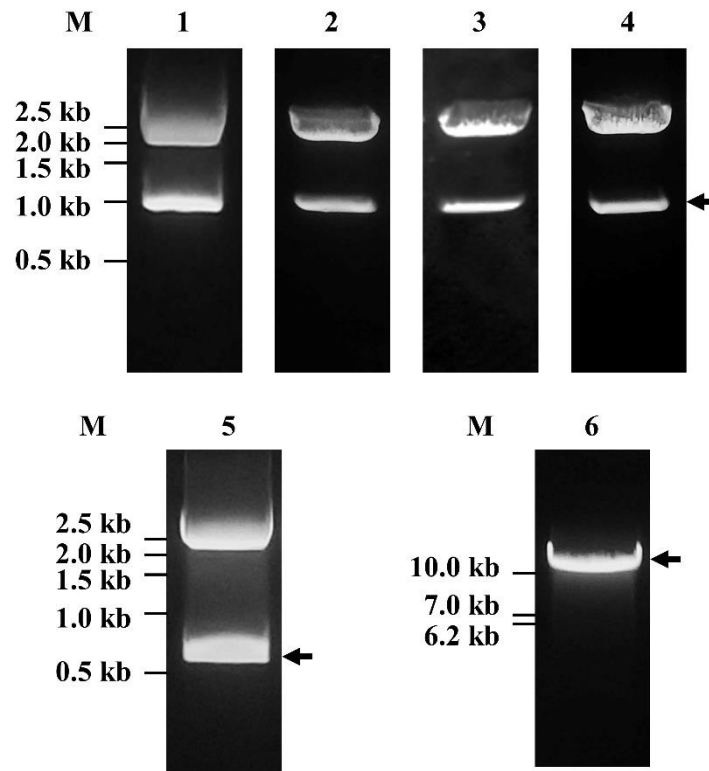
Figure 10 The restriction enzyme cleavage of recombinant pGEM®-T Easy-Gamma RBD, Epsilon RBD, Kappa RBD, Delta RBD, and 2XGGGGS-Fc, and pBYR2eK.
The recombinant pGEM®-T Easy variant RBD, 2XGGGGS-Fc, and pBYR2eK were cleaved by XbaI-BamHI, BamHI-SacI, and XbaI-SacI, respectively. Lane M: VC 1kb DNA Ladder; Lane 1: Gamma RBD; Lane 2: Epsilon RBD; Lane 3: Kappa RBD; Lane 4: Delta RBD; Lane 5: 2XGGGGS-Fc; Lane 6: pBYR2eK vector. Arrow mark indicated the expected band.

Then, the cleaved variant RBD, linker-Fc, and pBYR2eK were ligated with T4 DNA ligase overnight. After that, *E. coli* DH10B competent cell was transformed with each ligation mixture and was cultured in kanamycin selective LB agar. The positive colonies were screened by PCR with *Xba*I-SP-F/FC-KDEL-*Sac*I-R primers and the expected band was observed around 1,730 bp (Figure 10).
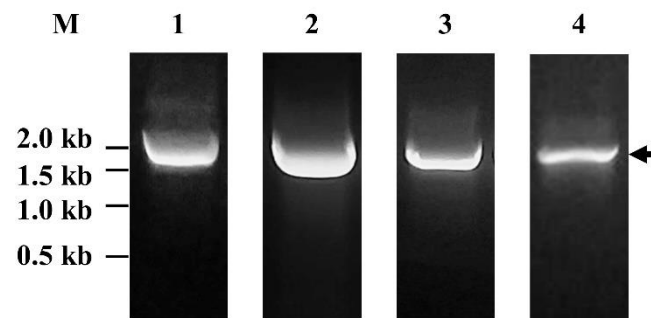
Figure 11 Screening of E. coli colony transformed with recombinant pBYR2eK Gamma

RBD-Fc, Epsilon RBD-Fc, Kappa RBD-Fc, and Delta RBD-Fc constructs by PCR.

The transformed E. coli DH10B were amplified by XbaI-SP-F/FC-KDEL-SacI-R primers.

Lane M: VC 1kb DNA Ladder; Lane 1: Gamma RBD-Fc; Lane 2: Epsilon RBD-Fc; Lane 3:

Kappa RBD-Fc; Lane 4: Delta RBD-Fc. Arrow mark indicated the expected band.

The positive variant RBD-Fc colonies were further cultured in kanamycin LB broth and then recombinant vectors were isolated. The recombinant pBYR2eK vectors were confirmed by cleaved at *Xba*I and *Sac*I enzymes with the expected size 1,726 bp of variant RBD-Fc genes and 12,446 bp of pBYR2eK vector (Figure 11).
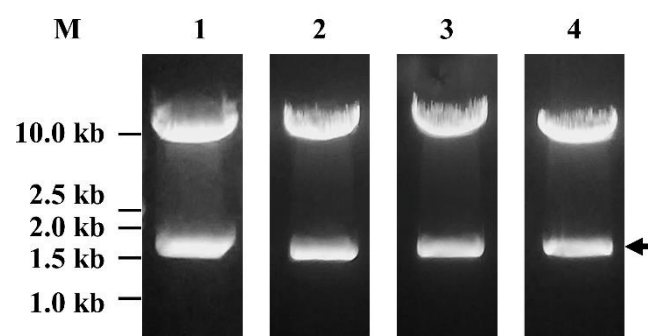
Figure 12 The confirmation of restriction enzyme cleavage of recombinant pBYR2eK

Gamma RBD-Fc, Epsilon RBD-Fc, Kappa RBD-Fc, and Delta RBD-Fc.

The recombinant pBYR2eK variant RBD-Fc were cleaved by XbaI-SacI. Lane M: VC 1kb

DNA Ladder; Lane 1: Gamma RBD-Fc; Lane 2: Epsilon RBD-Fc; Lane 3: Kappa RBD-Fc;

Lane 4: Delta RBD-Fc. Arrow mark indicated the expected band.

The confirmed recombinant pBYR2eK variant RBD-Fc vectors were transformed into *A. tumefaciens* strain GV3101 *via.,* electroporation. Next, the transformed *A. tumefaciens* was cultured in a selective LB RGK agar plate. The positive colonies were screened by colony PCR with *Xba*I-SP-F/FC-KDEL-*Sac*I-R primers (Figure 12). The recombinant *A. tumefaciens* containing pBYR2eK variant RBD-Fc were used for expressing recombinant RBD-Fc proteins in *N. benthamina.*
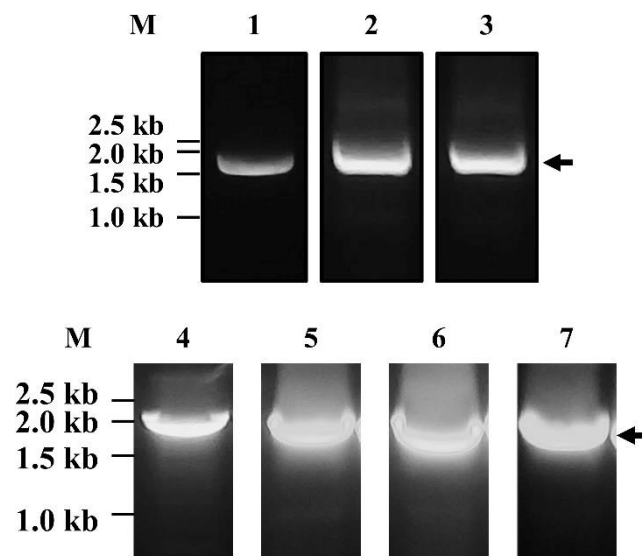
Figure 13 Screening of A. tumefaciens transformed with recombinant pBYR2eK RBD-Fc constructs by PCR.

The transformed A. tumefaciens GV3101 were amplified by XbaI-SP-F/FC-KDEL-SacI-R primers. Lane M: VC 1kb DNA Ladder; Lane 1: Wuhan RBD-Fc; Lane 2: Alpha RBD-Fc; Lane 3: Beta RBD-Fc; Lane 4: Gamma RBD-Fc; Lane 5: Epsilon RBD-Fc; Lane 6: Kappa RBD-Fc; Lane 7: Delta RBD-Fc. Arrow indicated the expected band.

2. Expression of RBD-Fc proteins in *N. benthamiana*

N. benthamiana plants (4-5 weeks old) were used to express the recombinant variant RBD-Fc proteins. In the preliminary expression analysis, *A. tumefaciens* transformed recombinant pBYR2eK RBD-Fc was cultured in LB RGK broth overnight. After that, bacterial cells were collected by centrifugation and resuspended in infiltration buffer (10 mM MES, 10 mM MgSO4, pH 5.5) at OD_{600} of 0.3-0.4. The plant

leaf was infiltrated by each *Agrobacterium* clone of variant RBD-Fc solution. After 3 dpi, the infiltrated leaf was harvested and extracted the crude extract for confirming the expression by western blot with goat anti-human IgG-HRP, specific to the Fc region. The crude extract from each clone of variant RBD-Fc was successfully expressed in *N. benthamiana* with the major band around 150 kDa under non-reducing conditions was observed, but not found any signal from wild type leaf (Figure 13).
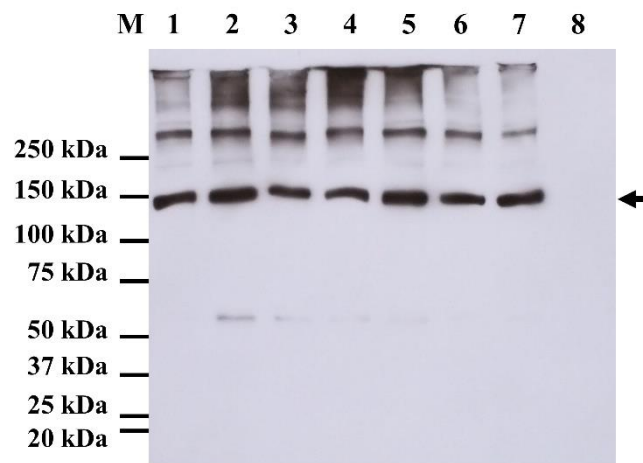
Figure 14 Confirmation preliminary expression of variant RBD-Fc proteins expressed from N. benthamiana by western blot.

The crude extraction of infiltrated leaves of variant RBD-Fc proteins were detected by goat anti-human IgG-HRP under non-reducing condition. Lane M: All Blue Prestained Protein Standard; Lane 1: Wuhan RBD-Fc; Lane 2: Alpha RBD-Fc; Lane 3: Beta RBD-Fc; Lane 4: Gamma RBD-Fc; Lane 5: Kappa RBD-Fc; Lane 6: Delta RBD-Fc; Lane 7: Epsilon RBD-Fc; Lane 8: Wild-type. Arrow mark indicated the expected band.

Further, each variant RBD-Fc clone was optimized for the highest expression level in each timepoint 3-5 dpi, based on the signal on the leaf or necrosis sign. After that, the infiltrated leaves were extracted for crude, and then, detected the expression by western blot with goat anti-human IgG-HRP. The recombinant variant RBD-Fc proteins demonstrated the highest expression level on 3 dpi, except Wuhan RBD-Fc which showed the highest expression level on 4 dpi (Figure 14)
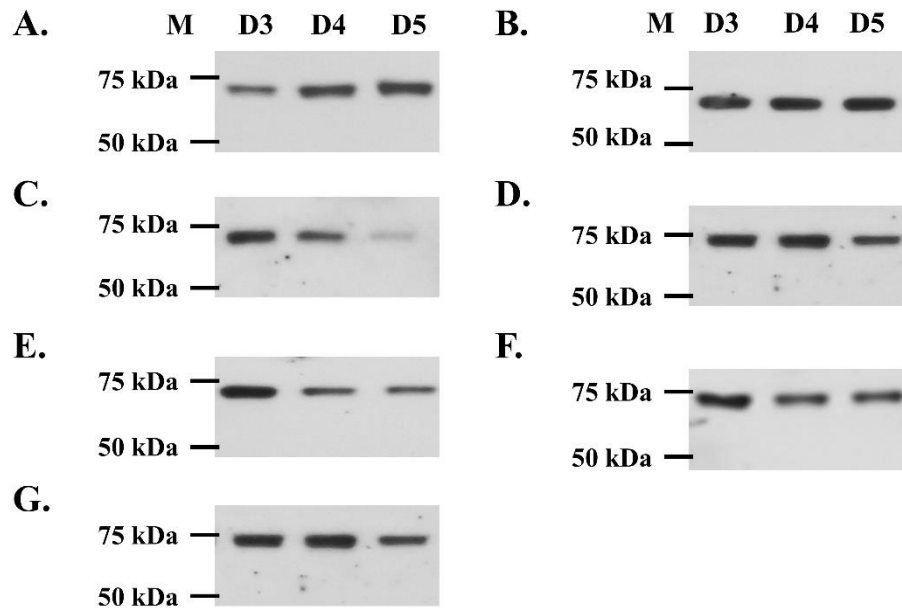
Figure 15 Day-optimized expression of variant RBD-Fc proteins expressed from N. benthamiana by western blot.

The crude extraction of infiltrated leaves of Wuhan RBD-Fc (A), Alpha RBD-Fc (B), Beta RBD-Fc (C), Gamma RBD-Fc (D), Kappa RBD-Fc (E), Delta RBD-Fc (F), and Epsilon RBD-Fc (G) were detected by goat anti-human IgG-HRP under reducing condition. Lane M: All Blue Prestained Protein Standards; Lane D3: 3 dpi; Lane D4: 4 dpi; Lane D5: 5 dpi. Arrow mark indicated the expected band.

For large-scale expression, 20-30 plants were used for expressing each recombinant variant RBD-Fc proteins by agroinfiltration under vacuum conditions. After 3 or 4 dpi, the leaves were harvested with an estimated yield of around 40-60 g fresh weight and purified by protein A chromatography. All variant RBD-Fc proteins were successfully purified and demonstrated the major band around 150 kDa in an eluted fraction under non-reducing conditions by SDS-PAGE (Figure 15).
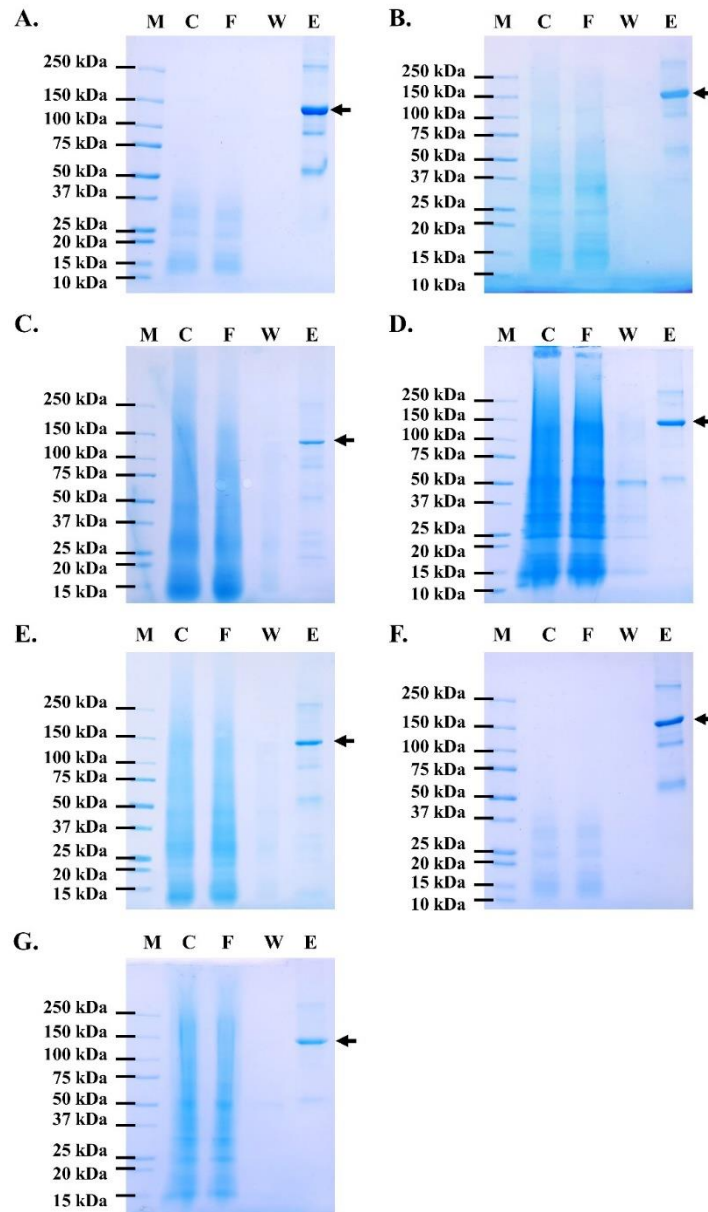
Figure 16 Purification profile of variant RBD-Fc proteins expressed from N. benthamiana by SDS-PAGE.

The crude extraction of Wuhan RBD-Fc (A), Alpha RBD-Fc (B), Beta RBD-Fc (C), Gamma RBD-Fc (D), Kappa RBD-Fc (E), Delta RBD-Fc (F), and Epsilon RBD-Fc (G) were purified by protein A chromatography and analyzed by SDS-PAGE under non-reducing condition. Lane M: All Blue Prestained Protein Standards; Lane C: Crude fraction; Lane F: Flow-through fraction; Lane W: Washed fraction; Lane E: Eluted fraction. Arrow mark indicated the expected band.

Next, the purified RBD-Fc proteins were concentrated and exchanged buffer with 1XPBS (Hyclone) by a centrifugal filter. After that, all recombinant variants RBD-Fc were filtered by 0.22 μm PES syringe filter. Then, the concentration of all proteins were measured by direct ELISA. The final concentration of Wuhan RBD-Fc, Alpha RBD-Fc, Beta RBD-Fc, Gamma RBD-Fc, Kappa RBD-Fc, Delta RBD-Fc, and Epsilon RBD-Fc were 2.0, 1.9, 2.0, 1.8, 2.1, 2.0, and 1.4 mg/mL, respectively, with yield 25.3, 23.8, 23.3, 21.9, 26.4, 28.0, and 20.0 μg/g fresh weight, respectively (Appendix D). Furthermore, the purified variant RBD-Fc proteins were characterized by SDS-PAGE and western blot. The results as presented in Figure 16 showed that all variants RBD-Fc were demonstrated the major around 150 kDa and 75 kDa under non-reducing and reducing conditions, respectively. Moreover, the western blot result of variants RBD-Fc also revealed the major around 150 kDa under non-reducing conditions in both detected with anti-human IgG-HRP and anti-SARS-CoV-2 RBD conjugated HRP.
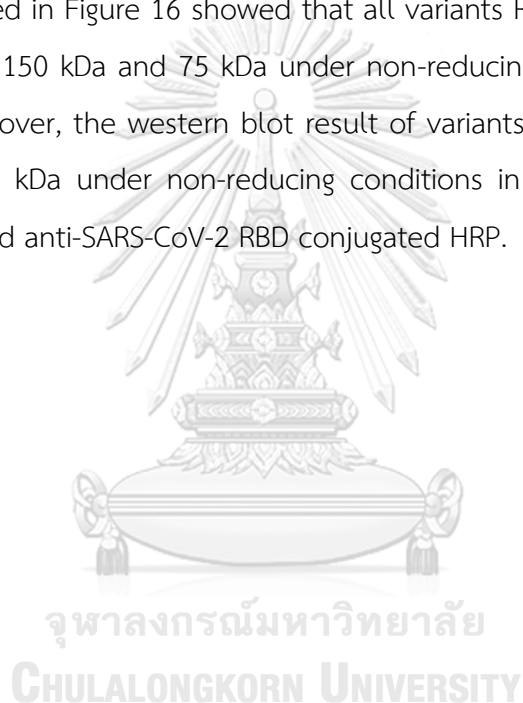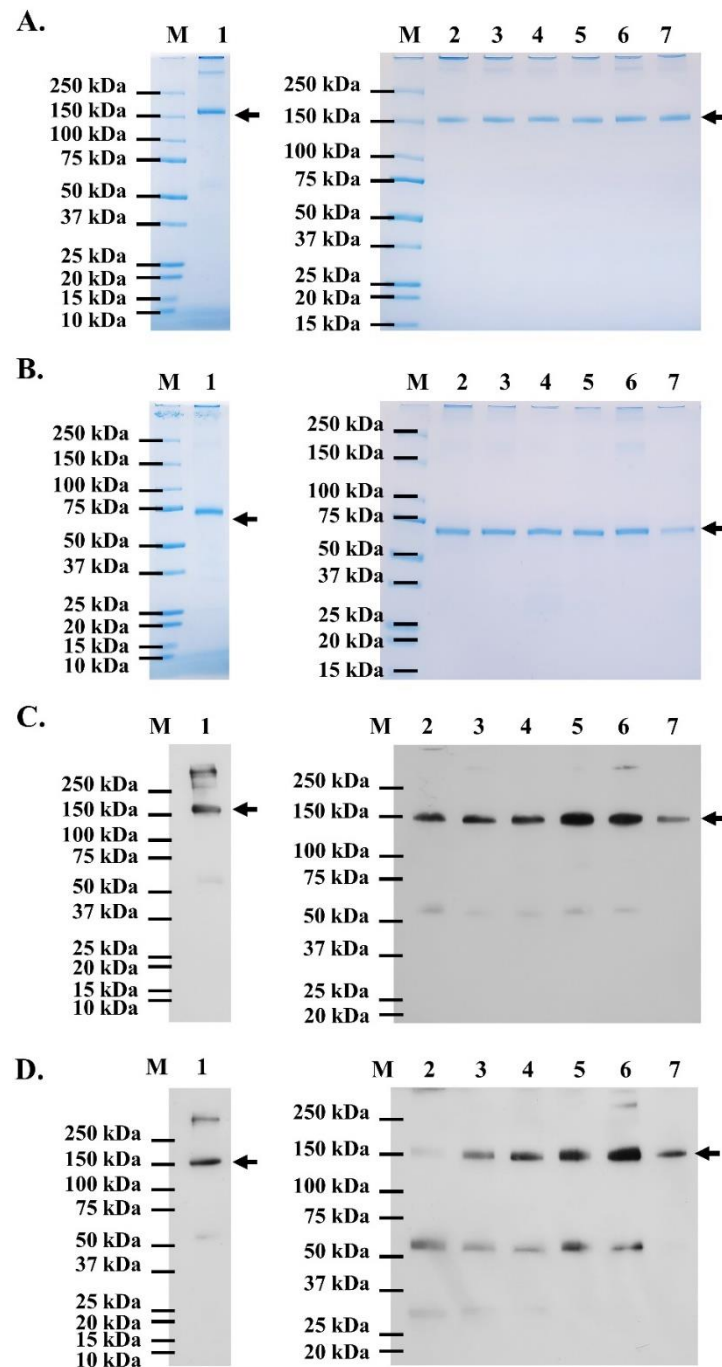
Figure 17 The purified variant RBD-Fc proteins expressed from N. benthamiana.

The purified Wuhan RBD-Fc (A), Alpha RBD-Fc (B), Beta RBD-Fc (C), Gamma RBD-Fc (D), Kappa RBD-Fc (E), Delta RBD-Fc (F), and Epsilon RBD-Fc (G) were analyzed by SDS-PAGE under non-reducing condition (A) and reducing-condition (B), and confirmed by western blot detected by goat anti-human IgG-HRP (C) and anti-SARS-CoV-2 RBD conjugated HRP (D) under non-reducing condition. Lane M: All Blue Prestained Protein

Standard; Lane 1: Wuhan RBD-Fc; Lane 2: Alpha RBD-Fc; Lane 3: Beta RBD-Fc; Lane 4: Gamma RBD-Fc; Lane 5: Kappa RBD-Fc; Lane 6: Delta RBD-Fc; Lane 7: Epsilon RBD-Fc. Arrow mark indicated the expected band.

3. Immunogenicity study of plant-produced variant RBD-Fc vaccines in monkeys

3.1 Baiya SARS-CoV-2 Vax 1 vaccine with 3 immunizations

For the immunization study in monkeys, the 10-µg dose of purified plant-produced Wuhan RBD-Fc was formulated with alum adjuvant and excipients, called Baiya SARS-CoV-2 Vax 1. Ten female monkeys were divided into vaccine and control groups (*n*=5). Monkeys were intramuscularly injected on Day 0, 21 as prime-boost (3-week interval) and another booster dose on Day 133 (16-week interval). Blood was collected before the first and third immunization and 14-day after each immunization (day 14, 35, 133, and 147) as shown in Figure 5A. After that, the sera from timepoints were analyzed for both anti-RBD and neutralizing antibodies response after immunizations.

As shown in Figure 17A, Baiya SARS-CoV-2 Vax 1 vaccine elicited a high anti-RBD total IgG titer after the second immunization on day 35 with geometric mean titer (GMT) = 11,143, which was significantly (*p*-value < 0.0001) higher than the titer on day 0 (GMT = 152). Then, the IgG titer was dropped to GMT = 1,600 after 16 weeks later (day 133). After the third immunization (day 147), the IgG titer of the vaccine group was regained to GMT = 11,143, which was significantly (*p*-value < 0.0001) higher than the titer on Day 0.

Furthermore, microneutralizing titer (MN_{50} titer) was assessed using the immunized monkey sera as shown in Figure 17B. The neutralizing titer against the Wuhan live virus was elicited after the second immunization on day 35 with GMT = 3,378, which was significantly (*p*-value < 0.0001) higher than the titer on day 0 (GMT = 10). After 16-week later (Day 133), the neutralizing titer of the vaccine group was decreased to GMT = 320. Then, the neutralizing titer was induced to GMT = 1,940 after

14 days after the third immunization on Day 147, which was significantly (p-value < 0.05) higher than the titer on day 0.
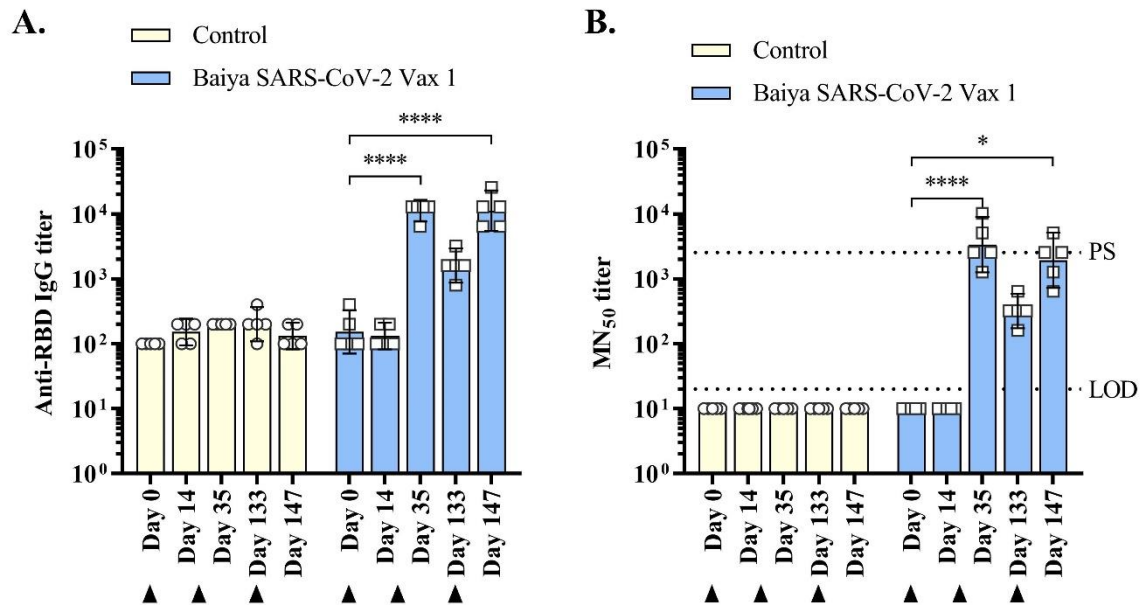
Figure 18 Immunogenicity of Baiya-SARS-CoV-2 Vax 1 in monkeys
Anti-RBD IgG (A) and 50% microneutralizing (MN$_{50}$) titers (B) were measured from immunized monkey sera. Data were plotted as GMT±95%CI, n = 5. Two-way ANOVA, Dunnett's test was used (*: p < 0.05, ****: p < 0.0001). Arrows indicated immunization times. LOD: limit of detection. PS: positive serum.

Moreover, the neutralizing antibodies against former VOCs also were investigated via., pseudovirus presenting SARS-CoV-2 variant Spike proteins neutralization (PVNT$_{50}$). In Baiya SARS-CoV-2 Vax 1 group, the neutralizing titers against SARS-CoV-2 variants were measurably elicited after the second immunization on day 35 (Figure 18). The neutralizing titers against both Wuhan (GMT = 4,937) and Alpha (GMT = 4,965) variants on day 35 were significantly higher than titers on day 14 (GMT = 3 for Wuhan, and 2 for Alpha) with p-value < 0.0001. On day 147, the PVNT$_{50}$ against Wuhan (GMT = 2,953) and Alpha (GMT = 4,197) were also significantly higher than the titers on day 14 with p-value < 0.001, but not in the titers on day 133 (GMT = 376 for Wuhan, and 159 for Alpha). On the other hand, only the PVNT$_{50}$ against Beta (GMT

=2,464) and Gamma (GMT = 1,852) on day 147 were significantly higher than the titers on day 14 with p-value < 0.01 and < 05, respectively, but not in the titers on day 35 (GMT = 343 for Beta, and 392 for Gamma) and 133 (GMT = 80 for Beta, and 83 for Gamma). Moreover, the $PVNT_{50}$ against Delta strain on day 35 (GMT =2,217) and 147 (GMT = 2,805) were significantly higher than the titer on day 14 (GMT = 38) with p-value < 0.01 and < 0001, respectively, but not in the titer on Day 133 (GMT = 132). Furthermore, the $PVNT_{50}$ against Omicron subvariants on day 147 were examined (Figure 18B). The result showed that the $PVNT_{50}$ against BA.1 (GMT = 484) and BA.2 (GMT = 396) variants were 6.1- and 7.5-fold decreased when compared with the Wuhan strain, respectively.
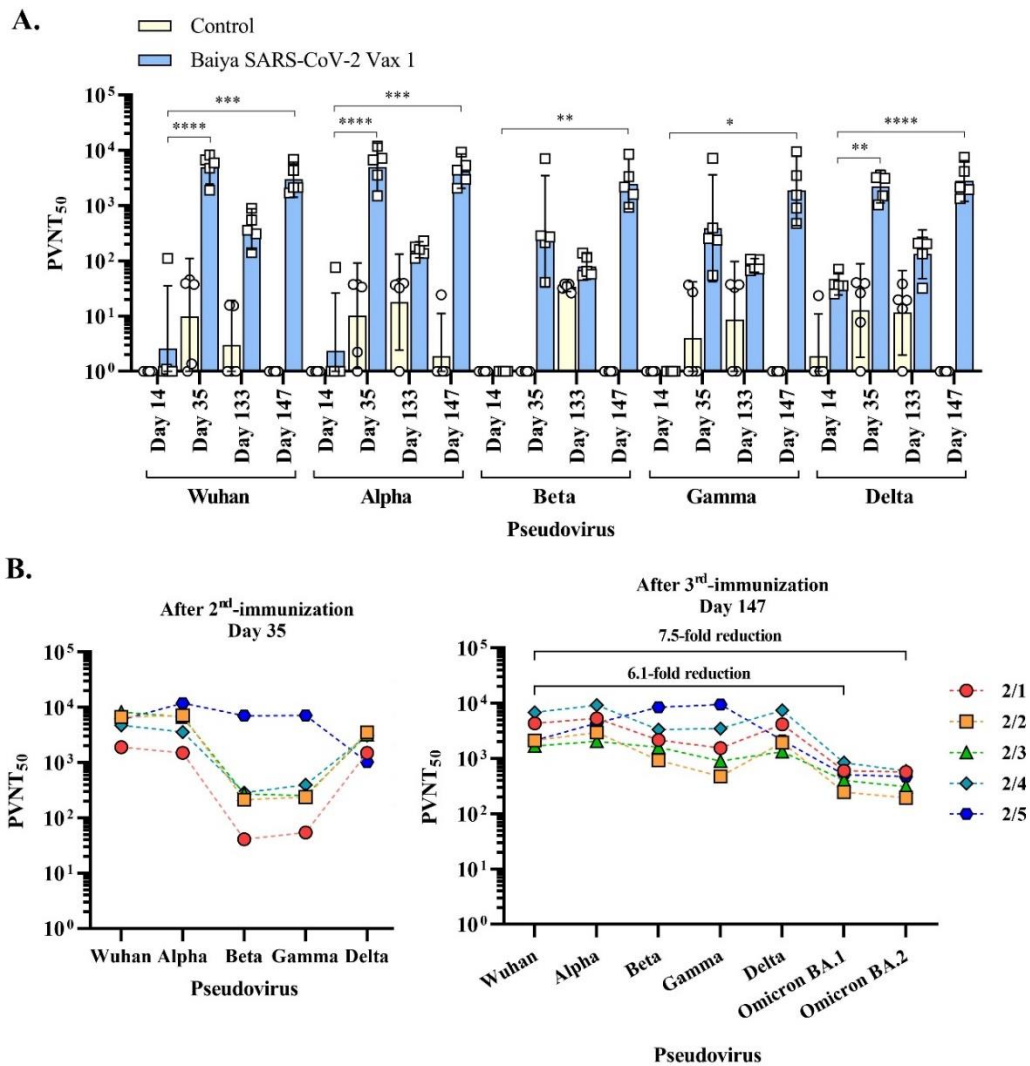
Figure 19 Neutralizing activity against SARS-CoV-2 variants of Baiya-SARS-CoV-2 Vax 1 immunized monkey sera

The 50% pseudovirus neutralizing titer ($PVNT_{50}$) against SARS-CoV-2 variants was measured from immunized monkey sera. Data were plotted as GMT±95%CI, n = 5. Two-way ANOVA, Dunnett's test was used (*: p < 0.05, **: p < 0.01, ***: p < 0.001, ****: p < 0.0001) (A). The $PVNT_{50}$ of vaccine group (No. 2/1-5) on day 35 and 147 were individually plotted (B).

3.2 Variant RBD-Fc vaccines with three immunizations

In the immunization study of variant RBD-Fc vaccines, the 10-µg dose of purified plant-produced Alpha, Beta, Gamma, Kappa, Delta, and Epsilon RBD-Fc proteins were adjuvanted with alum. Male and female monkeys were randomly separated into each variant vaccine group (n=5) and control group (*n*=3). Monkeys were intramuscularly injected on day 0, 21, and 42 (3-week intervals). Blood was collected before the first immunization and 14-day after each immunization (day 0, 14, 35, and 56) as shown in Figure 5B. Then, the immunized sera from timepoints were analyzed for both anti-RBD and neutralizing antibody responses.

In anti-RBD IgG response (Figure 19), Alpha (GMT = 174), Gamma (GMT = 115), Delta (GMT = 459), and Epsilon RBD-Fc (GMT = 1,213) vaccines induced the detectable titers after first immunization (day 14). Then, the antibody titer of Kappa RBD-Fc group (GMT = 16,890) was significantly higher than Alpha (GMT = 5,572), Beta (GMT = 4,222), and Gamma RBD-Fc (GMT = 3,805) vaccines with p-value < 0.05, and control group (GMT = 100) with p-value < 0.01, except Delta (GMT = 29,407) and Epsilon RBD-Fc (GMT = 12,800) vaccines. Moreover, the antibody titer of the Delta vaccine was significantly higher than Alpha, Beta, Gamma, and Epsilon vaccines and control groups with p-value < 0.0001, and Kappa group with p-value < 0.05. After the third immunization on day 56, the antibody titers of Delta and Epsilon vaccine groups, both GMT = 22,286, were significantly higher than the Beta RBD-Fc vaccine (GMT = 6,400) with p-value < 0.001, Gamma (GMT = 9,051) and Kappa (GMT = 11,143) groups with p-value < 0.05, and control groups (GMT = 100) with p-value < 0.0001, except Alpha RBD-Fc (GMT = 11,143).
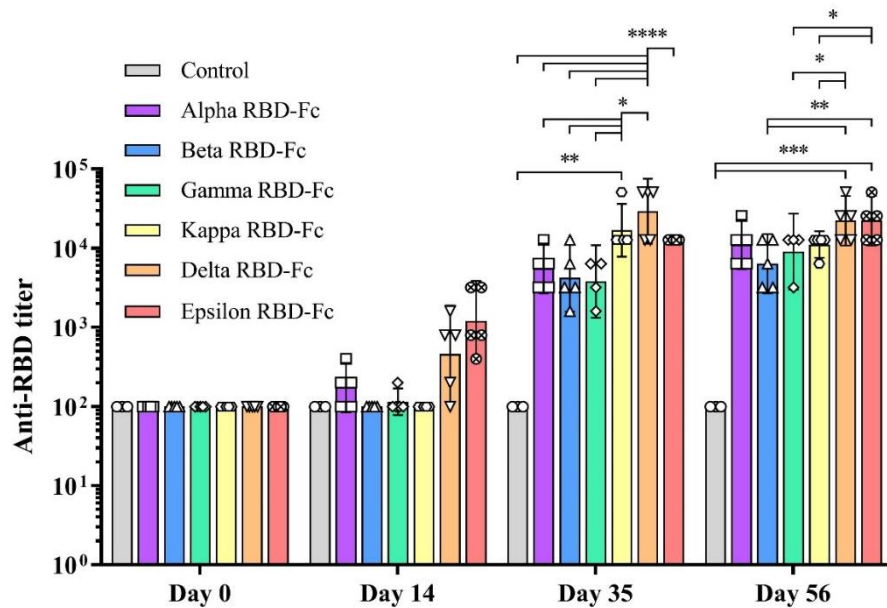
Figure 20 Anti-RBD IgG titer of plant-produced variant RBD-Fc vaccines in monkeys

The anti-RBD IgG titer was measured from immunized monkey sera. Data were plotted as GMT±95%CI, n = 5, n = 3 for control. Two-way ANOVA, Tukey's test was used (*: p < 0.05, **: p < 0.01, ***: p < 0.001, ****: p < 0.0001).

Subsequently, the neutralizing titer against live-virus, SARS-CoV-2 Wuhan, Alpha, Beta, and Delta strains were examined in monkeys immunized with variant RBD-Fc vaccine sera (Figure 20). After the first immunization on day 14, only MN_{50} titer against the Wuhan strain of Epsilon RBD-Fc vaccine (GMT = 80) was significantly higher than Alpha, Beta, Gamma, and Kappa RBD-Fc vaccines, GMTs were 15, 10, 11, and 15, respectively, with *p*-value < 0.01 and control group (GMT = 10) with *p*-value < 0.05, except Delta group with GMT = 35.

Then, after the second immunization detectable MN_{50} titers were observed. In neutralization against the Wuhan strain, the MN_{50} titer of only the Delta group, GMT = 2,560, was significantly higher than Alpha, GMT = 422, and Gamma, GMT = 538, vaccines with *p*-value < 0.05, and Beta, GMT = 92, Kappa, GMT = 368, and control, GMT = 10, groups with *p*-value < 0.01, except Epsilon vaccine with GMT of 2,229. After the second booster on day 56, the MN_{50} titer of only the Epsilon RBD-Fc vaccine rose GMT of 4,457 significantly higher than Beta (GMT = 211), Gamma RBD-Fc vaccines (GMT = 381), and

the control group (GMT = 10) with *p*-value < 0.01, but not in Alpha and Delta vaccine groups with GMT of 1,280 and 2,941, respectively.

For neutralization against the Alpha strain on day 35, the MN_{50} titer of the Delta RBD-Fc vaccine rose the GMT of 2,560 significantly higher than Beta (GMT = 139), Kappa RBD-Fc (GMT = 279) vaccines, and the control group (GMT = 10) with *p*-value < 0.05. Moreover, the MN_{50} titer against the Alpha variant of the Epsilon RBD-Fc vaccine (GMT = 3,378) was significantly higher than Alpha, GMT of 557, and Gamma RBD-Fc, GMT of 538, groups with *p*-value < 0.05, and Beta, Kappa vaccines, and the control group with *p*-value < 0.01. Then, the MN_{50} titer of the Delta RBD-Fc vaccine rose the GMT of 4,457 against the Alpha variant significantly higher than Beta (GMT = 279) and Kappa RBD-Fc vaccines (GMT of 368) with *p*-value < 0.01, and the Gamma vaccine (GMT = 538) and the control group (GMT of 10) with *p*-value < 0.05 after the third immunization on day 56. In addition, the MN_{50} titer of the Epsilon vaccine group (GMT = 4,457) was significantly higher than Beta, Gamma, and Kappa vaccines, and the control group with *p*-value < 0.01, except Alpha RBD-Fc (GMT = 1,280) and Delta vaccines.

The neutralization against the Beta variant after the second immunization, the MN_{50} titer of Alpha, Beta, Gamma, Kappa, Delta, and Epsilon RBD-Fc vaccines and the control group did not show any significant difference with GMT of 422, 970, 2,153, 844, 368, 735, and 13, respectively. After that, the MN_{50} titer against the Beta strain of Beta RBD-Fc vaccine (GMT of 3,378) was significantly higher than the Kappa vaccine (GMT = 1,689) with *p*-value < 0.05, and Delta (GMT = 735), Epsilon (GMT = 844) vaccines, and the control group (GMT = 13) with *p*-value < 0.01 after the third injection on day 56, but not in Alpha (GMT = 1689) and Gamma RBD-Fc (GMT = 3,620) vaccine groups.

Finally, the MN_{50} titer against the Delta variant of the Delta RBD-Fc vaccine group elicited GMT of 4,457 significantly higher titer than Alpha (GMT = 121), Beta (GMT = 23), Gamma (GMT = 57), Kappa RBD-Fc (GMT = 211), and control (GMT = 10) groups with *p*-value < 0.0001, and Epsilon (GMT = 1689) with *p*-value < 0.01 after the second immunization. After 14-day of the second booter (day 56), the MN_{50} titer against the Delta strain of the Delta RBD-Fc vaccine (GMT = 3,378) was significantly higher than

Beta (GMT = 121) and Gamma (GMT = 135) vaccine groups with *p*-value < 0.05, but not in Alpha (GMT = 844), Kappa (GMT = 422), Epsilon (GMT = 2,941) vaccines, and the control group (GMT = 10).

A.
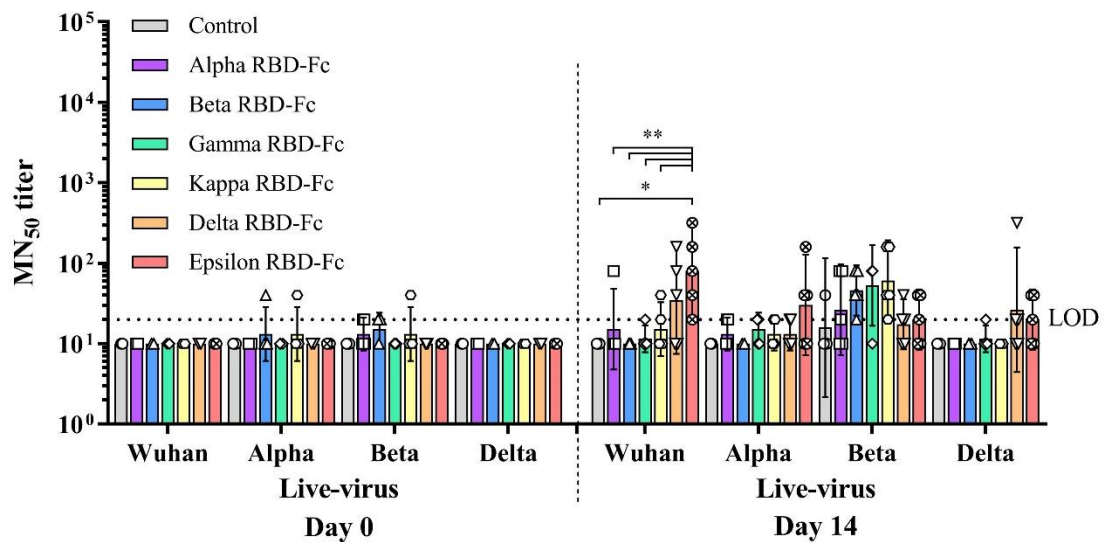
B.
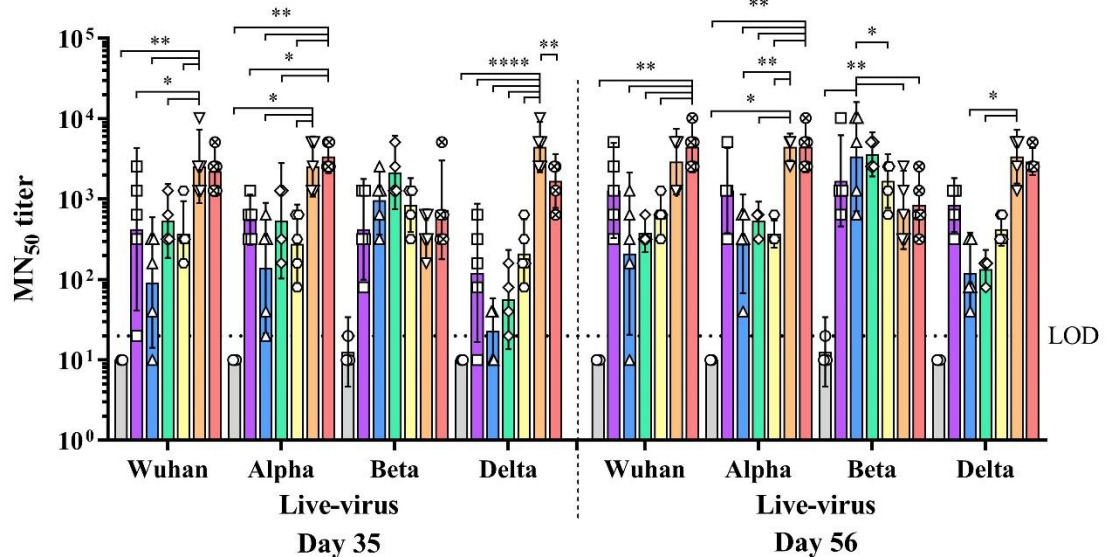
Figure 21 Live-virus neutralization against SARS-CoV-2 variants of plant-produced variant RBD-Fc vaccines in monkeys

The 50% microneutralizing (MN$_{50}$) titer was measured from immunized monkey sera on day 0, 14 (A), 35, and 56 (B). Data were plotted as GMT±95%CI, n = 5, n = 3 for

control. Two-way ANOVA, Tukey's test was used (*: p < 0.05, **: p < 0.01, ***: p < 0.001, ****: p < 0.0001). LOD: limit of detection.

Furthermore, the neutralizing antibody of variant vaccines immunized monkey sera against pseudovirus presenting SARS-CoV-2 spike protein of Wuhan, Alpha, Beta, Gamma, and Delta strains were also investigated (Figure 21). The 50% pseudovirus neutralizing titer ($PVNT_{50}$) of vaccines was observed a significant difference in the Delta variant after the first immunization. On day 14, the $PVNT_{50}$ against the Delta strain of Delta RBD-Fc vaccine (GMT = 133) was significantly higher than the Kappa vaccine (GMT = 9) and the control (GMT = 1) groups with p-value < 0.05, and Alpha (GMT = 7), Beta (GMT = 1), Gamma (GMT = 14) vaccine groups with p-value < 0.01. Moreover, the $PVNT_{50}$ of the Epsilon vaccine (GMT = 407) was significantly higher than all groups with p-value < 0.01, except the Gamma vaccine with p-value < 0.05.

After the second immunization on day 35, the $PVNT_{50}$ against the Wuhan strain of Epsilon RBD-Fc vaccine rose GMT of 6,228 significantly higher than Beta (GMT = 26) and Kappa vaccine (GMT = 520) groups with p-value < 0.05, except those of Alpha (GMT = 291), Gamma (GMT = 377), Delta (GMT = 4512) vaccines and the control (GMT = 1). Then, the $PVNT_{50}$ of the Alpha vaccine rose GMT of 4,157 significantly higher than the titer of Beta vaccine (GMT = 366) with p-value < 0.0001, and Gamma (GMT = 411), Kappa (GMT = 670) vaccines and control (GMT = 1) with p-value < 0.001 after the third immunization. Moreover, the neutralizing titer against Wuhan variant of Delta RBD-Fc vaccine (GMT = 2,674) was also significantly higher than the control group with p-value < 0.05. In addition, the $PVNT_{50}$ of the Epsilon vaccine (GMT = 4,222) was significantly higher than Gamma and Kappa vaccine groups with p-value < 0.01, and Beta and control groups with p-value < 0.001 on day 56.

For Alpha variant, the significant difference of the $PVNT_{50}$ of Alpha, Beta, Gamma, Kappa, Delta, and Epsilon vaccine and control groups (GMT of 327, 91, 617, 502, 5,969, 5,626, and 1, respectively) were not observed on day 35. After the third immunization on day 56, the $PVNT_{50}$ of Alpha RBD-Fc vaccine rose GMT of 3,951 significantly higher than Beta (GMT = 968) and Gamma (GMT = 959) vaccine groups with

p-value < 0.01, and Kappa vaccine (GMT = 748) and control group (GMT = 1) with *p*-value < 0.001. Moreover, the PVNT$_{50}$ of the Epsilon vaccine (GMT = 3,243) was also significantly higher than the control group with *p*-value < 0.05, without a significant difference, was observed in the Delta vaccine (GMT = 2,312) on Day 56.

In the pseudovirus neutralizing titer against the Beta variant, GMT of Alpha, Beta, Gamma, Kappa, Delta, and Epsilon RBD-Fc vaccines and the control were not significantly different both after the second (day 35) and third (day 56) immunizations, GMT of 27, 168, 1,357, 413, 445, 540, and 1 on day 35, and 196, 1653, 1632, 587, 619, 444, and 1 on day 56, respectively.

Likewise, GMT of Alpha, Beta, Gamma, Kappa, Delta, and Epsilon RBD-Fc vaccines and the control against the Gamma variant was not observed any significant difference in both on Day 35, GMT of 354, 1,639, 424, 587, 780, and 1, respectively, and 56, GMT of 1,368, 1,278, 487, 484, 472, and 1, respectively.

Finally, the PVNT$_{50}$ against the Delta variant of Delta RBD-Fc vaccine rose GMT of 19,684 significantly higher than Alpha, Beta, Gamma, Kappa, and Epsilon vaccine and control groups, GMT of 181, 31, 169, 536, 10,889, and 1, respectively, with *p*-value < 0.0001 after the second immunization. The PVNT$_{50}$ of Epsilon group was also significantly higher than Alpha, Beta, Gamma, Kappa, and Epsilon vaccine and control groups with *p*-value < 0.0001 on Day 35. Then, the PVNT$_{50}$ against the Delta strain of Delta vaccine (GMT = 5,241) was significantly higher than the Alpha vaccine (GMT = 1,603) with *p*-value < 0.01, and Beta (GMT = 148), Gamma (GMT = 174), and Kappa (GMT = 469) vaccines and the control (GMT = 1) with *p*-value < 0.0001 after the third immunization, except in the Epsilon vaccine (GMT = 2,584).
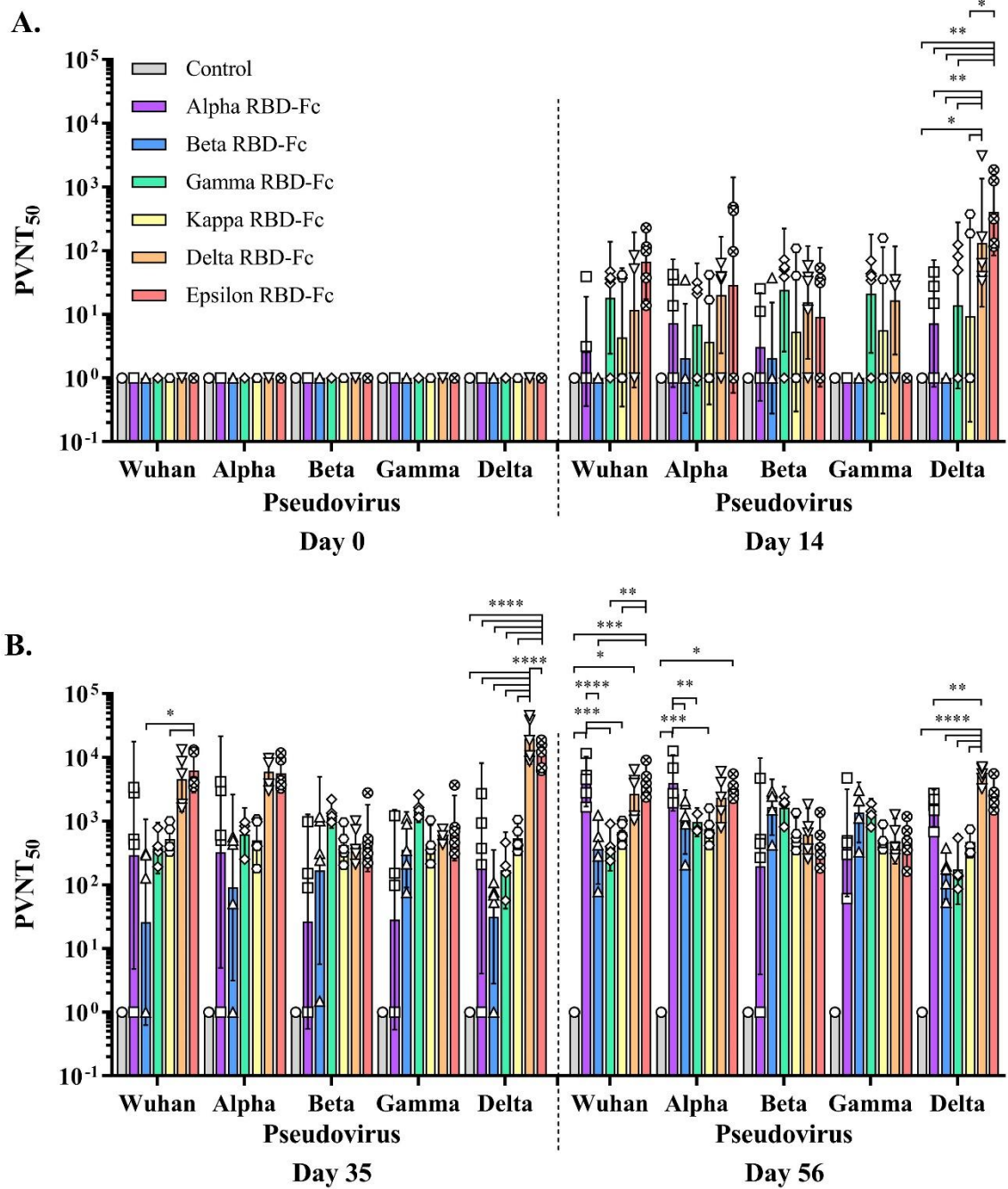
Figure 22 Pseudovirus neutralization against SARS-CoV-2 variants of plant-produced variant RBD-Fc vaccines in monkeys

The 50% pseudovirus neutralizing titer ($PVNT_{50}$) was measured from immunized monkey sera on day 0, 14 (A), 35, and 56 (B). Data were plotted as GMT±95%CI, n = 5, n = 3 for control. Two-way ANOVA, Tukey's test was used (*: $p < 0.05$, **: $p < 0.01$, ***: $p < 0.001$, ****: $p < 0.0001$).

CHAPTER V DISCUSSION

COVID-19 pandemic has adverse effects on health care and the nation's economic systems globally. More than six hundred million infected cases and six million deaths have been reported since 2019-2020 and still increasing (32). An effective vaccine is essential to prevent the spread of the virus and reduce the mortality. The radical vaccination may help to achieve herd immunity against the virus, in which some candidate vaccines are presently approved for human use (132, 189, 190). Now, the SARS-CoV-2 virus is evolving with multiple mutations that generate SARS-CoV-2 variants and predominately emerge worldwide. Furthermore, the emergence of variants, especially VOCs, increases concerns about the efficacy of the protection of existing vaccines against these variants' infection.

SARS-CoV-2 variants containing the mutations in the RBD region, increase the binding affinity between the virus and the host receptor, ACE2, thereby evading the host immunity (70, 191). The E484K, N501Y, and D614G sites in RBD involved in the virus interaction with ACE2 (62, 192, 193). Moreover, K417N/T, E484K, and L452R mutations were involved in the host immune escape function induced by convalescent plasma and immunized sera (68, 70, 192, 194, 195). Previously, many comparisons of the neutralizing activity against VOCs and ancestral (Wuhan) strain from vaccinated human samples were published (133). The minimal reduction of neutralizing titer against Alpha and Beta variants in mRNA, viral vector, inactivated, and subunit vaccine vaccinated recipients were observed. The minimal to moderate decrease neutralizing activity was also reported for Gamma, Delta, and Kappa strains. Moreover, a considerable reduction of neutralizing response in BNT162b2 recipients against the Omicron variant was reported, while undetectable neutralizing titer was demonstrated in CoronaVac recipients (137). Thus, the development of effective COVID-19 vaccines with coverage against VOCs is being a significance for worldwide (196). Moreover, the variant-specific SARS-CoV-2 vaccines might be required to manage the new variants outbreak, especially against those declining the immunity elicited by existing approved vaccines.

For subunit vaccines, several expression systems were used, including bacteria, yeast, mammalian or plant cells (197-200). The advantages of the plant expression system for producing vaccine antigens in response to viral pandemics or epidemics have been well described (201, 202). Previously, our team has developed the plant-produced SARS-CoV-2 Wuhan RBD-Fc subunit vaccine adjuvanted with alum, called Baiya SARS-CoV-2 Vax 1, that exhibited to elicit robust immune responses in both mice and monkeys against the ancestral SARS-CoV-2 (163). Moreover, our team has also published that the Alpha and Beta RBD-Fc can be successfully produced in plants (183). In this study, we have assessed the ancestral (Wuhan) strain and different variant-specific subunit vaccines which are constructed based on the variant SARS-CoV-2 RBD proteins produced in the *N. benthamiana* expression system. For new construct variant RBD-Fc proteins, Gamma, Kappa, Delta, and Epsilon RBD-Fc were successfully expressed from *N. benthamiana* and purified by protein A chromatography(163, 183). Plant-produced variant RBD-Fc proteins showed expected band at the molecular weight of approximately 150 kDa and 75 kDa under non-reducing and reducing conditions, respectively. However, in the western blot analysis, the affinity of anti-RBD HRP-conjugated secondary antibody was found to be different for each variant RBD-Fc protein. The most intense major band was observed in Delta RBD-Fc protein, whereas the band intensity was found to be lower in Kappa, Epsilon, Gamma, Beta, and Alpha RBD-Fc proteins. The yield of purified variant RBD-Fc proteins was found to be in the range of 20-28 µg/g fresh weight, which is comparable with the previous report of plant-produced Wuhan RBD-Fc which has the expression level of 25 µg/g fresh weight (163). The Fc region has been fused to the RBD owing to its advantages such as easy, rapid purification, longer half-life and also their polymeric nature provides an additional antigen depot effect (203). Fc-fused protein vaccines against SARS-CoV and influenza has also reported (204, 205).

Hereafter, the purified plant-produced variant RBD-Fc proteins were formulated with excipients and adjuvanted with alum as subunit vaccines. Alum exhibits excellent safety and efficacy profiles for long years and widely used in many available licensed vaccines, including tandem-repeat dimeric RBD subunit vaccine (206). Alum salts also

form a short-term depot at the injection site, while slowly releasing the adsorbed antigen to the recipient (207). Here, we performed two studies to investigate the booster dose effect of ancestral RBD-Fc vaccine, Baiya SARS-CoV-2 Vax 1, and three immunizations with 3-week interval of different SARS-CoV-2 variant RBD-Fc vaccines in cynomolgus monkeys. With the reduction the dose of vaccines to 10 μg-dose to increase the vaccine availability and accessibility during the outbreak.

First, two doses of 10 μg of Baiya SARS-CoV-2 Vax 1 elicited neutralizing antibody responses on day 35 in comparable levels to those of 25 and 50 μg Baiya SARS-CoV-2 Vax 1 (163). Moreover, this study showed that anti-RBD and neutralizing antibodies dramatically decreased after the second immunization for 16 weeks later (day 133). Which conformed to the recent research that the high immunogenic response after the second immunization of RBD subunit vaccine was reduced after 3 months later in mice (204). After the third immunization of Baiya SARS-CoV-2 Vax 1 (day 143), the anti-RBD and neutralizing antibody titers against the ancestral (Wuhan) variant were elicited in comparable levels after the second immunization (day 35). These results are in line with the previous studies in which the antibody response was shown to be increased after the booster dose (204, 208). Baiya SARS-CoV-2 Vax 1 vaccination elicits broadly neutralizing antibodies against VOCs, except Beta and Gamma variants, after the first booster dose. Relatively, the neutralization efficiency against Wuhan and variants of 4-month lapse was noticeably dropped as same as live-virus neutralization results. Surprisingly, the third vaccination markedly boosted the neutralizing response against these strains, including the highly transmission strain Delta variant. The neutralizing activity of the sera on day 147 against variants was comparable to the Wuhan strain, however, the minimal reduction in the $PVNT_{50}$ against Gamma variant compared to Wuhan strain was observed. On the other hand, the neutralizing titers against both Omicron BA.1 and BA.2 on day 147 were dramatically decreased compared to Wuhan with 6.1- and 7.1-fold reduction, respectively. Previous reports showed the resistance of variants against the antibody elicited after two doses of immunization (70, 209-211). Moreover, the booster dose showed increase in the vaccine efficacy against Omicron variant compared to non-booster vaccinated

recipients (212). Hence, the booster dose from 2-dose regimen of vaccine might be ideal for boosting the immunogenicity against further variants (210).

Then, the immunogenicity of 10 µg-dose of plant-produced variant RBD-Fc vaccines with three dose vaccination with 3-week intervals was investigated in monkeys. The results showed that both Delta and Epsilon RBD-Fc (sharing L452R and D614G mutations) vaccinated groups showed the high potential of inducing both anti-RBD and neutralizing antibodies against ancestral, Alpha and Delta strains after the third immunization on day 56. However, the neutralization activities against Beta and Gamma variants of both Delta and Epsilon vaccine groups were found to be lower, which related to Wuhan RBD-Fc vaccine as mentioned above. Besides, the neutralizing titer of Beta and Gamma RBD-Fc (sharing E484K, N501Y, D614G sites) vaccinated groups were found to be higher against Beta and Gamma strains compared to the rest of the immunized groups. Similar with the previous reports, recombinant spike proteins from the wild-type Wuhan, Alpha, Beta, and Gamma vaccines demonstrated high neutralizing titers against the homologous variants (213). In addition, the reduction of neutralizing activities was also noted, 4.8-fold reduction of Alpha vaccine against Beta strain, 4.4-fold reduction of Alpha vaccine against Gamma strain, and 4.2-fold reduction of Beta vaccine against Gamma strain. Based on these results, the SARS-CoV-2 variant-specific vaccine might not cross-protect or neutralize all or the further variants. However, further challenge experiments are required to support the findings. Recently, the concept of cocktail vaccine, antigens combination vaccine, has been proposed for eliciting the broad immune response against SARS-CoV-2 variants. Recently, the published data demonstrated that the designed RBD with mutation sites as the cocktail vaccine increased variant-specific antibodies than the single antigen vaccine formulation (214).

However, the Th2-bias of alum adjuvant was reported to be possibly associated with lung eosinophilic immunopathology in mice model (120). Consequently, U.S. Food and Drug Administration (FDA) guided to the industry that COVID-19 vaccine candidates should preferably elicit a strong Th1 response and high levels of neutralizing antibodies (215), like approved mRNA vaccines from both Pfizer/BioNTech and Moderna, and

Matrix-M adjuvanted subunit vaccine from Novavax. Hence, the second Th1-bias adjuvant might be considered to combine in the next formulation for balancing Th1/Th2 responses, such as CpG, Poly(I:C), and MPLA (174).

The limitation of this study is that the pseudovirus presenting the SARS-CoV-2 spike protein of variants was used instead of the live-viruses to test the neutralization activity of the immunized sera. However, this methodology is generally accepted, which offers the similarly results to the authentic virus neutralization. On the other hand, this assay can be applied even in the absence of specific variants in the local region and the requirement of facility is not restricted to the Biosafety Level 3 (BSL3) (216-218).

Further challenge studies are essential to evaluate the immunogenicity induced by plant-produced variant RBD-Fc vaccines have the potential to protect animals against SARS-CoV-2 infection, especially VOCs. Recently, prime-boost of Baiya SARS-CoV-2 Vax 1 was reported as the effective vaccine that protects the SARS-CoV-2 challenged K18-hACE2 mice (162). Taken together, these studies provide the clear evidence that the booster dose from prime-boost vaccination or the long-term of the third immunization elicit broad neutralizing antibody against SARS-CoV-2 variants better than variant-specific vaccines in monkeys.

In conclusion, our data highlights the potential of Baiya SARS-CoV-2 Vax 1 and different variant vaccines in eliciting a significant humoral immune response in cynomolgus macaques with three dose vaccination. Moreover, the sera from the booster dose of Baiya SARS-CoV-2 Vax 1 immunized monkeys were found to be effective in neutralizing SARS-CoV-2 variants recognized by the WHO as former VOCs, broader than variant-specific vaccines. These results revealed the potential for using the plant-produced protein subunit vaccines in the fight against SARS-COV-2. In addition, another possible approach is that the wild-type or variant antigens could be combined to develop as a cocktail vaccine. Further studies are needed to validate the cocktail vaccine strategy and its efficacy against the circulating SARS-CoV-2 or future variants. Furthermore, long-term three-dose regime can be suggested for the countries

where the infection is severe. Additionally, a three-dose vaccination regime can be employed for developing an effective vaccine against SARS-CoV-2 further variants. However, the durability immune response of booster dose needs to be investigated. Overall, these proof-of-concept results facilitate the design and development of plant-produced variant subunit vaccines against SARS-CoV-2 variants.

CHAPTER VI CONCLUSION

The efficacy of plant-produced SARS-CoV-2 variant RBD-Fc subunit vaccines was investigated in this study. Here, different variants, ancestral (Wuhan), Alpha, Beta, Gamma, Kappa, Delta, and Epsilon, RBD-Fc fusion proteins were successfully produced from *N. bethamiana* with yields of 25.3, 23.8, 23.3, 21.9, 26.4, 28.0, and 20.0 µg/g fresh weight, respectively. The outcomes of immunogenicity of Baiya SARS-CoV-2 Vax 1, Wuhan RBD-Fc adjuvanted with alum, in cynomolgus monkeys demonstrated that long-term immunization could induce a high level of cross-neutralizing antibodies against SARS-CoV-2 variants. Moreover, variant RBD-Fc vaccines also elicited a high level of neutralizing antibodies against homologous variants.

In conclusion, these findings revealed the potential to use the proper immunization manner and antigen formulations. The long-term booster dose of the original SARS-CoV-2 strain might be required for protecting the further SARS-CoV-2 variants. Whereas, the variant-specific vaccine may be considered as the booster dose or combined with another antigen as a cocktail vaccine to elicit broad neutralization against variants.

จุฬาลงกรณ์มหาวิทยาลัย
CHULALONGKORN UNIVERSITY

REFERENCES

1. Chen Y, Liu Q, Guo D. Emerging coronaviruses: Genome structure, replication, and pathogenesis. J Med Virol (2020) 92:doi: 10.1002/jmv.26234

2. Masters PS. The molecular biology of coronaviruses. Adv Virus Res (2006) 66:doi: 10.1016/S0065-3527(06)66005-3

3. Ziebuhr J, Snijder EJ, Gorbalenya AE. Virus-encoded proteinases and proteolytic processing in the Nidovirales. J Gen Virol (2000) 81:Pt 4. doi: 10.1099/0022-1317-81-4-853

4. Snijder EJ, van der Meer Y, Zevenhoven-Dobbe J, Onderwater JJ, van der Meulen J, Koerten HK, et al. Ultrastructure and origin of membrane vesicles associated with the severe acute respiratory syndrome coronavirus replication complex. J Virol (2006) 80:12. doi: 10.1128/JVI.02501-05

5. Hussain S, Pan J, Chen Y, Yang Y, Xu J, Peng Y, et al. Identification of novel subgenomic RNAs and noncanonical transcription initiation signals of severe acute respiratory syndrome coronavirus. J Virol (2005) 79:9. doi: 10.1128/JVI.79.9.5288-5295.2005

6. Perlman S, Netland J. Coronaviruses post-SARS: update on replication and pathogenesis. Nat Rev Microbiol (2009) 7:6. doi: 10.1038/nrmicro2147

7. Sawicki SG, Sawicki DL, Siddell SG. A contemporary view of coronavirus transcription. J Virol (2007) 81:1. doi: 10.1128/JVI.01358-06

8. Beniac DR, Andonov A, Grudeski E, Booth TF. Architecture of the SARS coronavirus prefusion spike. Nat Struct Mol Biol (2006) 13:8. doi: 10.1038/nsmb1123

9. Fehr AR, Perlman S. Coronaviruses: an overview of their replication and pathogenesis. Coronaviruses: Springer; 2015. p. 1-23.

10. Walls AC, Park YJ, Tortorici MA, Wall A, McGuire AT, Veesler D. Structure, Function, and Antigenicity of the SARS-CoV-2 Spike Glycoprotein. Cell (2020) 181:2. doi: 10.1016/j.cell.2020.02.058

11. Nal B, Chan C, Kien F, Siu L, Tse J, Chu K, et al. Differential maturation and subcellular localization of severe acute respiratory syndrome coronavirus surface proteins S, M and E. J Gen Virol (2005) 86:Pt 5. doi: 10.1099/vir.0.80671-0

12. Neuman BW, Kiss G, Kunding AH, Bhella D, Baksh MF, Connelly S, et al. A structural analysis of M protein in coronavirus assembly and morphology. J Struct Biol (2011) 174:1. doi: 10.1016/j.jsb.2010.11.021

13. DeDiego ML, Álvarez E, Almazán F, Rejas MT, Lamirande E, Roberts A, et al. A severe acute respiratory syndrome coronavirus that lacks the E gene is attenuated in vitro and in vivo. J Virol (2007) 81:4. doi: 10.1128/JVI.01467-06

14. Nieto-Torres JL, DeDiego ML, Verdia-Baguena C, Jimenez-Guardeno JM, Regla-Nava JA, Fernandez-Delgado R, et al. Severe acute respiratory syndrome coronavirus envelope protein ion channel activity promotes virus fitness and pathogenesis. PLoS Pathog (2014) 10:5. doi: 10.1371/journal.ppat.1004077

15. Schoeman D, Fielding BC. Coronavirus envelope protein: current knowledge. Virol J (2019) 16:1. doi: 10.1186/s12985-019-1182-0

16. Tai W, He L, Zhang X, Pu J, Voronin D, Jiang S, et al. Characterization of the receptor-binding domain (RBD) of 2019 novel coronavirus: implication for development of RBD protein as a viral attachment inhibitor and vaccine. Cell Mol Immunol (2020) 17:6. doi: 10.1038/s41423-020-0400-4

17. Hurst KR, Koetzner CA, Masters PS. Identification of in vivo-interacting domains of the murine coronavirus nucleocapsid protein. J Virol (2009) 83:14. doi: 10.1128/JVI.00440-09

18. Shanmugaraj B, Khorattanakulchai N, Phoolcharoen W. SARS-CoV-2 vaccines: current trends and prospects of developing plant-derived vaccines. Biomedical Innovations to Combat COVID-19: Elsevier; 2022. p. 213-29.

19. World Health Organization. SARS (Severe Acute Respiratory Syndrome) (2012). https://www.who.int/ith/diseases/sars/en/ [Accessed 6 December 2022].

20. Hon KL. Severe respiratory syndromes: travel history matters. Travel Med Infect Di (2013) 11:5. doi: 10.1016/j.tmaid.2013.06.005

21. World Health Organization. Case definitions for surveillance of severe acute respiratory syndrome (SARS) (2003). https://www.who.int/csr/sars/casedefinition/en/ [Accessed 6 December 2022].

22. World Health Organization. Middle East respiratory syndrome coronavirus (MERS-CoV) (2019). https://www.who.int/news-room/fact-sheets/detail/middle-east-respiratory-syndrome-coronavirus-(mers-cov) [Accessed 6 December 2022].

23. World Health Organization. WHO MERS global summary and assessment of risk, July 2019. World Health Organization; 2019.

24. Azhar EI, El-Kafrawy SA, Farraj SA, Hassan AM, Al-Saeed MS, Hashem AM, et al. Evidence for camel-to-human transmission of MERS coronavirus. New Engl J Med (2014) 370:26. doi: 10.1056/NEJMoa1401505

25. Faridi U. Middle East respiratory syndrome coronavirus (MERS-CoV): Impact on Saudi Arabia, 2015. Saudi J Biol Sci (2018) 25:7. doi: 10.1016/j.sjbs.2016.09.020

26. World Health Organization. WHO Director-General's opening remarks at the media briefing on COVID-19 - 11 March 2020 (2020). https://www.who.int/director-general/speeches/detail/who-director-general-s-opening-remarks-at-the-media-briefing-on-covid-19---11-march-2020 [Accessed 6 December 2022].

27. Huang C, Wang Y, Li X, Ren L, Zhao J, Hu Y, et al. Clinical features of patients infected with 2019 novel coronavirus in Wuhan, China. Lancet (2020) 395:10223. doi: 10.1016/S0140-6736(20)30183-5

28. Voskarides K. SARS-CoV-2: tracing the origin, tracking the evolution. BMC Med Genomics (2022) 15:1. doi: 10.1186/s12920-022-01208-w

29. Cyranoski D. Did pangolins spread the China coronavirus to people (2020). https://www.nature.com/articles/d41586-020-00364-2 [Accessed 6 December 2022].

30. Zhou P, Yang XL, Wang XG, Hu B, Zhang L, Zhang W, et al. A pneumonia outbreak associated with a new coronavirus of probable bat origin. Nature (2020) 579:7798. doi: 10.1038/s41586-020-2012-7

31. Carlos WG, Dela Cruz CS, Cao B, Pasnick S, Jamil S. Novel Wuhan (2019-nCoV) coronavirus. Am J Respir Crit Care (2020) 201:4. doi: 10.1164/rccm.2014P7

32. World Health Organization. WHO coronavirus (COVID-19) dashboard (2020). https://covid19.who.int/ [Accessed 6 December 2022].

33. World Health Organization. Coronavirus (2020). https://www.who.int/health-topics/coronavirus [Accessed 6 December 2022].

34. Mehta P, McAuley DF, Brown M, Sanchez E, Tattersall RS, Manson JJ, et al. COVID-19: consider cytokine storm syndromes and immunosuppression. Lancet (2020) 395:10229. doi: 10.1016/S0140-6736(20)30628-0

35. Russell CD, Millar JE, Baillie JK. Clinical evidence does not support corticosteroid treatment for 2019-nCoV lung injury. Lancet (2020) 395:10223. doi: 10.1016/S0140-6736(20)30317-2

36. Yu P, Zhu J, Zhang Z, Han Y. A familial cluster of infection associated with the 2019 novel coronavirus indicating possible person-to-person transmission during the incubation period. J Infect Dis (2020) 221:11. doi: 10.1093/infdis/jiaa077

37. Gralton J, Tovey ER, McLaws ML, Rawlinson WD. Respiratory virus RNA is detectable in airborne and droplet particles. J Med Virol (2013) 85:12. doi: 10.1002/jmv.23698

38. Morawska L, Cao J. Airborne transmission of SARS-CoV-2: The world should face the reality. Environ Int (2020) doi: 10.1016/j.envint.2020.105730

39. Rothe C, Schunk M, Sothmann P, Bretzel G, Froeschl G, Wallrauch C, et al. Transmission of 2019-nCoV Infection from an Asymptomatic Contact in Germany. New Engl J Med (2020) 382:10. doi: 10.1056/NEJMc2001468

40. Lei S, Jiang F, Su W, Chen C, Chen J, Mei W, et al. Clinical characteristics and outcomes of patients undergoing surgeries during the incubation period of COVID-19 infection. EClinicalMedicine (2020) doi: 10.1016/j.eclinm.2020.100331

41. Lauer SA, Grantz KH, Bi Q, Jones FK, Zheng Q, Meredith HR, et al. The incubation period of coronavirus disease 2019 (COVID-19) from publicly reported confirmed cases: estimation and application. Ann Intern Med (2020) 172:9. doi: 10.7326/M20-0504

42. Backer JA, Klinkenberg D, Wallinga J. Incubation period of 2019 novel coronavirus (2019-nCoV) infections among travellers from Wuhan, China, 20-28 January 2020. Eurosurveill (2020) 25:5. doi: 10.2807/1560-7917.ES.2020.25.5.2000062

43. Wei Y, Lu Y, Xia L, Yuan X, Li G, Li X, et al. Analysis of 2019 novel coronavirus infection and clinical characteristics of outpatients: An epidemiological study from a fever clinic in Wuhan, China. J Med Virol (2020) doi: 10.1002/jmv.26175

44. Varia M, Wilson S, Sarwal S, McGeer A, Gournis E, Galanis E, et al. Investigation of a nosocomial outbreak of severe acute respiratory syndrome (SARS) in Toronto, Canada. Can Med Assoc J (2003) 169:4. doi:

45. Virlogeux V, Fang VJ, Park M, Wu JT, Cowling BJ. Comparison of incubation period distribution of human infections with MERS-CoV in South Korea and Saudi Arabia. Sci Rep-UK (2016) 6:doi: 10.1038/srep35839

46. Lu R, Zhao X, Li J, Niu P, Yang B, Wu H, et al. Genomic characterisation and epidemiology of 2019 novel coronavirus: implications for virus origins and receptor binding. Lancet (2020) 395:10224. doi: 10.1016/S0140-6736(20)30251-8

47. Zhao Y, Zhao Z, Wang Y, Zhou Y, Ma Y, Zuo W. Single-cell RNA expression profiling of ACE2, the receptor of SARS-CoV-2. Am J Respir Crit Care Med (2020) 202:5. doi: 10.1164/rccm.202001-0179LE

48. Hoffmann M, Kleine-Weber H, Schroeder S, Krüger N, Herrler T, Erichsen S, et al. SARS-CoV-2 cell entry depends on ACE2 and TMPRSS2 and is blocked by a clinically proven protease inhibitor. Cell (2020) 181:2. doi: 10.1016/j.cell.2020.02.052

49. Shang J, Wan Y, Luo C, Ye G, Geng Q, Auerbach A, et al. Cell entry mechanisms of SARS-CoV-2. Proc Natl Acad Sci U S A (2020) 117:21. doi: 10.1073/pnas.2003138117

50. Smith TRF, Patel A, Ramos S, Elwood D, Zhu X, Yan J, et al. Immunogenicity of a DNA vaccine candidate for COVID-19. Nat Commun (2020) 11:1. doi: 10.1038/s41467-020-16505-0

51. Wang MY, Zhao R, Gao LJ, Gao XF, Wang DP, Cao JM. SARS-CoV-2: structure, biology, and structure-based therapeutics development. Front Cell Infect Microbiol (2020) 10:doi: 10.3389/fcimb.2020.587269

52. Shanmugaraj B, Siriwattananon K, Wangkanont K, Phoolcharoen W. Perspectives on monoclonal antibody therapy as potential therapeutic intervention for coronavirus disease-19 (COVID-19). Asian Pac J Allergy Immunol (2020) 38:1. doi: 10.12932/AP-200220-0773

53. Krammer F. SARS-CoV-2 vaccines in development. Nature (2020) 586:7830. doi: 10.1038/s41586-020-2798-3

54. Giovanetti M, Benedetti F, Campisi G, Ciccozzi A, Fabris S, Ceccarelli G, et al. Evolution patterns of SARS-CoV-2: Snapshot on its genome variants. Biochem Biophys Res Commun (2021) 538:doi: 10.1016/j.bbrc.2020.10.102

55. Korber B, Fischer WM, Gnanakaran S, Yoon H, Theiler J, Abfalterer W, et al. Tracking changes in SARS-CoV-2 spike: evidence that D614G increases infectivity of the COVID-19 virus. Cell (2020) 182:4. doi: 10.1016/j.cell.2020.06.043

56. Abdool Karim SS, de Oliveira T. New SARS-CoV-2 variants - clinical, public health, and vaccine implications. N Engl J Med (2021) 384:19. doi: 10.1056/NEJMc2100362

57. Singh J, Rahman SA, Ehtesham NZ, Hira S, Hasnain SE. SARS-CoV-2 variants of concern are emerging in India. Nat Med (2021) doi: 10.1038/s41591-021-01397-4

58. World Health Organization. Tracking SARS-CoV-2 variants (2021). https://www.who.int/en/activities/tracking-SARS-CoV-2-variants/ [Accessed 6 December 2022].

59. Galloway SE, Paul P, MacCannell DR, Johansson MA, Brooks JT, MacNeil A, et al. Emergence of SARS-CoV-2 B.1.1.7 Lineage - United States, December 29, 2020- January 12, 2021. MMWR Morb Mortal Wkly Rep (2021) 70:3. doi: 10.15585/mmwr.mm7003e2

60. Volz E, Mishra S, Chand M, Barrett JC, Johnson R, Geidelberg L, et al. Assessing transmissibility of SARS-CoV-2 lineage B.1.1.7 in England. Nature (2021) 593:7858. doi: 10.1038/s41586-021-03470-x

61. Choi A, Koch M, Wu K, Dixon G, Oestreicher J, Legault H, et al. Serum Neutralizing Activity of mRNA-1273 against SARS-CoV-2 Variants. J Virol (2021) 95:23. doi: 10.1128/JVI.01313-21

62. Liu Y, Liu J, Plante KS, Plante JA, Xie X, Zhang X, et al. The N501Y spike substitution enhances SARS-CoV-2 infection and transmission. Nature (2021) doi: 10.1038/s41586-021-04245-0

63. Davies NG, Abbott S, Barnard RC, Jarvis CI, Kucharski AJ, Munday JD, et al. Estimated transmissibility and impact of SARS-CoV-2 lineage B.1.1.7 in England. Science (2021) 372:6538. doi: 10.1126/science.abg3055

64. Davies NG, Jarvis CI, Group CC-W, Edmunds WJ, Jewell NP, Diaz-Ordaz K, et al. Increased mortality in community-tested cases of SARS-CoV-2 lineage B.1.1.7. Nature (2021) 593:7858. doi: 10.1038/s41586-021-03426-1

65. Grint DJ, Wing K, Williamson E, McDonald HI, Bhaskaran K, Evans D, et al. Case fatality risk of the SARS-CoV-2 variant of concern B.1.1.7 in England, 16 November to 5 February. Euro Surveill (2021) 26:11. doi: 10.2807/1560-7917.ES.2021.26.11.2100256

66. Tegally H, Wilkinson E, Giovanetti M, Iranzadeh A, Fonseca V, Giandhari J, et al. Detection of a SARS-CoV-2 variant of concern in South Africa. Nature (2021) 592:7854. doi: 10.1038/s41586-021-03402-9

67. Wibmer CK, Ayres F, Hermanus T, Madzivhandila M, Kgagudi P, Oosthuysen B, et al. SARS-CoV-2 501Y. V2 escapes neutralization by South African COVID-19 donor plasma. Nature medicine (2021) 27:4. doi: 10.1038/s41591-021-01285-x

68. Feder KA, Patel A, Vepachedu VR, Dominguez C, Keller EN, Klein L, et al. Association of E484K Spike Protein Mutation With Severe Acute Respiratory Syndrome Coronavirus 2 (SARS-CoV-2) Infection in Vaccinated Persons: Maryland, January–May 2021. Clinical Infectious Diseases (2021) doi: 10.1093/cid/ciab762

69. Liu Y, Liu J, Xia H, Zhang X, Fontes-Garfias CR, Swanson KA, et al. Neutralizing Activity of BNT162b2-Elicited Serum. N Engl J Med (2021) 384:15. doi: 10.1056/NEJMc2102017

70. Wang P, Nair MS, Liu L, Iketani S, Luo Y, Guo Y, et al. Antibody resistance of SARS-CoV-2 variants B.1.351 and B.1.1.7. Nature (2021) 593:7857. doi: 10.1038/s41586-021-03398-2

71. Wu K, Werner AP, Koch M, Choi A, Narayanan E, Stewart-Jones GBE, et al. Serum Neutralizing Activity Elicited by mRNA-1273 Vaccine. N Engl J Med (2021) 384:15. doi: 10.1056/NEJMc2102179

72. Faria NR, Mellan TA, Whittaker C, Claro IM, Candido DDS, Mishra S, et al. Genomics and epidemiology of the P.1 SARS-CoV-2 lineage in Manaus, Brazil. Science (2021) 372:6544. doi: 10.1126/science.abh2644

73. Mlcochova P, Kemp SA, Dhar MS, Papa G, Meng B, Ferreira I, et al. SARS-CoV-2 B.1.617.2 Delta variant replication and immune evasion. Nature (2021) 599:7883. doi: 10.1038/s41586-021-03944-y

74. McCallum M, Bassi J, De Marco A, Chen A, Walls AC, Di Iulio J, et al. SARS-CoV-2 immune evasion by the B.1.427/B.1.429 variant of concern. Science (2021) 373:6555. doi: 10.1126/science.abi7994

75. Ferreira IA, Kemp SA, Datir R, Saito A, Meng B, Rakshit P, et al. SARS-CoV-2 B. 1.617 mutations L452R and E484Q are not synergistic for antibody evasion. The Journal of infectious diseases (2021) 224:6. doi: 10.1093/infdis/jiab368.

76. Wilhelm A, Toptan T, Pallas C, Wolf T, Goetsch U, Gottschalk R, et al. Antibody-Mediated Neutralization of Authentic SARS-CoV-2 B.1.617 Variants Harboring L452R and T478K/E484Q. Viruses (2021) 13:9. doi: 10.3390/v13091693

77. Baral P, Bhattarai N, Hossen ML, Stebliankin V, Gerstman BS, Narasimhan G, et al. Mutation-induced changes in the receptor-binding interface of the SARS-CoV-2 Delta variant B.1.617.2 and implications for immune evasion. Biochem Biophys Res Commun (2021) 574:doi: 10.1016/j.bbrc.2021.08.036

78. Vaughan A. Delta to dominate world. New Sci (2021) 250:3341. doi: 10.1016/S0262-4079(21)01121-0

79. Vaughan A. Omicron emerges. New Sci (2021) 252:3363. doi: 10.1016/S0262-4079(21)02140-0

80. Centers for Disease Control and Prevention. SARS-CoV-2 Variant Classifications and Definitions (2021). https://www.cdc.gov/coronavirus/2019-ncov/variants/variant-classifications.html [Accessed 6 December 2022].

81. Khandia R, Singhal S, Alqahtani T, Kamal MA, El-Shall NA, Nainu F, et al. Emergence of SARS-CoV-2 Omicron (B.1.1.529) variant, salient features, high global health concerns and strategies to counter it amid ongoing COVID-19 pandemic. Environ Res (2022) 209:doi: 10.1016/j.envres.2022.112816

82. Cele S, Jackson L, Khoury DS, Khan K, Moyo-Gwete T, Tegally H, et al. Omicron extensively but incompletely escapes Pfizer BNT162b2 neutralization. Nature (2022) 602:7898. doi: 10.1038/s41586-021-04387-1

83. Islam F, Dhawan M, Nafady MH, Emran TB, Mitra S, Choudhary OP, et al. Understanding the omicron variant (B.1.1.529) of SARS-CoV-2: Mutational impacts, concerns, and the possible solutions. Ann Med Surg (Lond) (2022) 78:doi: 10.1016/j.amsu.2022.103737

84. Bhattacharya M, Sharma AR, Dhama K, Agoramoorthy G, Chakraborty C. Omicron variant (B.1.1.529) of SARS-CoV-2: understanding mutations in the genome, S-glycoprotein, and antibody-binding regions. Geroscience (2022) 44:2. doi: 10.1007/s11357-022-00532-4

85. Dhawan M, Priyanka, Choudhary OP. Omicron SARS-CoV-2 variant: Reasons of emergence and lessons learnt. Int J Surg (2022) 97:doi: 10.1016/j.ijsu.2021.106198

86. World Health Organization. DRAFT landscape of COVID-19 candidate vaccines (2021). https://www.who.int/publications/m/item/draft-landscape-of-covid-19-candidate-vaccines [Accessed 6 December 2022].

87. Stern PL. Key steps in vaccine development. Ann Allergy Asthma Im (2020) 125:1. doi: 10.1016/j.anai.2020.01.025

88. Minor PD. Live attenuated vaccines: Historical successes and current challenges. Virology (2015) 479-480:doi: 10.1016/j.virol.2015.03.032

89. Poon B, Hsu JF, Gudeman V, Chen IS, Grovit-Ferbas K. Formaldehyde-treated, heat-inactivated virions with increased human immunodeficiency virus type 1 env can be used to induce high-titer neutralizing antibody responses. J Virol (2005) 79:16. doi: 10.1128/JVI.79.16.10210-10217.2005

90. Wang Q, Zhang L, Kuwahara K, Li L, Liu Z, Li T, et al. Immunodominant SARS coronavirus epitopes in humans elicited both enhancing and neutralizing effects on infection in non-human primates. ACS Infect Dis (2016) 2:5. doi: 10.1021/acsinfecdis.6b00006

91. Yang ZY, Werner HC, Kong WP, Leung K, Traggiai E, Lanzavecchia A, et al. Evasion of antibody neutralization in emerging severe acute respiratory syndrome coronaviruses. P Natl Acad Sci USA (2005) 102:3. doi: 10.1073/pnas.0409065102

92. Gao Q, Bao L, Mao H, Wang L, Xu K, Yang M, et al. Development of an inactivated vaccine candidate for SARS-CoV-2. Science (2020) 369:6499. doi: 10.1126/science.abc1932

93. Wang H, Zhang Y, Huang B, Deng W, Quan Y, Wang W, et al. Development of an Inactivated Vaccine Candidate, BBIBP-CorV, with Potent Protection against SARS-CoV-2. Cell (2020) 182:3. doi: 10.1016/j.cell.2020.06.008

94. Thanh Le T, Andreadakis Z, Kumar A, Gomez Roman R, Tollefsen S, Saville M, et al. The COVID-19 vaccine development landscape. Nat Rev Drug Discov (2020) 19:5. doi: 10.1038/d41573-020-00073-5

95. Robert-Guroff M. Replicating and non-replicating viral vectors for vaccine development. Curr Opin Biotech (2007) 18:6. doi: 10.1016/j.copbio.2007.10.010

96. van Riel D, de Wit E. Next-generation vaccine platforms for COVID-19. Nat Mater (2020) 19:8. doi: 10.1038/s41563-020-0746-0

97. Case JB, Rothlauf PW, Chen RE, Kafai NM, Fox JM, Smith BK, et al. Replication-competent vesicular stomatitis virus vaccine vector protects against SARS-CoV-2-mediated pathogenesis in mice. Cell Host Microbe (2020) 28:3. doi: 10.1016/j.chom.2020.07.018

98. Zhu FC, Guan XH, Li YH, Huang JY, Jiang T, Hou LH, et al. Immunogenicity and safety of a recombinant adenovirus type-5-vectored COVID-19 vaccine in healthy adults aged 18 years or older: a randomised, double-blind, placebo-controlled, phase 2 trial. Lancet (2020) 396:10249. doi: 10.1016/S0140-6736(20)31605-6

99. Zhao Z, Anselmo AC, Mitragotri S. Viral vector-based gene therapies in the clinic. Bioeng Transl Med (2022) 7:1. doi: 10.1002/btm2.10258

100. Zhu FC, Li YH, Guan XH, Hou LH, Wang WJ, Li JX, et al. Safety, tolerability, and immunogenicity of a recombinant adenovirus type-5 vectored COVID-19 vaccine: a dose-escalation, open-label, non-randomised, first-in-human trial. Lancet (2020) 395:10240. doi: 10.1016/S0140-6736(20)31208-3

101. Tebas P, Kraynyak KA, Patel A, Maslow JN, Morrow MP, Sylvester AJ, et al. Intradermal SynCon® Ebola GP DNA vaccine is temperature stable and safely demonstrates cellular and humoral immunogenicity advantages in healthy volunteers. J Intfect Dis (2019) 220:3. doi: 10.1093/infdis/jiz132

102. Martin JE, Louder MK, Holman LA, Gordon IJ, Enama ME, Larkin BD, et al. A SARS DNA vaccine induces neutralizing antibody and cellular immune responses in

healthy adults in a Phase I clinical trial. Vaccine (2008) 26:50. doi: 10.1016/j.vaccine.2008.09.026

103. Yang ZY, Kong WP, Huang Y, Roberts A, Murphy BR, Subbarao K, et al. A DNA vaccine induces SARS coronavirus neutralization and protective immunity in mice. Nature (2004) 428:6982. doi: 10.1038/nature02463

104. Modjarrad K, Roberts CC, Mills KT, Castellano AR, Paolino K, Muthumani K, et al. Safety and immunogenicity of an anti-Middle East respiratory syndrome coronavirus DNA vaccine: a phase 1, open-label, single-arm, dose-escalation trial. Lancet Infect Dis (2019) 19:9. doi: 10.1016/S1473-3099(19)30266-X

105. Muthumani K, Falzarano D, Reuschel EL, Tingey C, Flingai S, Villarreal DO, et al. A synthetic consensus anti-spike protein DNA vaccine induces protective immunity against Middle East respiratory syndrome coronavirus in nonhuman primates. Sci Transl Med (2015) 7:301. doi: 10.1126/scitranslmed.aac7462

106. Yu J, Tostanoski LH, Peter L, Mercado NB, McMahan K, Mahrokhian SH, et al. DNA vaccine protection against SARS-CoV-2 in rhesus macaques. Science (2020) 369:6505. doi: 10.1126/science.abc6284

107. He Y, Zhou Y, Liu S, Kou Z, Li W, Farzan M, et al. Receptor-binding domain of SARS-CoV spike protein induces highly potent neutralizing antibodies: implication for developing subunit vaccine. Biochem Bioph Res Co (2004) 324:2. doi: 10.1016/j.bbrc.2004.09.106

108. Zost SJ, Gilchuk P, Chen RE, Case JB, Reidy JX, Trivette A, et al. Rapid isolation and profiling of a diverse panel of human monoclonal antibodies targeting the SARS-CoV-2 spike protein. Nat Med (2020) 26:9. doi: 10.1038/s41591-020-0998-x

109. Pardi N, Tuyishime S, Muramatsu H, Kariko K, Mui BL, Tam YK, et al. Expression kinetics of nucleoside-modified mRNA delivered in lipid nanoparticles to mice by various routes. J Control Release (2015) 217:doi: 10.1016/j.jconrel.2015.08.007

110. Wang F, Kream RM, Stefano GB. An Evidence Based Perspective on mRNA-SARS-CoV-2 Vaccine Development. Med Sci Monit (2020) 26:doi: 10.12659/MSM.924700

111. Pardi N, Hogan MJ, Porter FW, Weissman D. mRNA vaccines - a new era in vaccinology. Nat Rev Drug Discov (2018) 17:4. doi: 10.1038/nrd.2017.243

112. Schlake T, Thess A, Fotin-Mleczek M, Kallen KJ. Developing mRNA-vaccine technologies. RNA Biol (2012) 9:11. doi: 10.4161/rna.22269

113. Sahin U, Muik A, Derhovanessian E, Vogler I, Kranz LM, Vormehr M, et al. COVID-19 vaccine BNT162b1 elicits human antibody and T(H)1 T cell responses. Nature (2020) 586:7830. doi: 10.1038/s41586-020-2814-7

114. Khehra N, Padda I, Jaferi U, Atwal H, Narain S, Parmar MS. Tozinameran (BNT162b2) Vaccine: The Journey from Preclinical Research to Clinical Trials and Authorization. AAPS PharmSciTech (2021) 22:5. doi: 10.1208/s12249-021-02058-y

115. Teo SP. Review of COVID-19 mRNA Vaccines: BNT162b2 and mRNA-1273. J Pharm Pract (2021) doi: 10.1177/08971900211009650

116. Kruse RL. Therapeutic strategies in an outbreak scenario to treat the novel coronavirus originating in Wuhan, China. F1000Res (2020) 9:doi: 10.12688/f1000research.22211.2

117. Jiang S, Du L, Shi Z. An emerging coronavirus causing pneumonia outbreak in Wuhan, China: calling for developing therapeutic and prophylactic strategies. Emerg Microbes Infec (2020) 9:1. doi: 10.1080/22221751.2020.1723441

118. Sekimukai H, Iwata-Yoshikawa N, Fukushi S, Tani H, Kataoka M, Suzuki T, et al. Gold nanoparticle-adjuvanted S protein induces a strong antigen-specific IgG response against severe acute respiratory syndrome-related coronavirus infection, but fails to induce protective antibodies and limit eosinophilic infiltration in lungs. Microbiol Immunol (2020) 64:1. doi: 10.1111/1348-0421.12754

119. Weingartl H, Czub M, Czub S, Neufeld J, Marszal P, Gren J, et al. Immunization with modified vaccinia virus Ankara-based recombinant vaccine against severe acute respiratory syndrome is associated with enhanced hepatitis in ferrets. Journal of virology (2004) 78:22. doi: 10.1128/JVI.78.22.12672-12676.2004

120. Honda-Okubo Y, Barnard D, Ong CH, Peng B-H, Tseng C-TK, Petrovsky N. Severe acute respiratory syndrome-associated coronavirus vaccines formulated with delta inulin adjuvants provide enhanced protection while ameliorating lung eosinophilic immunopathology. Journal of virology (2015) 89:6. doi: 10.1128/JVI.02980-14

121. Lee JS, Poo H, Han DP, Hong SP, Kim K, Cho MW, et al. Mucosal immunization with surface-displayed severe acute respiratory syndrome coronavirus spike protein on

Lactobacillus casei induces neutralizing antibodies in mice. J Virol (2006) 80:8. doi: 10.1128/JVI.80.8.4079-4087.2006

122. Zhou Z, Post P, Chubet R, Holtz K, McPherson C, Petric M, et al. A recombinant baculovirus-expressed S glycoprotein vaccine elicits high titers of SARS-associated coronavirus (SARS-CoV) neutralizing antibodies in mice. Vaccine (2006) 24:17. doi: 10.1016/j.vaccine.2006.01.059

123. Bhattacharya M, Sharma AR, Patra P, Ghosh P, Sharma G, Patra BC, et al. Development of epitope-based peptide vaccine against novel coronavirus 2019 (SARS-CoV-2): Immunoinformatics approach. J Med Virol (2020) 92:6. doi: 10.1002/jmv.25736

124. Li Y, Tenchov R, Smoot J, Liu C, Watkins S, Zhou Q. A Comprehensive Review of the Global Efforts on COVID-19 Vaccine Development. ACS Cent Sci (2021) 7:4. doi: 10.1021/acscentsci.1c00120

125. Heath PT, Galiza EP, Baxter DN, Boffito M, Browne D, Burns F, et al. Safety and Efficacy of NVX-CoV2373 Covid-19 Vaccine. N Engl J Med (2021) doi: 10.1056/NEJMoa2107659

126. Tian JH, Patel N, Haupt R, Zhou H, Weston S, Hammond H, et al. SARS-CoV-2 spike glycoprotein vaccine candidate NVX-CoV2373 immunogenicity in baboons and protection in mice. Nat Commun (2021) 12:1. doi: 10.1038/s41467-020-20653-8

127. Keech C, Albert G, Cho I, Robertson A, Reed P, Neal S, et al. Phase 1-2 Trial of a SARS-CoV-2 Recombinant Spike Protein Nanoparticle Vaccine. N Engl J Med (2020) 383:24. doi: 10.1056/NEJMoa2026920

128. Ghorbani A, Zare F, Sazegari S, Afsharifar A, Eskandari MH, Pormohammad A. Development of a novel platform of virus-like particle (VLP) based vaccine against coronavirus 2019 (SARS-CoV-2) by exposing of epitopes: an immunoinformatics approach. New Microbes and New Infections (2020) doi: 10.1016/j.nmni.2020.100786

129. Xu R, Shi M, Li J, Song P, Li N. Construction of SARS-CoV-2 Virus-Like Particles by Mammalian Expression System. Front Bioeng Biotechnol (2020) 8:doi: 10.3389/fbioe.2020.00862

130. Mohsen MO, Augusto G, Bachmann MF. The 3Ds in virus-like particle based-vaccines: "Design, Delivery and Dynamics". Immunol Rev (2020) 296:1. doi: 10.1111/imr.12863

131. Health Canada. Health Canada authorizes Medicago COVID-19 vaccine for adults 18 to 64 years of age (2022). https://www.canada.ca/en/health-canada/news/2022/02/health-canada-authorizes-medicago-covid-19-vaccine-for-adults-18-to-64-years-of-age.html [Accessed 6 December 2022].

132. World Health Organization. COVID-19 Vaccines with WHO Emergency Use Listing (2022). https://extranet.who.int/pqweb/vaccines/vaccinescovid-19-vaccine-eul-issued [Accessed 6 December 2022].

133. Fiolet T, Kherabi Y, MacDonald C-J, Ghosn J, Peiffer-Smadja N. Comparing COVID-19 vaccines for their characteristics, efficacy and effectiveness against SARS-CoV-2 and variants of concern: A narrative review. Clinical Microbiology and Infection (2021) doi: 10.1016/j.cmi.2021.10.005

134. Bates TA, Leier HC, Lyski ZL, McBride SK, Coulter FJ, Weinstein JB, et al. Neutralization of SARS-CoV-2 variants by convalescent and BNT162b2 vaccinated serum. Nat Commun (2021) 12:1. doi: 10.1038/s41467-021-25479-6

135. Planas D, Veyer D, Baidaliuk A, Staropoli I, Guivel-Benhassine F, Rajah MM, et al. Reduced sensitivity of SARS-CoV-2 variant Delta to antibody neutralization. Nature (2021) 596:7871. doi: 10.1038/s41586-021-03777-9

136. Mahase E. Covid-19: Novavax vaccine efficacy is 86% against UK variant and 60% against South African variant. BMJ (2021) 372:doi: 10.1136/bmj.n296

137. Lu L, Mok BW, Chen LL, Chan JM, Tsang OT, Lam BH, et al. Neutralization of SARS-CoV-2 Omicron variant by sera from BNT162b2 or Coronavac vaccine recipients. Clin Infect Dis (2021) doi: 10.1093/cid/ciab1041

138. Capell T, Twyman RM, Armario-Najera V, Ma JK, Schillberg S, Christou P. Potential applications of plant biotechnology against SARS-CoV-2. Trends Plant Sci (2020) 25:7. doi: 10.1016/j.tplants.2020.04.009

139. Kumar M, Kumari N, Thakur N, Bhatia SK, Saratale GD, Ghodake G, et al. A comprehensive overview on the production of vaccines in plant-based expression

systems and the scope of plant biotechnology to combat against SARS-CoV-2 virus pandemics. Plants (2021) 10:6. doi: 10.3390/plants10061213

140. Lobato Gomez M, Huang X, Alvarez D, He W, Baysal C, Zhu C, et al. Contributions of the international plant science community to the fight against human infectious diseases - part 1: epidemic and pandemic diseases. Plant Biotechnol J (2021) doi: 10.1111/pbi.13657

141. Singh R, Ren Z, Shi Y, Lin S, Kwon KC, Balamurugan S, et al. Affordable oral health care: dental biofilm disruption using chloroplast made enzymes with chewing gum delivery. Plant Biotechnology Journal (2021) 19:10. doi: 10.1111/pbi.13643

142. Yao J, Weng Y, Dickey A, Wang KY. Plants as factories for human pharmaceuticals: Applications and challenges. Int J Mol Sci (2015) 16:12. doi: 10.3390/ijms161226122

143. Sabalza M, Christou P, Capell T. Recombinant plant-derived pharmaceutical proteins: current technical and economic bottlenecks. Biotechnol Lett (2014) 36:12. doi: 10.1007/s10529-014-1621-3

144. Moussavou G, Ko K, Lee JH, Choo YK. Production of monoclonal antibodies in plants for cancer immunotherapy. Biomed Res Int (2015) 2015:doi: 10.1155/2015/306164

145. Ecker DM, Jones SD, Levine HL. The therapeutic monoclonal antibody market. MAbs (2015) 7:1. doi: 10.4161/19420862.2015.989042

146. Buyel JF, Fischer R. Predictive models for transient protein expression in tobacco (Nicotiana tabacum L.) can optimize process time, yield, and downstream costs. Biotechnol Bioeng (2012) 109:10. doi: 10.1002/bit.24523

147. Chen Q, Davis KR. The potential of plants as a system for the development and production of human biologics. F1000Research (2016) 5:doi: 10.12688/f1000research.8010.1

148. Sack M, Rademacher T, Spiegel H, Boes A, Hellwig S, Drossard J, et al. From gene to harvest: insights into upstream process development for the GMP production of a monoclonal antibody in transgenic tobacco plants. Plant Biotechnol J (2015) 13:8. doi: 10.1111/pbi.12438

149. Ma JK, Christou P, Chikwamba R, Haydon H, Paul M, Ferrer MP, et al. Realising the value of plant molecular pharming to benefit the poor in developing countries and emerging economies. Plant Biotechnol J (2013) 11:9. doi: 10.1111/pbi.12127

150. Moon KB, Park JS, Park YI, Song IJ, Lee HJ, Cho HS, et al. Development of Systems for the Production of Plant-Derived Biopharmaceuticals. Plants (Basel) (2019) 9:1. doi: 10.3390/plants9010030

151. Santos RB, Abranches R, Fischer R, Sack M, Holland T. Putting the Spotlight Back on Plant Suspension Cultures. Front Plant Sci (2016) 7:doi: 10.3389/fpls.2016.00297

152. Goodin MM, Zaitlin D, Naidu RA, Lommel SA. Nicotiana benthamiana: its history and future as a model for plant-pathogen interactions. Mol Plant Microbe Interact (2008) 21:8. doi: 10.1094/MPMI-21-8-1015

153. Diamos AG, Mason HS. High-level expression and enrichment of norovirus virus-like particles in plants using modified geminiviral vectors. Protein expression and purification (2018) 151:doi: 10.1016/j.pep.2018.06.011

154. Lomonossoff GP, D'Aoust MA. Plant-produced biopharmaceuticals: A case of technical developments driving clinical deployment. Science (2016) 353:6305. doi: 10.1126/science.aaf6638

155. Krenek P, Samajova O, Luptovciak I, Doskocilova A, Komis G, Samaj J. Transient plant transformation mediated by Agrobacterium tumefaciens: Principles, methods and applications. Biotechnol Adv (2015) 33:6 Pt 2. doi: 10.1016/j.biotechadv.2015.03.012

156. Olinger GG, Jr., Pettitt J, Kim D, Working C, Bohorov O, Bratcher B, et al. Delayed treatment of Ebola virus infection with plant-derived monoclonal antibodies provides protection in rhesus macaques. Proc Natl Acad Sci U S A (2012) 109:44. doi: 10.1073/pnas.1213709109

157. Chen Q, He J, Phoolcharoen W, Mason HS. Geminiviral vectors based on bean yellow dwarf virus for production of vaccine antigens and monoclonal antibodies in plants. Hum Vaccin (2011) 7:3. doi: 10.4161/hv.7.3.14262

158. Ahmad AR, Kaewpungsup P, Khorattanakulchai N, Rattanapisit K, Pavasant P, Phoolcharoen W. Recombinant Human Dentin Matrix Protein 1 (hDMP1) Expressed

in Nicotiana benthamiana Potentially Induces Osteogenic Differentiation. Plants (Basel) (2019) 8:12. doi: 10.3390/plants8120566

159. Ma JK, Drake PM, Christou P. The production of recombinant pharmaceutical proteins in plants. Nat Rev Genet (2003) 4:10. doi: 10.1038/nrg1177

160. Yusibov V, Streatfield SJ, Kushnir N. Clinical development of plant-produced recombinant pharmaceuticals: vaccines, antibodies and beyond. Hum Vaccin (2011) 7:3. doi: 10.4161/hv.7.3.14207

161. Hager KJ, Perez Marc G, Gobeil P, Diaz RS, Heizer G, Llapur C, et al. Efficacy and Safety of a Recombinant Plant-Based Adjuvanted Covid-19 Vaccine. N Engl J Med (2022) 386:22. doi: 10.1056/NEJMoa2201300

162. Shanmugaraj B, Khorattanakulchai N, Panapitakkul C, Malla A, Im-Erbsin R, Inthawong M, et al. Preclinical evaluation of a plant-derived SARS-CoV-2 subunit vaccine: Protective efficacy, immunogenicity, safety, and toxicity. Vaccine (2022) 40:32. doi: 10.1016/j.vaccine.2022.05.087

163. Siriwattananon K, Manopwisedjaroen S, Shanmugaraj B, Rattanapisit K, Phumiamorn S, Sapsutthipas S, et al. Plant-produced receptor-binding domain of SARS-CoV-2 elicits potent neutralizing responses in mice and non-human primates. Front Plant Sci (2021) 12:-. doi: 10.3389/fpls.2021.682953

164. Shanmugaraj B, Siriwattananon K, Malla A, Phoolcharoen W. Potential for Developing Plant-Derived Candidate Vaccines and Biologics against Emerging Coronavirus Infections. Pathogens (2021) 10:8. doi: 10.3390/pathogens10081051

165. COVID19 Vaccine Tracker. Baiya Phytopharm Co Ltd: Baiya SARS-CoV-2 Vax 2 (2022). https://covid19.trackvaccines.org/vaccines/182/ [Accessed 6 December 2022].

166. Ward BJ, Makarkov A, Séguin A, Pillet S, Trépanier S, Dhaliwall J, et al. Efficacy, immunogenicity, and safety of a plant-derived, quadrivalent, virus-like particle influenza vaccine in adults (18–64 years) and older adults (≥ 65 years): two multicentre, randomised phase 3 trials. Lancet (2020) doi: 10.1016/S0140-6736(20)32014-6

167. TrialSiteNews. Kentucky Bioprocessing Selects Meridian Clinical Research to Conduct Phase I Influenza Vaccine Clinical Trial of KBP-V001 (2020). https://www.trialsitenews.com/kentucky-bioprocessing-selects-meridian-clinical-

research-to-conduct-phase-i-influenza-vaccine-clinical-trial-of-kbp-v001/

[Accessed 6 December 2022].

168. Pillet S, Aubin E, Trepanier S, Poulin JF, Yassine-Diab B, Ter Meulen J, et al. Humoral and cell-mediated immune responses to H5N1 plant-made virus-like particle vaccine are differentially impacted by alum and GLA-SE adjuvants in a Phase 2 clinical trial. NPJ Vaccines (2018) 3:doi: 10.1038/s41541-017-0043-3

169. Loh HS, Green BJ, Yusibov V. Using transgenic plants and modified plant viruses for the development of treatments for human diseases. Curr Opin Virol (2017) 26:doi: 10.1016/j.coviro.2017.07.019

170. Hodgins B, Pillet S, Landry N, Ward BJ. A plant-derived VLP influenza vaccine elicits a balanced immune response even in very old mice with co-morbidities. PloS one (2019) 14:1. doi: 10.1371/journal.pone.0210009

171. Pillet S, Racine T, Nfon C, Di Lenardo TZ, Babiuk S, Ward BJ, et al. Plant-derived H7 VLP vaccine elicits protective immune response against H7N9 influenza virus in mice and ferrets. Vaccine (2015) 33:46. doi: 10.1016/j.vaccine.2015.09.065

172. Bendandi M, Marillonnet S, Kandzia R, Thieme F, Nickstadt A, Herz S, et al. Rapid, high-yield production in plants of individualized idiotype vaccines for non-Hodgkin's lymphoma. Ann Oncol (2010) 21:12. doi: 10.1093/annonc/mdq256

173. Yusibov V, Hooper DC, Spitsin SV, Fleysh N, Kean RB, Mikheeva T, et al. Expression in plants and immunogenicity of plant virus-based experimental rabies vaccine. Vaccine (2002) 20:25-26. doi: 10.1016/s0264-410x(02)00260-8

174. Pollet J, Chen WH, Strych U. Recombinant protein vaccines, a proven approach against coronavirus pandemics. Adv Drug Deliv Rev (2021) 170:-. doi: 10.1016/j.addr.2021.01.001

175. Reed SG, Orr MT, Fox CB. Key roles of adjuvants in modern vaccines. Nat Med (2013) 19:12. doi: 10.1038/nm.3409

176. Lindblad EB. Aluminium compounds for use in vaccines. Immunology and cell biology (2004) 82:5. doi: 10.1111/j.0818-9641.2004.01286.x

177. Glenny A, Pope C, Waddington H, Wallace U. Immunological notes. xvii–xxiv. The Journal of Pathology and Bacteriology (1926) 29:1. doi: 10.1002/path.1700290106

178. Clements CJ, Griffiths E. The global impact of vaccines containing aluminium adjuvants. Vaccine (2002) 20 Suppl 3:doi: 10.1016/s0264-410x(02)00168-8

179. Reed SG, Bertholet S, Coler RN, Friede M. New horizons in adjuvants for vaccine development. Trends Immunol (2009) 30:1. doi: 10.1016/j.it.2008.09.006

180. Brewer JM, Conacher M, Hunter CA, Mohrs M, Brombacher F, Alexander J. Aluminium hydroxide adjuvant initiates strong antigen-specific Th2 responses in the absence of IL-4- or IL-13-mediated signaling. J Immunol (1999) 163:12. doi:

181. Kool M, Soullie T, van Nimwegen M, Willart MA, Muskens F, Jung S, et al. Alum adjuvant boosts adaptive immunity by inducing uric acid and activating inflammatory dendritic cells. J Exp Med (2008) 205:4. doi: 10.1084/jem.20071087

182. Coffman RL, Sher A, Seder RA. Vaccine adjuvants: putting innate immunity to work. Immunity (2010) 33:4. doi: 10.1016/j.immuni.2010.10.002

183. Rattanapisit K, Bulaon CJI, Khorattanakulchai N, Shanmugaraj B, Wangkanont K, Phoolcharoen W. Plant-produced SARS-CoV-2 receptor binding domain (RBD) variants showed differential binding efficiency with anti-spike specific monoclonal antibodies. Plos one (2021) 16:8. doi: 10.1371/journal.pone.0253574

184. Frey A, Di Canzio J, Zurakowski D. A statistically defined endpoint titer determination method for immunoassays. J Immunol Methods (1998) 221:1-2. doi: 10.1016/s0022-1759(98)00170-7

185. Vacharathit V, Aiewsakun P, Manopwisedjaroen S, Srisaowakarn C, Laopanupong T, Ludowyke N, et al. CoronaVac induces lower neutralising activity against variants of concern than natural infection. The Lancet Infectious Diseases (2021) 21:10. doi: 10.1016/S1473-3099(21)00568-5

186. Seephetdee C, Buasri N, Bhukhai K, Srisanga K, Manopwisedjaroen S, Lertjintanakit S, et al. Mice immunized with the vaccine candidate hexapro spike produce neutralizing antibodies against SARS-CoV-2. Vaccines (2021) 9:5. doi: 10.3390/vaccines9050498

187. Hyseni I, Molesti E, Benincasa L, Piu P, Casa E, Temperton NJ, et al. Characterisation of SARS-CoV-2 lentiviral pseudotypes and correlation between pseudotype-based neutralisation assays and live virus-based micro neutralisation assays. Viruses (2020) 12:9. doi: 10.3390/v12091011

188. Ferrara F, Temperton N. Pseudotype neutralization assays: from laboratory bench to data analysis. Methods Protoc (2018) 1:1. doi: 10.3390/mps1010008

189. Frederiksen LSF, Zhang Y, Foged C, Thakur A. The long road toward COVID-19 herd immunity: vaccine platform technologies and mass immunization strategies. Front Immunol (2020) 11:-. doi: 10.3389/fimmu.2020.01817

190. Malla A, Shanmugaraj B, Ramalingam S. Severe acute respiratory syndrome coronavirus-2 (SARS-CoV-2): an emerging zoonotic respiratory pathogen in humans. J Pure Appl Microbiol (2020) 14:6327. doi: 10.22207/JPAM.14.SPL1.30

191. Hoffmann M, Arora P, Gross R, Seidel A, Hornich BF, Hahn AS, et al. SARS-CoV-2 variants B.1.351 and P.1 escape from neutralizing antibodies. Cell (2021) 184:9. doi: 10.1016/j.cell.2021.03.036

192. Barton MI, MacGowan SA, Kutuzov MA, Dushek O, Barton GJ, van der Merwe PA. Effects of common mutations in the SARS-CoV-2 Spike RBD and its ligand, the human ACE2 receptor on binding affinity and kinetics. Elife (2021) 10:doi: 10.7554/eLife.70658

193. Groves DC, Rowland-Jones SL, Angyal A. The D614G mutations in the SARS-CoV-2 spike protein: Implications for viral infectivity, disease severity and vaccine design. Biochem Biophys Res Commun (2021) 538:doi: 10.1016/j.bbrc.2020.10.109

194. Jensen B, Luebke N, Feldt T, Keitel V, Brandenburger T, Kindgen-Milles D, et al. Emergence of the E484K mutation in SARS-COV-2-infected immunocompromised patients treated with bamlanivimab in Germany. The Lancet Regional Health-Europe (2021) 8:doi: 10.1016/j.lanepe.2021.100164

195. Wang P, Casner RG, Nair MS, Wang M, Yu J, Cerutti G, et al. Increased resistance of SARS-CoV-2 variant P. 1 to antibody neutralization. Cell host & microbe (2021) 29:5. doi: 10.1016/j.chom.2021.04.007

196. Burgos RM, Badowski ME, Drwiega E, Ghassemi S, Griffith N, Herald F, et al. The race to a COVID-19 vaccine: opportunities and challenges in development and distribution. Drugs Context (2021) 10:-. doi: 10.7573/dic.2020-12-2

197. Chen TH, Liu WC, Chen IC, Liu CC, Huang MH, Jan JT, et al. Recombinant hemagglutinin produced from Chinese hamster ovary (CHO) stable cell clones and

a PELC/CpG combination adjuvant for H7N9 subunit vaccine development. Vaccine (2019) 37:47. doi: 10.1016/j.vaccine.2019.02.040

198. Hartwig DD, Oliveira TL, Seixas FK, Forster KM, Rizzi C, Hartleben CP, et al. High yield expression of leptospirosis vaccine candidates ligA and LipL32 in the methylotrophic yeast *Pichia pastoris*. Microb Cell Fact (2010) 9:-. doi: 10.1186/1475-2859-9-98

199. He J, Peng L, Lai H, Hurtado J, Stahnke J, Chen Q. A plant-produced antigen elicits potent immune responses against West Nile virus in mice. Biomed Res Int (2014) 2014:-. doi: 10.1155/2014/952865

200. Tebianian M, Hoseini AZ, Ebrahimi SM, Memarnejadian A, Mokarram AR, Mahdavi M, et al. Cloning, expression, and immunogenicity of novel fusion protein of *Mycobacterium tuberculosis* based on ESAT-6 and truncated C-terminal fragment of HSP70. Biologicals (2011) 39:3. doi: 10.1016/j.biologicals.2011.02.002

201. Hefferon KL. The role of plant expression platforms in biopharmaceutical development: possibilities for the future. Expert Rev Vaccines (2019) 18:12. doi: 10.1080/14760584.2019.1704264

202. He W, Baysal C, Lobato Gomez M, Huang X, Alvarez D, Zhu C, et al. Contributions of the international plant science community to the fight against infectious diseases in humans - part 2: affordable drugs in edible plants for endemic and re-emerging diseases. Plant Biotechnol J (2021) doi: 10.1111/pbi.13658

203. Sun S, He L, Zhao Z, Gu H, Fang X, Wang T, et al. Recombinant vaccine containing an RBD-Fc fusion induced protection against SARS-CoV-2 in nonhuman primates and mice. Cell Mol Immunol (2021) 18:4. doi: 10.1038/s41423-021-00658-z

204. Du L, Zhao G, He Y, Guo Y, Zheng B-J, Jiang S, et al. Receptor-binding domain of SARS-CoV spike protein induces long-term protective immunity in an animal model. Vaccine (2007) 25:15. doi: 10.1016/j.vaccine.2006.10.031

205. Li Y, Du L, Qiu H, Zhao G, Wang L, Zhou Y, et al. A recombinant protein containing highly conserved hemagglutinin residues 81-122 of influenza H5N1 induces strong humoral and mucosal immune responses. Biosci Trends (2013) 7:3. doi: 10.5582/bst.2013.v7.3.129

206. Yang S, Li Y, Dai L, Wang J, He P, Li C, et al. Safety and immunogenicity of a recombinant tandem-repeat dimeric RBD-based protein subunit vaccine (ZF2001) against COVID-19 in adults: two randomised, double-blind, placebo-controlled, phase 1 and 2 trials. Lancet Infect Dis (2021) doi: 10.1016/S1473-3099(21)00127-4

207. Gupta RK, Relyveld EH, Lindblad EB, Bizzini B, Ben-Efraim S, Gupta CK. Adjuvants—a balance between toxicity and adjuvanticity. Vaccine (1993) 11:3. doi: 10.1016/0264-410X(93)90190-9

208. Yang L, Tian D, Han JB, Fan W, Zhang Y, Li Y, et al. A recombinant receptor-binding domain in trimeric form generates protective immunity against SARS-CoV-2 infection in nonhuman primates. Innovation (N Y) (2021) 2:3. doi: 10.1016/j.xinn.2021.100140

209. Zhou D, Dejnirattisai W, Supasa P, Liu C, Mentzer AJ, Ginn HM, et al. Evidence of escape of SARS-CoV-2 variant B.1.351 from natural and vaccine-induced sera. Cell (2021) 184:9. doi: 10.1016/j.cell.2021.02.037

210. Cao Y, Yisimayi A, Bai Y, Huang W, Li X, Zhang Z, et al. Humoral immune response to circulating SARS-CoV-2 variants elicited by inactivated and RBD-subunit vaccines. Cell Res (2021) 31:7. doi: 10.1038/s41422-021-00514-9

211. Chen Y, Shen H, Huang R, Tong X, Wu C. Serum neutralising activity against SARS-CoV-2 variants elicited by CoronaVac. Lancet Infect Dis (2021) doi: 10.1016/S1473-3099(21)00287-5

212. Abu-Raddad LJ, Chemaitelly H, Ayoub HH, AlMukdad S, Yassine HM, Al-Khatib HA, et al. Effect of mRNA Vaccine Boosters against SARS-CoV-2 Omicron Infection in Qatar. N Engl J Med (2022) 386:19. doi: 10.1056/NEJMoa2200797

213. Amanat F, Strohmeier S, Meade PS, Dambrauskas N, Muhlemann B, Smith DJ, et al. Vaccination with SARS-CoV-2 variants of concern protects mice from challenge with wild-type virus. PLoS Biol (2021) 19:12. doi: 10.1371/journal.pbio.3001384

214. Wang E, Chakraborty AK. Design of immunogens for eliciting antibody responses that may protect against SARS-CoV-2 variants. PLoS Comput Biol (2022) 18:9. doi: 10.1371/journal.pcbi.1010563

215. U.S. Food and Drug Administration. Development and Licensure of Vaccines to Prevent COVID-19 (2020). https://www.fda.gov/regulatory-information/search-fda-

guidance-documents/development-and-licensure-vaccines-prevent-covid-19
[Accessed 6 December 2022].

216. Schmidt F, Weisblum Y, Muecksch F, Hoffmann H-H, Michailidis E, Lorenzi JC, et al. Measuring SARS-CoV-2 neutralizing antibody activity using pseudotyped and chimeric viruses. J Exp Med (2020) 217:11. doi: 10.1084/jem.20201181

217. Shen X, Tang H, McDanal C, Wagh K, Fischer W, Theiler J, et al. SARS-CoV-2 variant B.1.1.7 is susceptible to neutralizing antibodies elicited by ancestral spike vaccines. Cell Host Microbe (2021) 29:4. doi: 10.1101/2021.01.27.428516

218. Shen X, Tang H, Pajon R, Smith G, Glenn GM, Shi W, et al. Neutralization of SARS-CoV-2 variants B.1.429 and B.1.351. N Engl J Med (2021) doi: 10.1056/NEJMc2103740

APPENDICES

APPENDIX A

pGEM®-T Easy Cloning Vector map (Promega, USA)
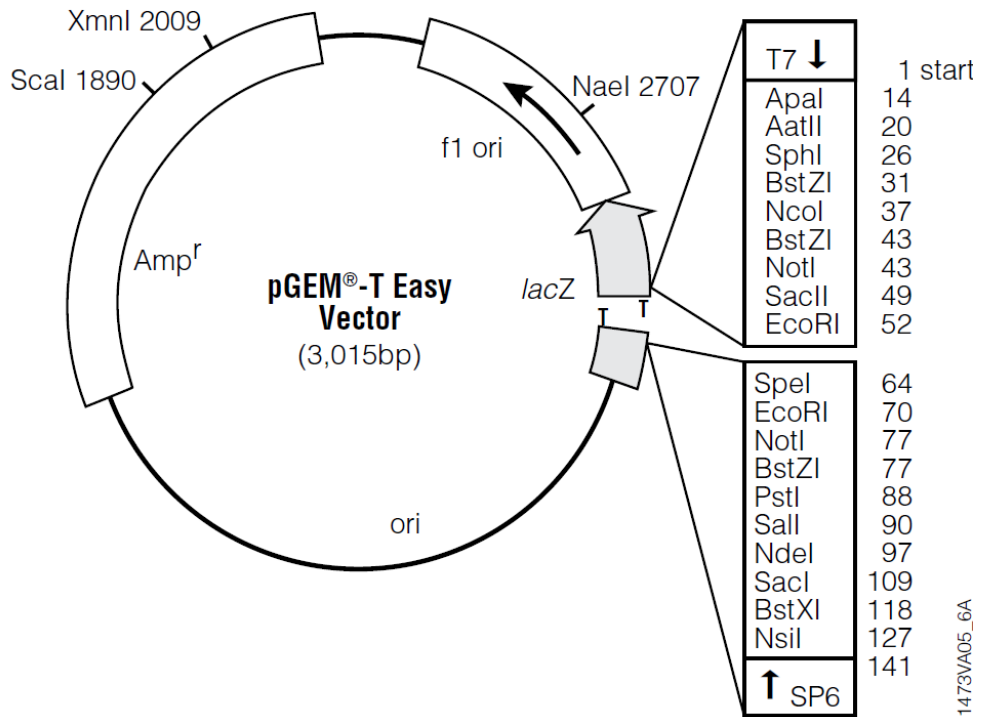
APPENDIX B

pBYR2eK2Md Plant Expression Vector Map

pBYR2eK2Md-GFP
(13179 bp)

จุฬาลงกรณ์มหาวิทยาลัย
CHULALONGKORN UNIVERSITY
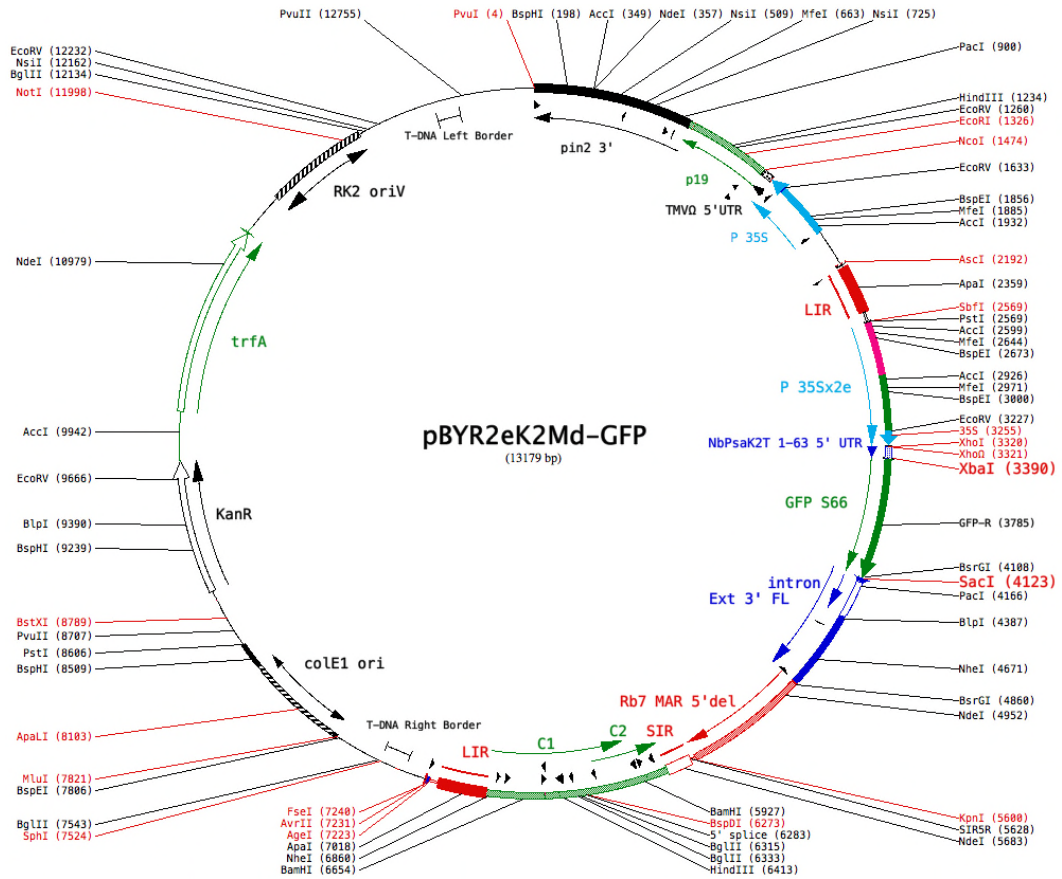
APPENDIX C

The amino acid sequence alignment of variant RBD regions

```
Wuhan RBD    318 FRVQPTESIVRFPNITNLCPFGEVFNATRFASVYAWNRKRISNCVADYSV 367
Alpha RBD        -------------------------------------------------
Beta RBD         -------------------------------------------------
Gamma RBD        -------------------------------------------------
Kappa RBD        -------------------------------------------------
Delta RBD        -------------------------------------------------
Epsilon RBD      -------------------------------------------------


Wuhan RBD    368 LYNSASFSTFKCYGVSPTKLNDLCFTNVYADSFVIRGDEVRQIAPGQTGK 417
Alpha RBD        -------------------------------------------------
Beta RBD         ------------------------------------------------N
Gamma RBD        ------------------------------------------------T
Kappa RBD        -------------------------------------------------
Delta RBD        -------------------------------------------------
Epsilon RBD      -------------------------------------------------


Wuhan RBD    418 IADYNYKLPDDFTGCVIAWNSNNLDSKVGGNYNYLYRLFRKSNLKPFERD 467
Alpha RBD        -------------------------------------------------
Beta RBD         -------------------------------------------------
Gamma RBD        -------------------------------------------------
Kappa RBD        ----------------------------------R--------------
Delta RBD        ----------------------------------R--------------
Epsilon RBD      ----------------------------------R--------------


Wuhan RBD    468 ISTEIYQAGSTPCNGVEGFNCYFPLQSYGFQPTNGVGYQPYRVVVLSFEL 517
Alpha RBD        -------------------------------Y-----------------
Beta RBD         ---------------K---------------Y-----------------
Gamma RBD        ---------------K---------------------------------
Kappa RBD        ---------------Q---------------------------------
Delta RBD        ----------K--------------------------------------
Epsilon RBD      -------------------------------------------------


Wuhan RBD    518 LHAPATVCGPKKSTNLVKNKCVNFNFNGLTGTGVLTESNKKFLPFQQFGR 567
Alpha RBD        -------------------------------------------------
Beta RBD         -------------------------------------------------
Gamma RBD        -------------------------------------------------
Kappa RBD        -------------------------------------------------
Delta RBD        -------------------------------------------------
Epsilon RBD      -------------------------------------------------


Wuhan RBD    568 DIADTTDAVRDPQTLEILDITPCSFGGVSVITPGTNTSNQVAVLYQDVNC 617
Alpha RBD        --D---------------------------------------------G---
Beta RBD         ------------------------------------------------G---
Gamma RBD        ------------------------------------------------G---
Kappa RBD        ------------------------------------------------G---
Delta RBD        ------------------------------------------------G---
Epsilon RBD      ------------------------------------------------G---
```

APPENDIX D

The quantification of plant-produced variant RBD-Fc by ELISA Assay.

Standard curve
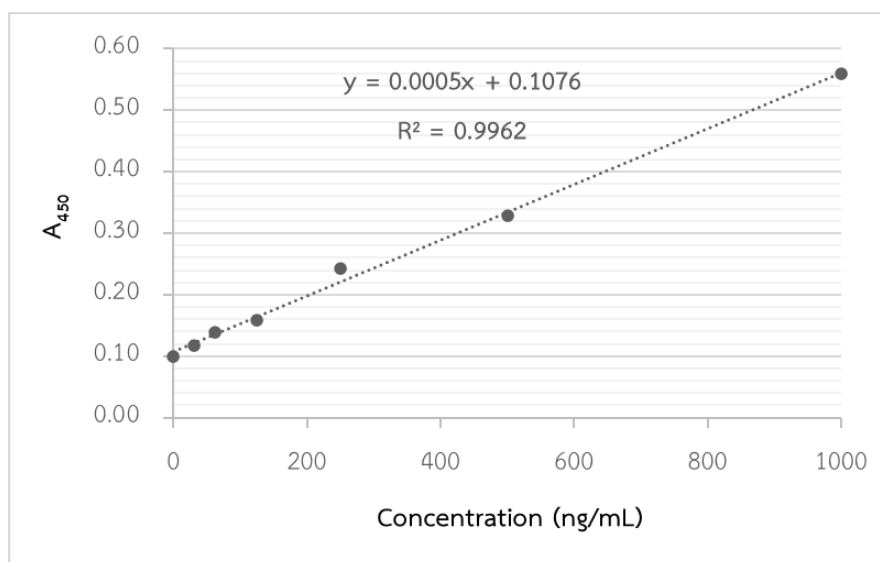
Raw data of the standard curve

Concentration	A_{450}		
(ng/mL)	Rep1	Rep2	Average
0	0.101	0.099	0.100
31.25	0.115	0.120	0.118
62.5	0.137	0.140	0.139
125	0.162	0.157	0.159
250	0.240	0.245	0.243
500	0.320	0.337	0.329
1000	0.574	0.543	0.559

The calculated concentration of plant-produced variant RBD-Fc proteins

Protein	Dilution	A450			Calculated concentration (ng/mL)		Calculated concentration (mg/mL)		Final volume (mL)	Fresh weight (g)	Yield (µg/g fresh weight)
		Rep1	Rep2	Average		X Dilution		Average			
Wuhan RBD-Fc	16,000	0.144	0.129	0.137	57.8	924,800	0.9248		0.67	53	25.3
	8,000	0.248	0.225	0.237	257.8	2,062,400	2.0624	2.00			
	4,000	0.339	0.359	0.349	482.8	1,931,200	1.9312				
	2,000	0.511	0.528	0.520	823.8	1,647,600	1.6476				
Alpha RBD-Fc	16,000	0.128	0.142	0.135	54.8	876,800	0.8768		0.64	51	23.8
	8,000	0.212	0.233	0.223	229.8	1,838,400	1.8384	1.90			
	4,000	0.349	0.356	0.353	489.8	1,959,200	1.9592				
	2,000	0.480	0.502	0.491	766.8	1,533,600	1.5336				
Beta RBD-Fc	16,000	0.148	0.161	0.155	93.8	1,500,800	1.5008		0.57	48	23.3
	8,000	0.224	0.228	0.226	236.8	1,894,400	1.8944	1.96			
	4,000	0.354	0.369	0.362	507.8	2,031,200	2.0312				
	2,000	0.518	0.496	0.507	798.8	1,597,600	1.5976				
Gamma RBD-Fc	16,000	0.127	0.131	0.129	42.8	684,800	0.6848		0.73	59	21.9
	8,000	0.222	0.218	0.220	224.8	1,798,400	1.7984	1.77			
	4,000	0.324	0.329	0.327	437.8	1,751,200	1.7512				
	2,000	0.488	0.491	0.490	763.8	1,527,600	1.5276				
Kappa RBD-Fc	16,000	0.178	0.185	0.182	147.8	2,364,800	2.3648		0.51	41	26.4
	8,000	0.240	0.232	0.236	256.8	2,054,400	2.0544	2.12			
	4,000	0.388	0.372	0.380	544.8	2,179,200	2.1792				

Protein	Dilution	A450			Calculated concentration (ng/mL)		Calculated concentration (mg/mL)		Final volume (mL)	Fresh weight (g)	Yield (µg/g fresh weight)
		Rep1	Rep2	Average		X Dilution		Average			
Delta RBD-Fc	2,000	0.598	0.575	0.587	957.8	1,915,600	1.9156		0.58	42	28.0
	16,000	0.155	0.162	0.159	101.8	1,628,800	1.6288				
	8,000	0.233	0.239	0.236	256.8	2,054,400	2.0544	2.03			
	4,000	0.362	0.355	0.359	501.8	2,007,200	2.0072				
	2,000	0.567	0.575	0.571	926.8	1,853,600	1.8536				
Epsilon RBD-Fc	16,000	0.127	0.131	0.129	42.8	684,800	0.6848		0.65	45	20.0
	8,000	0.201	0.194	0.198	179.8	1,438,400	1.4384	1.39			
	4,000	0.277	0.272	0.275	333.8	1,335,200	1.3352				
	2,000	0.470	0.461	0.466	715.8	1,431,600	1.4316				

APPENDIX E

Antibody titers of Baiya SARS-CoV-2 Vax 1 immunized monkey sera

Anti-RBD IgG titer

Group	Vaccination Group	No.	Anti-RBD IgG titer				
			Day 0	Day 14	Day 35	Day 133	Day 147
1	Control	G1/1	100	100	200	200	100
		G1/2	100	200	200	400	200
		G1/3	100	200	200	100	100
		G1/4	100	200	200	200	200
		G1/5	100	100	200	200	100
		GMT	100	152	200	200	132
		95% CI	100 - 100	95 - 243	200 - 200	109 - 368	82 - 211
2	10 μg Baiya SARS-CoV-2 Vax 1	G2/1	100	200	6,400	1600	12,800
		G2/2	100	200	12,800	1600	6,400
		G2/3	100	400	12,800	3200	12,800
		G2/4	100	100	12,800	1600	25,600
		G2/5	200	200	12,800	800	6,400
		GMT	115	200	11,143	1600	11,143
		95% CI	78 - 169	109 - 368	7,583 - 16,374	871 - 2,940	5,423 - 22,894

MN$_{50}$ titer

Group	Vaccination Group	No.	MN$_{50}$ titer				
			Day 0	Day 14	Day 35	Day 133	Day 147
1	Control	G1/1	10	10	10	10	10
		G1/2	10	10	10	10	10
		G1/3	10	10	10	10	10
		G1/4	10	10	10	10	10
		G1/5	10	10	10	10	10
		GMT	10	10	10	10	10
		95% CI	10 - 10	10 - 10	10 - 10	10 - 10	10 - 10
2	10 µg Baiya SARS-CoV-2 Vax 1	G2/1	10	10	1,280	160	2560
		G2/2	10	10	5,120	320	640
		G2/3	10	10	2,560	320	1280
		G2/4	10	10	2,560	640	5120
		G2/5	10	10	10,240	320	2560
		GMT	10	10	3,378	320	1,940
		95% CI	10 - 10	10 - 10	1,266 - 9,012	147 - 588	727 - 5,176

<u>PVNT$_{50}$</u>

Group	Vaccination Group	No.	PVNT$_{50}$ (Day 14)				
			Wuhan	Alpha	Beta	Gamma	Delta
1	Control	G1/1	1.00	1.00	1.00	1.00	1.00
		G1/2	1.00	1.00	1.00	1.00	1.00
		G1/3	1.00	1.00	1.00	1.00	1.00
		G1/4	1.00	1.00	1.00	1.00	1.00
		G1/5	1.00	1.00	1.00	1.00	23.60
		GMT	1.00	1.00	1.00	1.00	1.88
		95% CI	1.00 - 1.00	1.00 - 1.00	1.00 - 1.00	1.00 - 1.00	0.33 - 10.89
2	10 µg Baiya SARS-CoV-2 Vax 1	G2/1	111.53	76.10	1.00	1.00	70.79
		G2/2	1.00	1.00	1.00	1.00	37.39
		G2/3	1.00	1.00	1.00	1.00	35.43
		G2/4	1.10	1.00	1.00	1.00	35.44
		G2/5	1.00	1.00	1.00	1.00	25.26
		GMT	2.62	2.38	1.00	1.00	38.44
		95% CI	0.19 - 35.41	0.21 - 26.36	1.00 - 1.00	1.00 - 1.00	24.12 - 61.26

Group	Vaccination Group	No.	PVNT$_{50}$ (Day 35)				
			Wuhan	Alpha	Beta	Gamma	Delta
1	Control	G1/1	45.81	37.63	1.00	27.35	7.81
		G1/2	39.44	33.79	1.00	36.87	39.25
		G1/3	37.39	2.25	1.00	1.00	26.24
		G1/4	1.00	1.00	1.00	1.00	1.00
		G1/5	1.38	37.65	1.00	1.00	40.40
		GMT	9.86	10.15	1.00	3.99	12.66
		95% CI	0.88 - 110.60	1.13 - 91.32	1.00 - 1.00	0.38 - 42.04	1.81 - 88.70
2	10 µg Baiya SARS-CoV-2 Vax 1	G2/1	1,896.29	1,494.70	41.18	54.14	1,500.40
		G2/2	6,683.56	7,165.83	212.68	237.51	3,538.13
		G2/3	8,235.94	6,667.37	271.17	252.59	3,189.89
		G2/4	4,715.25	3,564.03	285.61	396.08	3,101.90
		G2/5	5,958.11	11,858.21	7,047.86	7,154.37	1,020.55
		GMT	4,936.83	4,965.32	343.48	391.56	2,217.40
		95% CI	2,427.96 - 10,038.14	1,849.42 - 133,330.88	33.80 - 3,490.19	42.48 - 3,608.72	1,117.58 - 4,399.55

Group	Vaccination Group	No.	PVNT$_{50}$ (Day 133)				
			Wuhan	Alpha	Beta	Gamma	Delta
1	Control	G1/1	1.00	1.00	31.97	33.07	19.87
		G1/2	15.43	39.20	38.18	37.39	38.57
		G1/3	15.83	36.59	38.25	37.15	19.34
		G1/4	1.00	39.36	35.36	1.00	1.00
		G1/5	1.00	32.24	26.27	1.00	13.52
		GMT	3.00	17.87	33.68	8.56	11.49
		95% CI	0.46 - 19.48	2.41 - 132.48	27.71 - 40.94	0.75 - 97.64	1.98 - 66.71
2	10 μg Baiya SARS-CoV-2 Vax 1	G2/1	306.18	136.96	54.20	66.97	133.29
		G2/2	887.64	179.01	64.87	73.11	220.22
		G2/3	545.72	159.88	57.16	71.31	209.04
		G2/4	357.67	230.90	138.24	104.69	204.31
		G2/5	141.63	111.68	115.66	106.71	32.08
		GMT	375.98	158.83	79.69	82.84	132.09
		95% CI	160.70 - 879.68	113.02 - 223.20	46.66 - 136.11	62.66 - 109.51	47.94 - 363.96

Group	Vaccination Group	No.	PVNT$_{50}$ (Day 147)						
			Wuhan	Alpha	Beta	Gamma	Delta	Omicron BA.1	Omicron BA.2
1	Control	G1/1	1.00	1.00	1.00	1.00	1.00		
		G1/2	1.00	1.00	1.00	1.00	1.00		
		G1/3	1.00	24.35	1.00	1.00	1.00		
		G1/4	1.00	1.00	1.00	1.00	1.00		
		G1/5	1.00	1.00	1.00	1.00	1.00		
		GMT	1.00	1.89	1.00	1.00	1.00		
		95% CI	1.00 - 1.00	0.32 - 11.15	1.00 - 1.00	1.00 - 1.00	1.00 - 1.00		
2	10 µg Baiya SARS-CoV-2 Vax 1	G2/1	4,321.60	5,311.81	2,159.17	1,549.15	4,148.60	605.95	571.34
		G2/2	2,110.86	2,951.86	926.59	474.15	1,950.37	247.70	194.18
		G2/3	1,691.40	2,052.36	1,592.80	899.84	1,334.08	405.54	310.08
		G2/4	6,836.76	9,286.19	3,339.24	3,496.39	7,490.19	846.68	597.99
		G2/5	2,127.99	4,360.26	8,534.70	9,419.19	2,148.54	512.92	470.84
		GMT	2,952.80	4,197.48	2,463.96	1,851.66	2,805.22	483.54	395.57
		95% CI	1,423.82 - 6,123.68	2,055.09 - 8,573.24	871.87 - 6,963.30	434.14 - 7,897.66	1,199.33 - 6,561.40	273.12 - 856.08	219.37 - 713.32

APPENDIX F

Antibody titers of plant-produced variant RBD-Fc vaccines immunized monkey sera

*Note: G4/4 monkey (Gamma RBD-Fc vaccine) died on day 8 (11 June 21) which acute upper airway obstruction and respiratory failure caused by choking the digested food. Accordingly, the data of G3/4 monkey was presented only on day 0 or day 8 as day 14 in some experiments by using the serum on day 8 for day 14 data with other monkeys.

Anti-RBD IgG titer

Group	Vaccination Group	No.	Sex	Anti-RBD IgG titer			
				Day 0	Day 14	Day 35	Day 56
1	Control	G1/1	M	100	100	100	100
		G1/2	M	100	100	100	100
		G1/3	F	100	100	100	100
		GMT		100	100	100	100
		95% CI		100 - 100	100 - 100	100 - 100	100 - 100
2	10 μg Alpha RBD-Fc vaccine	G2/1	M	100	200	6,400	12,800
		G2/2	M	100	100	3,200	6,400
		G2/3	M	100	400	3,200	6,400
		G2/4	F	100	200	12,800	25,600
		G2/5	F	100	100	6,400	12,800
		GMT		100	174	5,572	11,143
		95% CI		100 - 100	85 - 358	2,712 - 11,447	5,423 - 22,894
3	10 μg Beta RBD-Fc vaccine	G3/1	M	100	100	1,600	12,800
		G3/2	M	100	100	12,800	12,800
		G3/3	M	100	100	3,200	6,400
		G3/4	F	100	100	6,400	3,200
		G3/5	F	100	100	3,200	3,200
		GMT		100	100	4,222	6,400
		95% CI		100 - 100	100 - 100	1,583 - 11,265	2,706 - 15,134
4	10 μg Gamma RBD-Fc vaccine	G4/1	M	100	100	1,600	12,800
		G4/2	M	100	200	6,400	12,800
		G4/3	M	100	100	6,400	12,800
		G4/4*	F	100	100		
		G4/5	F	100	100	3,200	3,200
		GMT		100	115	3,805	9,051
		95% CI		100 - 100	78 - 168	1,324 - 10,940	3,004 - 27271

Group	Vaccination Group	No.	Sex	Anti-RBD IgG titer			
				Day 0	Day 14	Day 35	Day 56
5	10 µg Kappa RBD-Fc vaccine	G5/1	M	100	100	12,800	12,800
		G5/2	M	100	100	12,800	12,800
		G5/3	M	100	100	12,800	6,400
		G5/4	F	100	100	12,800	12,800
		G5/5	F	100	100	51,200	12,800
		GMT		100	100	16,890	11,143
		95% CI		100 - 100	100 - 100	7,822 - 36,470	7,583 - 16,374
6	10 µg Delta RBD-Fc vaccine	G6/1	M	100	800	51,200	12,800
		G6/2	M	100	800	12,800	12,800
		G6/3	F	100	200	12,800	25,600
		G6/4	F	100	100	51,200	25,600
		G6/5	F	100	1,600	51,200	51,200
		GMT		100	459	29,407	22,286
		95% CI		100 - 100	112 - 1,890	11,455 - 75,492	10,847 - 45,789
7	10 µg Epsilon RBD-Fc vaccine	G7/1	M	100	3,200	12,800	12,800
		G7/2	M	100	3,200	12,800	12,800
		G7/3	F	100	400	12,800	51,200
		G7/4	F	100	800	12,800	25,600
		G7/5	F	100	800	12,800	25,600
		GMT		100	1,213	12,800	22,286
		95% CI		100 - 100	382 - 3,848	12,800 - 12,800	10,847 - 45,789

จุฬาลงกรณ์มหาวิทยาลัย

CHULALONGKORN UNIVERSITY

MN$_{50}$ titer

Group	Vaccination Group	No.	Sex	MN$_{50}$ titer (Wuhan)				MN$_{50}$ titer (Alpha)			
				Day 0	Day 14	Day 35	Day 56	Day 0	Day 14	Day 35	Day 56
1	Control	G1/1	M	10	10	10	10	10	10	10	10
		G1/2	M	10	10	10	10	10	10	10	10
		G1/3	F	10	10	10	10	10	10	10	10
		GMT		10	10	10	10	10	10	10	10
		95% CI		10 - 10	10 - 10	10 - 10	10 - 10	10 - 10	10 - 10	10 - 10	10 - 10
2	10 μg Alpha RBD-Fc vaccine	G2/1	M	10	10	2,560	2,560	10	10	1,280	1,280
		G2/2	M	10	10	640	320	10	10	320	320
		G2/3	M	10	10	20	1,280	10	10	10	1,280
		G2/4	F	10	10	1,280	5,120	10	20	640	5,120
		G2/5	F	10	80	320	640	10	20	640	1,280
		GMT		10	15	422	1,280	10	13	279	1,280
		95% CI		10 - 10	5 - 48	41 - 4,320	328 - 4,991	10 - 10	8 - 21	26 - 3,3035	379 - 4,323
3	10 μg Beta RBD-Fc vaccine	G3/1	M	10	10	320	640	10	10	640	640
		G3/2	M	10	10	160	1,280	10	10	320	640
		G3/3	M	10	10	10	160	10	10	20	320
		G3/4	F	10	10	320	320	10	10	320	320
		G3/5	F	10	10	40	10	40	10	40	40
		GMT		10	10	92	211	13	10	139	279
		95% CI		10 - 10	10 - 10	14 - 594	21 - 2,160	6 - 28	10 - 10	22 - 900	68 - 1,146
4	10 μg Gamma RBD-Fc vaccine	G4/1	M	10	10	1,280	640	10	20	1,280	640
		G4/2	M	10	10	640	320	10	10	1,280	640

Group	Vaccination Group	No.	Sex	MN$_{50}$ titer (Wuhan)				MN$_{50}$ titer (Alpha)			
				Day 0	Day 14	Day 35	Day 56	Day 0	Day 14	Day 35	Day 56
		G4/3	M	10	10	320	320	10	10	160	640
		G4/4*	F	10	20			10	20		
		G4/5	F	10	10	320	320	10	20	320	320
		GMT		10	11	538	381	10	15	538	538
		95% CI		10 - 10	8 - 17	187 - 1,547	219 - 661	10 - 10	9 - 24	103 - 2,815	310 - 934
5	10 µg Kappa RBD-Fc vaccine	G5/1	M	10	10	320	320	10	10	320	320
		G5/2	M	10	40	320	1,280	40	20	640	640
		G5/3	M	10	10	320	640	10	10	160	320
		G5/4	F	10	20	160	640	10	10	80	320
		G5/5	F	10	10	1,280	640	10	20	640	320
		GMT		10	15	368	640	13	13	279	368
		95% CI		10 - 10	7 - 33	143 - 944	348 - 1,176	6 - 28	8 - 21	91 - 856	250 - 540
6	10 µg Delta RBD-Fc vaccine	G6/1	M	10	40	2,560	1,280	10	20	1,280	5,120
		G6/2	M	10	80	1,280	1,280	10	10	1,280	2,560
		G6/3	F	10	10	1,280	5,120	10	10	2,560	5,120
		G6/4	F	10	10	10,240	5,120	10	10	5,120	5,120
		G6/5	F	10	160	2,560	5,120	10	20	5,120	5,120
		GMT		10	35	2,560	2,941	10	13	2,560	4,457
		95% CI		10 - 10	7 - 162	892 - 7,346	1,145 - 7,549	10 - 10	8 - 21	1,083 - 6,054	3,033 - 6,550
7	10 µg Epsilon RBD-Fc vaccine	G7/1	M	10	160	2,560	2,560	10	40	5,120	5,120
		G7/2	M	10	320	2,560	5,120	10	160	5,120	5,120
		G7/3	F	10	40	5,120	10,240	10	10	2,560	10,240
		G7/4	F	10	80	1,280	2,560	10	10	2,560	2,560

Group	Vaccination Group	No.	Sex	MN$_{50}$ titer (Wuhan)				MN$_{50}$ titer (Alpha)			
				Day 0	Day 14	Day 35	Day 56	Day 0	Day 14	Day 35	Day 56
		G7/5	F	10	20	1,280	5,120	10	40	2,560	2,560
		GMT		10	80	2,229	4,457	10	30	3,378	4,457
		95% CI		10 - 10	21 - 312	1,085 - 4,579	2,169 - 9,158	10 - 10	7 - 128	2,108 - 5,412	2,169 - 9,158

Group	Vaccination Group	No.	Sex	MN$_{50}$ titer (Beta)				MN$_{50}$ titer (Delta)			
				Day 0	Day 14	Day 35	Day 56	Day 0	Day 14	Day 35	Day 56
1	Control	G1/1	M	10	10	10	20	10	10	10	10
		G1/2	M	10	40	10	10	10	10	10	10
		G1/3	F	10	10	20	10	10	10	10	10
		GMT		10	16	13	13	10	10	10	10
		95% CI		10 - 10	2 - 116	5 - 34	5 - 34	10 - 10	10 - 10	10 - 10	10 - 10
2	10 µg Alpha RBD-Fc vaccine	G2/1	M	20	20	1,280	1,280	10	10	640	1,280
		G2/2	M	10	80	320	640	10	10	80	320
		G2/3	M	10	10	80	1,280	10	10	10	1,280
		G2/4	F	10	10	1,280	10,240	10	10	320	1,280
		G2/5	F	20	80	320	1,280	10	10	160	640
		GMT		13	26	422	1,689	10	10	121	844
		95% CI		8 - 21	7 - 97	100 - 1,782	458 -6,230	10 - 10	10 - 10	17 - 879	391 - 1,824
3	10 µg Beta RBD-Fc vaccine	G3/1	M	20	80	1,280	10,240	10	10	40	320
		G3/2	M	20	20	2,560	10,240	10	10	40	320
		G3/3	M	10	40	320	5,120	10	10	10	80
		G3/4	F	10	80	1,280	1,280	10	10	40	80

Group	Vaccination Group	No.	Sex	MN$_{50}$ titer (Beta)				MN$_{50}$ titer (Delta)			
				Day 0	Day 14	Day 35	Day 56	Day 0	Day 14	Day 35	Day 56
		G3/5	F	20	40	640	640	10	10	10	40
		GMT		15	46	970	3,378	10	10	23	121
		95% CI		9 - 24	22 - 94	364 - 2,588	707 - 16,131	10 - 10	10 - 10	9 - 59	38 - 385
4	10 µg Gamma RBD-Fc vaccine	G4/1	M	10	80	2,560	5,120	10	10	160	160
		G4/2	M	10	80	5,120	5,120	10	10	20	80
		G4/3	M	10	80	1,280	2,560	10	10	80	160
		G4/4*	F	10	10			10	20		
		G4/5	F	10	80	1,280	2,560	10	10	40	160
		GMT		10	53	2,153	3,620	10	11	57	135
		95% CI		10 - 10	17 - 167	749 - 6,189	1,915 - 6,844	10 - 10	8 - 17	14 - 235	78 - 234
5	10 µg Kappa RBD-Fc vaccine	G5/1	M	10	40	320	640	10	10	80	320
		G5/2	M	10	160	1,280	2,560	10	10	320	640
		G5/3	M	10	20	1,280	2,560	10	10	160	320
		G5/4	F	40	40	640	2,560	10	10	160	320
		G5/5	F	10	160	1,280	1,280	10	10	640	640
		GMT		13	61	844	1,689	10	10	211	422
		95% CI		6 - 28	19 - 192	391 - 1,824	782 - 3,647	10 - 10	10 - 10	79 - 563	264 - 677
6	10 µg Delta RBD-Fc vaccine	G6/1	M	10	20	320	320	10	20	2,560	1,280
		G6/2	M	10	10	160	320	10	320	5,120	2,560
		G6/3	F	10	10	640	2,560	10	10	2,560	5,120
		G6/4	F	10	20	320	640	10	10	10,240	5,120
		G6/5	F	10	40	640	1,280	10	20	5,120	5,120
		GMT		10	17	368	735	10	26	4,457	3,378

Group	Vaccination Group	No.	Sex	MN$_{50}$ titer (Beta)				MN$_{50}$ titer (Delta)			
				Day 0	Day 14	Day 35	Day 56	Day 0	Day 14	Day 35	Day 56
			95% CI	10 - 10	8 - 36	179 - 755	239 - 2,258	10 - 10	4 - 157	2,169 - 9,158	1,564 - 7,294
7	10 µg Epsilon RBD-Fc vaccine	G7/1	M	10	40	640	640	10	40	1,280	2,560
		G7/2	M	10	40	320	320	10	40	2,560	2,560
		G7/3	F	10	10	640	2,560	10	10	2,560	5,120
		G7/4	F	10	10	5,120	1,280	10	10	2,560	2,560
		G7/5	F	10	20	320	640	10	20	640	2,560
		GMT		10	20	735	844	10	20	1,689	2,941
		95% CI		10 - 10	8 - 47	179 - 3,024	317 - 2,253	10 - 10	8 - 47	782 - 3,647	2,001 - 4,321

PVNT$_{50}$

Group	Vaccination Group	No.	Sex	PVNT50 (Day 0)				
				Wuhan	Alpha	Beta	Gamma	Delta
1	Control	G1/1	M	1.00	1.00	1.00	1.00	1.00
		G1/2	M	1.00	1.00	1.00	1.00	1.00
		G1/3	F	1.00	1.00	1.00	1.00	1.00
		GMT		1.00	1.00	1.00	1.00	1.00
		95% CI		1.00 - 1.00	1.00 - 1.00	1.00 - 1.00	1.00 - 1.00	1.00 - 1.00
2	10 µg Alpha RBD-Fc vaccine	G2/1	M	1.00	1.00	1.00	1.00	1.00
		G2/2	M	1.00	1.00	1.00	1.00	1.00
		G2/3	M	1.00	1.00	1.00	1.00	1.00
		G2/4	F	1.00	1.00	1.00	1.00	1.00
		G2/5	F	1.00	1.00	1.00	1.00	1.00
		GMT		1.00	1.00	1.00	1.00	1.00
		95% CI		1.00 - 1.00	1.00 - 1.00	1.00 - 1.00	1.00 - 1.00	1.00 - 1.00
3	10 µg Beta RBD-Fc vaccine	G3/1	M	1.00	1.00	1.00	1.00	1.00
		G3/2	M	1.00	1.00	1.00	1.00	1.00
		G3/3	M	1.00	1.00	1.00	1.00	1.00
		G3/4	F	1.00	1.00	1.00	1.00	1.00
		G3/5	F	1.00	1.00	1.00	1.00	1.00
		GMT		1.00	1.00	1.00	1.00	1.00
		95% CI		1.00 - 1.00	1.00 - 1.00	1.00 - 1.00	1.00 - 1.00	1.00 - 1.00
4	10 µg Gamma RBD-Fc vaccine	G4/1	M	1.00	1.00	1.00	1.00	1.00
		G4/2	M	1.00	1.00	1.00	1.00	1.00

Group	Vaccination Group	No.	Sex	PVNT50 (Day 0)				
				Wuhan	Alpha	Beta	Gamma	Delta
		G4/3	M	1.00	1.00	1.00	1.00	1.00
		G4/4*	F	1.00	1.00	1.00	1.00	1.00
		G4/5	F	1.00	1.00	1.00	1.00	1.00
		GMT		1.00	1.00	1.00	1.00	1.00
		95% CI		1.00 - 1.00	1.00 - 1.00	1.00 - 1.00	1.00 - 1.00	1.00 - 1.00
5	10 µg Kappa RBD-Fc vaccine	G5/1	M	1.00	1.00	1.00	1.00	1.00
		G5/2	M	1.00	1.00	1.00	1.00	1.00
		G5/3	M	1.00	1.00	1.00	1.00	1.00
		G5/4	F	1.00	1.00	1.00	1.00	1.00
		G5/5	F	1.00	1.00	1.00	1.00	1.00
		GMT		1.00	1.00	1.00	1.00	1.00
		95% CI		1.00 - 1.00	1.00 - 1.00	1.00 - 1.00	1.00 - 1.00	1.00 - 1.00
6	10 µg Delta RBD-Fc vaccine	G6/1	M	1.00	1.00	1.00	1.00	1.00
		G6/2	M	1.00	1.00	1.00	1.00	1.00
		G6/3	F	1.00	1.00	1.00	1.00	1.00
		G6/4	F	1.00	1.00	1.00	1.00	1.00
		G6/5	F	1.00	1.00	1.00	1.00	1.00
		GMT		1.00	1.00	1.00	1.00	1.00
		95% CI		1.00 - 1.00	1.00 - 1.00	1.00 - 1.00	1.00 - 1.00	1.00 - 1.00
7	10 µg Epsilon RBD-Fc vaccine	G7/1	M	1.00	1.00	1.00	1.00	1.00
		G7/2	M	1.00	1.00	1.00	1.00	1.00
		G7/3	F	1.00	1.00	1.00	1.00	1.00
		G7/4	F	1.00	1.00	1.00	1.00	1.00

106

PVNT50 (Day 0)

Group	Vaccination Group	No.	Sex	Wuhan	Alpha	Beta	Gamma	Delta
		G7/5	F	1.00	1.00	1.00	1.00	1.00
		GMT		1.00	1.00	1.00	1.00	1.00
		95% CI		1.00 - 1.00	1.00 - 1.00	1.00 - 1.00	1.00 - 1.00	1.00 - 1.00

PVNT50 (Day 14)

Group	Vaccination Group	No.	Sex	Wuhan	Alpha	Beta	Gamma	Delta
1	Control	G1/1	M	1.00	1.00	1.00	1.00	1.00
		G1/2	M	1.00	1.00	1.00	1.00	1.00
		G1/3	F	1.00	1.00	1.00	1.00	1.00
		GMT		1.00	1.00	1.00	1.00	1.00
		95% CI		1.00 - 1.00	1.00 - 1.00	1.00 - 1.00	1.00 - 1.00	1.00 - 1.00
2	10 µg Alpha RBD-Fc vaccine	G2/1	M	1.00	1.00	1.00	1.00	27.71
		G2/2	M	1.00	34.77	1.00	1.00	1.00
		G2/3	M	1.00	1.00	11.16	1.00	1.00
		G2/4	F	39.14	13.73	1.00	1.00	14.94
		G2/5	F	3.13	42.38	25.20	1.00	46.26
		GMT		2.62	7.26	3.09	1.00	7.19
		95% CI		0.36 - 18.86	0.72 - 73.11	0.44 - 21.72	1.00 - 1.00	0.73 - 70.94
3	10 µg Beta RBD-Fc vaccine	G3/1	M	1.00	34.84	1.00	1.00	1.00
		G3/2	M	1.00	1.00	1.00	1.00	1.00
		G3/3	M	1.00	1.00	37.52	1.00	1.00
		G3/4	F	1.00	1.00	1.00	1.00	1.00

Group	Vaccination Group	No.	Sex	PVNT50 (Day 14)				
				Wuhan	Alpha	Beta	Gamma	Delta
		G3/5	F	1.00	1.00	1.00	1.00	1.00
		GMT		1.00	2.03	2.06	1.00	1.00
		95% CI		1.00 - 1.00	0.28 - 14.61	0.28 - 15.45	1.00 - 1.00	1.00 - 1.00
4	10 µg Gamma RBD-Fc vaccine	G4/1	M	30.84	20.97	72.63	69.86	124.15
		G4/2	M	36.00	1.00	1.00	1.00	1.00
		G4/3	M	1.00	31.55	38.72	34.27	49.65
		G4/4*	F	47.31	24.49	51.03	43.66	81.49
		G4/5	F	37.77	1.00	55.28	40.07	1.00
		GMT		18.18	6.95	23.98	21.11	13.81
		95% CI		2.41 - 137.29	0.77 - 63.02	2.60 - 221.45	2.48 - 179.79	0.69 - 278.20
5	10 µg Kappa RBD-Fc vaccine	G5/1	M	1.00	1.00	1.00	1.00	1.00
		G5/2	M	37.32	41.88	109.02	157.98	378.01
		G5/3	M	1.00	1.00	1.00	1.00	1.00
		G5/4	F	1.00	1.00	1.00	1.00	1.00
		G5/5	F	41.67	16.89	40.21	35.70	186.16
		GMT		4.35	3.71	5.35	5.63	9.32
		95% CI		0.36 - 52.95	0.39 - 35.83	0.30 - 95.78	0.28 - 114.02	0.21 - 420.07
6	10 µg Delta RBD-Fc vaccine	G6/1	M	51.48	39.10	11.72	35.29	62.69
		G6/2	M	51.83	63.51	1.00	27.79	3,098.63
		G6/3	F	1.00	34.91	58.26	36.57	39.49
		G6/4	F	1.00	1.00	38.32	1.00	33.16
		G6/5	F	83.93	38.32	32.86	34.80	163.90
		GMT		11.75	20.15	15.38	16.57	133.05

108

PVNT50 (Day 14)

Group	Vaccination Group	No.	Sex	Wuhan	Alpha	Beta	Gamma	Delta
		95% CI		0.71 - 193.90	2.46 - 165.31	2.01 - 117.48	2.35 - 116.83	13.12 - 1,349.46
7	10 µg Epsilon RBD-Fc vaccine	G7/1	M	115.09	96.83	36.16	1.00	314.82
		G7/2	M	228.38	481.50	31.67	1.00	1,245.25
		G7/3	F	13.86	1.00	1.00	1.00	116.47
		G7/4	F	99.22	1.00	53.64	1.00	131.28
		G7/5	F	37.54	429.16	1.00	1.00	1,862.73
		GMT		67.07	28.86	9.07	1.00	406.98
		95% CI		17.29 - 260.21	0.59 - 1,413.17	0.74 - 111.74	1.00 - 1.00	83.84 - 1,975.57

PVNT50 (Day 35)

Group	Vaccination Group	No.	Sex	Wuhan	Alpha	Beta	Gamma	Delta
1	Control	G1/1	M	1.00	1.00	1.00	1.00	1.00
		G1/2	M	1.00	1.00	1.00	1.00	1.00
		G1/3	F	1.00	1.00	1.00	1.00	1.00
		GMT		1.00	1.00	1.00	1.00	1.00
		95% CI		1.00 - 1.00	1.00 - 1.00	1.00 - 1.00	1.00 - 1.00	1.00 - 1.00
2	10 µg Alpha RBD-Fc vaccine	G2/1	M	2771.11	3012.35	89.55	98.33	2703.42
		G2/2	M	518.41	499.49	1.00	1.00	208.78
		G2/3	M	1.00	1.00	1.00	1.00	1.00
		G2/4	F	3380.81	4133.97	976.20	1217.37	932.97
		G2/5	F	432.21	598.77	149.94	152.08	371.28
		GMT		291.35	326.75	26.52	28.32	181.23

Group	Vaccination Group	No.	Sex	PVNT50 (Day 35)				
				Wuhan	Alpha	Beta	Gamma	Delta
		95% CI		4.79 - 17,710.16	4.97 - 21,461.01	0.55 - 1,278.54	0.53 - 1,499.33	4.03 - 8,140.83
3	10 µg Beta RBD-Fc vaccine	G3/1	M	312.45	566.61	1008.75	1110.89	76.50
		G3/2	M	127.97	432.59	309.91	346.18	53.31
		G3/3	M	1.00	1.00	1.50	75.58	1.00
		G3/4	F	294.92	499.45	1162.71	906.72	107.81
		G3/5	F	1.00	50.38	241.82	211.39	69.11
		GMT		25.96	90.79	167.50	354.15	31.37
		95% CI		0.63 - 1,068.31	3.14 - 2,625.76	5.67 - 4,944.00	90.33 - 1,388.51	2.81 - 350.09
4	10 µg Gamma RBD-Fc vaccine	G4/1	M	784.10	838.16	2204.38	2586.56	462.54
		G4/2	M	332.32	958.33	1333.32	1633.85	56.59
		G4/3	M	192.66	253.41	1203.99	1476.12	153.75
		G4/4*	F					
		G4/5	F	403.07	711.87	959.08	1157.40	200.35
		GMT		377.16	616.97	1357.30	1639.21	168.51
		95% CI		150.00 - 948.34	235.40 - 1,617.08	775.95 - 2,374.20	959.25 - 2,801.15	42.50 - 668.20
5	10 µg Kappa RBD-Fc vaccine	G5/1	M	328.68	418.29	203.84	214.39	333.67
		G5/2	M	743.74	1068.85	962.79	1033.36	1059.53
		G5/3	M	399.54	404.19	318.67	352.69	416.40
		G5/4	F	388.60	179.05	362.89	420.55	436.91
		G5/5	F	1006.05	982.79	531.18	419.36	689.40
		GMT		520.45	501.74	413.27	424.47	536.24
		95% CI		286.15 - 946.58	201.24 - 1,250.99	200.24 - 852.96	209.55 - 859.82	301.74 - 953.01
6	10 µg Delta RBD-Fc vaccine	G6/1	M	1,846.21	3,827.48	359.34	744.84	8,705.59

110

| Group | Vaccination Group | No. | Sex | PVNT50 (Day 35) | | | | |
				Wuhan	Alpha	Beta	Gamma	Delta
		G6/2	M	1,606.79	3,007.73	211.22	501.12	18,487.50
		G6/3	F	8,595.94	9,593.84	1,007.36	589.58	10,660.14
		G6/4	F	13,212.18	8,180.64	310.13	432.67	38,108.90
		G6/5	F	5,570.64	8,384.96	736.83	732.48	45,191.61
		GMT		4,515.26	5,968.79	445.11	587.08	19,683.61
		95% CI		1,418.38 - 14,373.81	3,105.77 - 11,471.06	200.35 - 988.87	437.66 - 787.52	7,882.50 - 49,152.50
7	10 µg Epsilon RBD-Fc vaccine	G7/1	M	3,494.35	4,294.95	455.03	794.29	6,221.99
		G7/2	M	13,040.98	9,110.93	220.63	309.53	15,686.81
		G7/3	F	12,068.73	11,752.49	528.93	685.94	18,823.85
		G7/4	F	4,214.97	3,306.81	2,771.18	3,699.94	12,157.61
		G7/5	F	4,041.87	3,705.57	312.43	463.14	6,852.45
		GMT		6,227.92	5,625.78	540.14	780.14	10,888.63
		95% CI		2,800.61 - 13,849.47	2,768.27 - 11432.95	160.90 - 1,813.21	241.54 - 2,519.72	5,902.65 - 20,086.30

| Group | Vaccination Group | No. | Sex | PVNT50 (Day 56) | | | | |
				Wuhan	Alpha	Beta	Gamma	Delta
1	Control	G1/1	M	1.00	1.00	1.00	1.00	1.00
		G1/2	M	1.00	1.00	1.00	1.00	1.00
		G1/3	F	1.00	1.00	1.00	1.00	1.00
		GMT		1.00	1.00	1.00	1.00	1.00
		95% CI		1.00 - 1.00	1.00 - 1.00	1.00 - 1.00	1.00 - 1.00	1.00 - 1.00
2	10 µg Alpha RBD-Fc vaccine	G2/1	M	5187.36	6783.84	266.61	296.92	2732.30

111

Group	Vaccination Group	No.	Sex	PVNT50 (Day 56)				
				Wuhan	Alpha	Beta	Gamma	Delta
		G2/2	M	1652.64	2171.56	1.00	60.98	676.37
		G2/3	M	4534.49	2694.90	516.16	494.56	1768.19
		G2/4	F	11550.24	12536.15	4713.50	4743.97	2196.53
		G2/5	F	2766.15	1935.02	444.61	458.10	1474.69
		GMT		4157.42	3951.19	195.88	454.81	1603.01
		95% CI		1,684.46 - 10,260.93	1,441.02 - 10,833.89	3.92 - 9,779.03	65.62 - 3,152.20	825.00 - 3,114.70
3	10 µg Beta RBD-Fc vaccine	G3/1	M	1232.37	1864.34	2752.64	3041.10	195.10
		G3/2	M	572.75	2068.48	2936.36	2064.39	377.68
		G3/3	M	281.58	896.44	2448.57	2087.32	103.85
		G3/4	F	424.49	1197.99	1491.76	1115.54	176.09
		G3/5	F	78.17	205.09	418.47	327.85	52.88
		GMT		366.31	967.87	1653.36	1368.09	148.10
		95% CI		103.44 - 1,297.18	304.71 - 3,074.33	602.68 - 4,535.69	461.12 - 4,058.93	59.36 - 369.53
4	10 µg Gamma RBD-Fc vaccine	G4/1	M	907.40	1299.93	2398.79	1874.44	542.99
		G4/2	M	398.24	1241.71	1838.94	1421.08	86.68
		G4/3	M	239.14	745.98	1980.11	1246.08	136.65
		G4/4*	F					
		G4/5	F	331.28	701.85	812.56	804.85	143.36
		GMT		411.34	958.80	1632.21	1278.46	174.26
		95% CI		166.59 - 1,015.66	570.29 - 1,611.99	762.51 - 3,493.89	729.80 - 2,239.59	49.50 - 613.41
5	10 µg Kappa RBD-Fc vaccine	G5/1	M	611.25	647.77	438.61	388.03	403.06
		G5/2	M	1014.39	1588.56	1366.91	898.58	743.84
		G5/3	M	417.36	626.39	345.44	359.46	306.27

Group	Vaccination Group	No.	Sex	PVNT50 (Day 56)				
				Wuhan	Alpha	Beta	Gamma	Delta
		G5/4	F	577.93	413.97	534.21	447.17	321.39
		G5/5	F	905.27	878.20	630.11	488.04	770.25
		GMT		670.37	748.11	587.03	486.86	469.16
		95% CI		429.01 - 1,047.54	402.71 - 1,389.77	306.62 - 1,123.91	310.31 - 763.85	268.67 - 819.26
6	10 µg Delta RBD-Fc vaccine	G6/1	M	1,200.43	1,453.13	651.52	382.98	3,229.24
		G6/2	M	1,041.90	789.65	366.33	296.12	4,696.50
		G6/3	F	6,456.55	5,995.54	1,828.85	1,259.59	5,514.74
		G6/4	F	4,335.18	2,366.83	254.63	260.72	6,667.17
		G6/5	F	3,905.38	4,058.17	818.60	712.80	7,089.92
		GMT		2,674.03	2,312.13	619.14	483.95	5,240.79
		95% CI		967.7 - 7,393.91	850.53 - 6,285.47	240.57 - 1,593.48	213.20 - 1,098.57	3,541.76 - 7,754.85
7	10 µg Epsilon RBD-Fc vaccine	G7/1	M	3,138.91	2,966.68	598.73	491.15	2,512.75
		G7/2	M	3,934.39	3,629.42	182.53	162.51	2,826.09
		G7/3	F	9,063.67	5,507.39	384.13	706.99	5,554.59
		G7/4	F	2,375.01	2,663.08	1,383.22	1,177.28	1,491.29
		G7/5	F	5,047.74	2,271.12	298.80	352.30	1,957.25
		GMT		4,222.26	3,242.92	444.49	471.91	2,583.68
		95% CI		2,242.14 - 7,951.08	2,121.90 - 4,956.18	171.65 - 1,150.99	187.02 - 1,190.77	1,400.14 - 4,767.69

VITA

NAME	Mr. Narach Khorattanakulchai
DATE OF BIRTH	2 March 1992
PLACE OF BIRTH	Bangkok, Thailand
INSTITUTIONS ATTENDED	Department of Biochemistry, Faculty of Science, Chulalongkorn University, Bangkok, Thailand (B.Sc.) Biochemistry and Molecular Biology Program, Faculty of Science,Chulalongkorn University, Bangkok, Thailand (M.Sc.)
HOME ADDRESS	Bangkapi, Huaikhwang, Bangkok, Thailand
PUBLICATION	Khorattanakulchai N, Amparyup P, Tassanakajon A. Binding of PmClipSP2 to microbial cell wall components and activation of the proPO-activating system in the black tiger shrimp Penaeus monodon. Dev Comp Immunol (2017) 77:doi: 10.1016/j.dci.2017.07.016

Khorattanakulchai N, Manopwisedjaroen S, Rattanapisit K, Panapitakkul C, Kemthong T, Suttisan N, et al. Receptor binding domain proteins of SARS-CoV-2 variants produced in Nicotiana benthamiana elicit neutralizing antibodies against variants of concern. J Med Virol (2022) 94:9. doi: 10.1002/jmv.27881

Khorattanakulchai N, Srisutthisamphan K, Shanmugaraj B, Manopwisedjaroen S, Rattanapisit K, Panapitakkul C, et al. A recombinant subunit vaccine candidate produced in plants elicits neutralizing antibodies against SARS-CoV-2 variants in macaques. Front Plant Sci (2022) 13:doi: 10.3389/fpls.2022.901978